LBL-23495
UC-94c

# Lawrence Berkeley Laboratory
UNIVERSITY OF CALIFORNIA

## APPLIED SCIENCE DIVISION

RECEIVED
LAWRENCE
BERKELEY LABORATORY

OCT 1 1987

LIBRARY AND
DOCUMENTS SECTION

**Technology Base Research Project for Electrochemical Energy Storage: Annual Report for 1986**

July 1987

TWO-WEEK LOAN COPY
This is a Library Circulating Copy
which may be borrowed for two weeks.

**APPLIED SCIENCE DIVISION**

Prepared for the U.S. Department of Energy under Contract DE-AC03-76SF00098

LBL-23495 c.2

## DISCLAIMER

This document was prepared as an account of work sponsored by the United States Government. While this document is believed to contain correct information, neither the United States Government nor any agency thereof, nor the Regents of the University of California, nor any of their employees, makes any warranty, express or implied, or assumes any legal responsibility for the accuracy, completeness, or usefulness of any information, apparatus, product, or process disclosed, or represents that its use would not infringe privately owned rights. Reference herein to any specific commercial product, process, or service by its trade name, trademark, manufacturer, or otherwise, does not necessarily constitute or imply its endorsement, recommendation, or favoring by the United States Government or any agency thereof, or the Regents of the University of California. The views and opinions of authors expressed herein do not necessarily state or reflect those of the United States Government or any agency thereof or the Regents of the University of California.

LBL-23495

# TECHNOLOGY BASE RESEARCH PROJECT FOR ELECTROCHEMICAL ENERGY STORAGE

## ANNUAL REPORT FOR 1986

Applied Science Division
Lawrence Berkeley Laboratory
University of California
Berkeley, California 94720

Edited by Kim Kinoshita, Technical Manager

July 1987

This work was supported by the Assistant Secretary for Conservation and Renewable Energy, Office of Energy Storage and Distribution of the U.S. Department of Energy under Contract No. DE-AC03-76SF00098.

# CONTENTS

EXECUTIVE SUMMARY ..... vii

I. INTRODUCTION ..... 1

II. EXPLORATORY RESEARCH

*A. MOLTEN SALT CELLS*

1. Molten-Electrolyte Cell Research ..... 3
2. Investigation of the $FeS_2$ Electrodes in High-Temperature Li/FeS Cells ..... 5

*B. AMBIENT-TEMPERATURE LITHIUM CELLS*

1. Inorganic Ambient-Temperature Rechargeable Lithium Battery ..... 6
2. Ambient-Temperature Secondary Lithium Batteries Using LiAl or Lithium Insertion Anodes ..... 7

III. APPLIED SCIENCE RESEARCH

*A. ALKALINE CELLS*

1. Zinc Electrode Studies ..... 9
2. Stable Ionic Polymers for Electrochemical Applications ..... 10

*B. ZINC/HALOGEN CELLS*

1. Surface Morphology of Metals in Electrodeposition ..... 11
2. Dendritic Zinc Deposition from Flowing Zinc Halide Solutions ..... 12
3. Zinc Electrode Morphology in Acid Electrolytes ..... 13
4. Transport in Aqueous Battery Systems ..... 14

*C. COMPONENTS FOR ALKALI/SULFUR CELLS*

1. Low-Temperature Beta″-Alumina Cell ..... 15
2. Mathematical Modeling of the Sodium/Sulfur Cell ..... 16
3. Electrical Conduction and Corrosion Processes in Fast-Ion Conducting Glasses ..... 16
4. Glass Electrolytes and Advanced Cell Concepts ..... 17
5. New Battery Materials ..... 18

*D. CORROSION PROCESSES IN HIGH-TEMPERATURE, HIGH-SULFUR-ACTIVITY MOLTEN SALTS*

1. Polysulfide Containment Materials ..... 19
2. Corrosion Resistant Coatings for High-Temperature High-Sulfur-Activity Applications ..... 20

*E. COMPONENTS FOR AMBIENT-TEMPERATURE NONAQUEOUS CELLS*

1. Surface Layers on Battery Materials ..... 21
2. Spectroscopic Studies of the Passive Film on Alkali and Alkaline Earth Metals in Nonaqueous Solvents ..... 22
3. *In Situ* Raman Spectroscopy of Lithium Electrode Surface in Ambient-Temperature Lithium Secondary Battery ..... 23
4. Polymeric Electrolytes for Ambient-Temperature Lithium Batteries ..... 24
5. Exploratory Cell Research and Fundamental Processes Study in Solid State Electrochemical Cells ..... 24
6. Metal Couples in Nonaqueous Electrolytes ..... 25
7. Corrosion, Passivity and Breakdown of Alloys Used in High Energy Density Batteries ..... 26

*F. CROSS-CUTTING RESEARCH*

1. Analysis and Simulation of Electrochemical Systems ..... 27
2. Ambient-Temperature Alkaline Sulfur-Polysulfide Electrodes ..... 28
3. Engineering Analysis of Gas Evolution ..... 29

**IV. AIR SYSTEMS RESEARCH**

*A. METAL/AIR CELL RESEARCH*

1. Electrocatalysts for Oxygen Electrodes ..... 31
2. Electrode Research for Electrically Rechargeable Zinc/Air Alkaline Battery ..... 32
3. Electrical and Electrochemical Behavior of Particulate Electrodes ..... 33
4. Technology Base Research on Zn/Air Battery Systems ..... 34

*B. ALUMINUM/AIR BATTERIES*

1. Aluminum/Air Power Cell Research and Development ..... 35

*C. FUEL CELL RESEARCH*

1. Fuel Cells for Transportation ..... 38
2. Advanced Chemistry and Materials for Fuel Cells ..... 42
3. Oxygen Reduction on Platinum in Fuel Cell Electrolytes ..... 43

# EXECUTIVE SUMMARY

The U.S. Department of Energy's Office of Energy Storage and Distribution provides continuing support for an Energy Storage Program, which includes R&D on advanced electrochemical energy storage and conversion systems. A major goal of this program is to develop electrochemical power sources suitable for application in electric vehicles and/or electric load-leveling devices. The program centers on advanced secondary batteries and fuel cells that offer the potential for high performance and low life-cycle costs, both of which are necessary to permit significant penetration into commercial markets.

The DOE Electrochemical Energy Storage Program is divided into two projects: the Exploratory Technology Development and Testing (ETD) Project and the Technology Base Research (TBR) Project. ETD Project management responsibility has been assigned to Sandia National Laboratory (SNL), and the Lawrence Berkeley Laboratory* (LBL) is responsible for management of the TBR Project. The ETD and TBR Projects include an integrated matrix of research and development efforts designed to advance progress on several candidate electrochemical systems. The role of the TBR Project is to perform supporting research for the advanced battery systems under development by the ETD Project, and to evaluate new systems with potentially superior performance, durability and/or cost characteristics. The specific goal of the TBR Project is to identify the most promising electrochemical technologies and transfer them to industry and/or the ETD Project for further development and scale-up. This report summarizes the research, financial and management activities relevant to the TBR Project in CY 1986. This is a continuing project, and reports for prior years have been published; they are listed at the end of the Executive Summary.

General problem areas addressed by the project include identification of new electrochemical couples for advanced batteries, determination of technical feasibility of the new couples, improvements in battery components and materials, establishment of engineering principles applicable to electrochemical energy storage and conversion, and the development of air-system (fuel cell, metal/air) technology for transportation applications. Major emphasis is given to applied research which will lead to superior performance and lower life-cycle costs.

*Participants in the TBR Project include the following LBL scientists: E. Cairns, K. Kinoshita and F. McLarnon of the Applied Science Division; and L. DeJonghe, J. Evans, R. Muller, J. Newman, P. Ross and C. Tobias of the Materials and Chemical Sciences Division.

The TBR Project is divided into three major project elements: Exploratory Research, Applied Science Research, and Air Systems Research. Highlights of each project element are summarized according to the appropriate battery system or electrochemical research area.

## EXPLORATORY RESEARCH

The objectives of this project element are to identify, evaluate and initiate development of new electrochemical couples with the potential to meet or exceed advanced battery and electrochemical performance goals. Research projects were conducted on molten-salt cells and ambient-temperature lithium cells.

**Molten-Salt Cells** based on lithium alloy negative electrodes and metal disulfide positive electrodes can exhibit very high performance, ease of manufacture, and freeze-thaw capability. Two organizations are pursuing techniques to stabilize the performance of $FeS_2$ electrodes in these cells.

- ANL has achieved over 400 cycles and 5400-h operation at 397°C with a small prismatic upper-plateau Li-Al/$FeS_2$ cell with LiCl-LiBr-KBr electrolyte. The cell performance (coulombic efficiency >90%, utilization 89%) remained nearly constant throughout the cycle test (discharge at 50 mA/cm$^2$ for 4 h, charge at 25 mA/cm$^2$ to a cut-off voltage of 2.05 V). Based on the stable cycle life demonstrated in this cell test, at least 1000 cycles with ≤20% capacity loss should be achievable.

- Gould, Inc. has observed that identical Li-alloy/$FeS_2$ cells containing LiCl-LiF-LiI electrolyte, which were cycled at 350 and 450°C, lost upper-plateau capacity at the rate of 0.14 and 0.29% per cycle, respectively. The life of the cell operated at 350°C was also significantly longer than that of the cell operated at 450°C, i.e., 250 vs 115 cycles. These results, and observations from other tests, clearly demonstrate that capacity decline is reduced at lower operating temperatures, and reaction kinetics are also lower.

**Ambient-Temperature Lithium Cells** have the potential for high specific energy and specific power, but they typically exhibit short lifetimes when tested under deep-discharge regimens. Various anodes containing Li combined with metal oxide cathodes in an organic-electrolyte system are being investigated to develop ambient-temperature Li cells which do not have the safety and cycle-life problems associated with elemental Li.

- The draft final report from Duracell, Inc. on studies of the ambient-temperature $Li/LiAlCl_4$-$SO_2/C$ system has been completed. The capability of the inorganic electrolyte systems to accept overcharge was demonstrated, but is limited by the chemical stability of the separator to the overcharge products. Further research studies to improve the cycle life, specific energy, and stability of separators are recommended.

- A novel low-temperature chemical synthesis method has been developed by EIC Laboratories, Inc. to produce Li anode materials such as Li-Al, $Li_xWO_2$, $Li_xFe_2O_3$ and $LiCoO_2$. Cycle tests of these materials in cells with $LiClO_4$-propylene carbonate and metal oxide cathodes ($V_2O_5$, $Fe_2O_3$, $Cr_3O_8$) are underway.

## APPLIED SCIENCE RESEARCH

The objectives of this project element are to provide and establish scientific and engineering principles applicable to batteries and electrochemical systems; and to identify, characterize and improve materials and components for use in batteries and electrochemical systems. Projects in this element provide research that supports a wide range of battery systems – alkaline, metal/air, flow, solid-electrolyte, and nonaqueous. Other research efforts are directed at improving the understanding of electrochemical engineering principles, minimizing corrosion of battery components, analyzing the surfaces of electrodes, and electrocatalysis.

**Alkaline Cells** often use zinc as the negative electrode, and it is this electrode that typically limits the lifetime of these cells. Efforts are underway to identify cell components that will improve the cycle-life performance of the Zn electrode.

- LBL has achieved more than 500 deep-discharge (100%) cycles with a pulse-charged ZnCa/KOH-KF/NiOOH cell. The performance of this system is expected to be comparable to that of standard Zn/KOH/NiOOH batteries, because the Ca and KF additions replaced equal quantities of Zn and KOH.

- LBL has used micro-electrodes to provide new insight into the chemical and transport processes that occur in secondary porous Zn electrodes in KOH electrolytes. Preliminary measurements show significant variations in local Zn species concentrations, and only modest variations in local hydroxyl-ion concentra-

tion. The response of the micro-electrodes also indicates that higher KOH concentrations stabilize the supersaturated zincate solution.

- SNL has found that replacement of a tertiary hydrogen by a methyl group in sulfonated polyphenylenes enhances the stability of the membrane in alkaline ferro/ferricyanide electrolytes.

**Zinc/Halogen Cells** use flowing electrolytes to promote the transport of Zn ions across the cell and to remove halogen as the cell is charged. The cell performance is limited by the tendency of the electrodeposited Zn to assume unwanted shapes, and efforts are aimed at understanding the complex phenomena that control the Zn electrode morphology.

- LBL has observed that the current efficiency for Zn deposition from acidic chloride solutions increased with Zn concentration and decreased with pH. The presence of impurities (i.e., Ni, Fe and Cd) was found to lower the current efficiency.

- Illinois Institute of Technology (IIT) investigated the kinetics of Zn dissolution at a rotating hemispherical electrode in brominated (0.05-0.35 M) $ZnBr_2$, and concluded that the exchange current density is ~20 $mA/cm^2$.

- EXAFS (extended X-ray absorption fine structure) studies on Zn electrolytes (acidic and basic) at Brookhaven National Laboratory (BNL) were able to determine the bond distances in Zn complexes. A tetrahedral $Zn(OH)_4^{=}$ species with a Zn-O distance of 1.77 Å was detected in alkaline electrolytes. In $ZnBr_2$ electrolytes, the Zn-Br distance is 2.37 Å and the Zn-O distance is 1.83 Å.

- Lawrence Livermore National Laboratory (LLNL) has completed isopiestic measurements of the $ZnCl_2$-$H_2O$ system over the concentration range 0.31358 to 13.143 mol/kg. These data show fairly good agreement, within 0.1 to 0.5%, with previous isopiestic data for concentrations up to 11 mol/kg.

**Improved Components for Alkali/Sulfur Cells**, such as superior alternatives to the $\beta''$-$Al_2O_3$ ceramic electrolyte and high-temperature sulfur-polysulfide electrode used in Na/S cells, stable lithium-ion conductors for Li/S cells, and a class of organosulfur electrodes for low-temperature $\beta''$-$Al_2O_3$ cells are under investigation.

- A novel, low-temperature (120-150°C) secondary cell has been developed at LBL which contains a liquid sodium negative, $\beta''$-$Al_2O_3$ electrolyte, and a class of organosulfur positives. The Na/tetraethylthiuram disulfide cell, which has a theoretical specific energy of 360 Wh/kg (OCV = 2.3 V), has been studied in most detail. Small-scale laboratory cells were capable of peak discharge rates of over 100 mA/cm$^2$, and cycling at 5 mA/cm$^2$ was demonstrated.

- ANL has selected a glass electrolyte with the composition (mol%) of 42 $Na_2O$, 8 $Al_2O_3$, 5 $ZrO_2$ and 45 $SiO_2$ for further testing in Na/S cells. Small-scale cells (1-3 mAh) were successfully cycled at 3 to 6 mA/cm$^2$ for 36 to 40 cycles (10-20% DOD) before a capacity loss was observed.

- Massachusetts Institute of Technology (MIT) has observed that the addition of KCl to potassium borate generally enhances $K^+$ transport in these glasses. At a fixed O/B ratio of 1.7, $K^+$ conductivity increased monotonically with increasing chloride content.

- Stanford University is exploring the use of compositions from the Li-Si-S system for both positive electrode and electrolyte materials. The Li-Si-S phase diagram and Gibbs free energies of formation of $Li_2SiS_3$ and $Li_4SiS_4$ have been determined from electrochemical measurements. X-ray diffraction analyses have indexed for the first time the lattice parameters of $Li_2SiS_3$ and $Li_4SiS_4$.

**Corrosion Processes in High-Temperature, High-Sulfur Activity Molten Salts** are under investigation, and the aim is to develop low-cost container and current-collector materials for use in alkali/sulfur and other molten-salt cells.

- Work at ANL to develop new alloys for positive current collector and containment materials for Na/S cells was completed. The corrosion behavior of 33 metals and alloys in S and $NaS_x$ at 350°C was examined. It was concluded that the continued development of new alloys would probably not result in an alloy material of sufficient low cost, low density and low corrosion rate to be useful for Na/S cells.

- IIT observed no weight loss or discoloration of $Mo_2C$ coatings in $Na_2S_3$ melt after 24 h at 300°C. However, in $Na_2S_4$ at 310°C, a black color was observed on the surface after 24 h immersion. Results to date are encouraging and suggest that $Mo_2C$ appears to resist S attack.

**Components for Ambient-Temperature Nonaqueous Cells**, particularly metal/electrolyte combinations that improve the rechargeability of these cells, are under investigation.

- Mercury porosimetry measurements at LBL show that $Li_3N$ layers formed by reaction of Li with gaseous nitrogen are microporous, with most of the pore radii less than 25 A. The slow filling of these pores and reaction of Li with the electrolyte at the base of the pores were observed by impedance spectroscopy.

- Case Western Reserve University (CWRU) has completed testing of ultrahigh vacuum apparatus and spectroscopic techniques for investigations of alkali and alkaline-earth metals. Auger electron spectroscopy measurements indicate that K free of impurities can be deposited on Ni substrates, and that K on the surface shifts the desorption of CO to higher temperatures. These findings will be useful for understanding the interaction of decomposition products (i.e., CO) from the reaction of propylene carbonate (PC) and alkali and alkaline earth metals.

- A research project has been initiated at Jackson State University to study the electrode/electrolyte interface by *in situ* Raman spectroscopy. Preliminary measurements indicate that $Li_2O$ and $Li_2CO_3$ are formed during the electrodeposition of Li on Ag from 0.75 M $LiAsF_6$ in PC.

- The University of Minnesota was awarded a contract from a RFP on applied research on novel concepts for advanced batteries. A research project has been initiated to investigate the electrochemical performance of thin-film polymer electrolytes and electrodes.

- The University of Pennsylvania has found that the ionic transport of $Ni^{2+}$ in $NiBr_2$ complexes with poly(ethylene oxide) (PEO) can be activated by hydration and dehydration of the sample. At 145°C, the $Ni^{2+}$ transport number for a dehydrated sample is $<0.1$, and it increases to 0.7 upon hydration.

- Experiments at LBL showed that 0.3 to 20 ppm $H_2O$ in PC electrolytes can be detected by electrochemical measurements using cyclic voltammetry and rotating disk electrodes. The onset of reduction of $H_2O$ occurred over a wide range of cathodic potentials (vs $K/K^+$ reference electrode), depending on the electrolyte. In $KPF_6$/PC, $H_2O$ reduction occurred at 0.48 V, whereas in $KAlCl_4$/PC, reduction occurred at 2.8 V. Experiments to understand these results are underway.

- Johns Hopkins University has observed that the presence of small quantities of $H_2O$ has a strong influence on the corrosion of Armco Fe in 0.5 M $LiClO_4$-PC. In nominally dry PC, only small pits ($\sim$20 $\mu$m) which are widely separated are formed. Aggressive pitting corrosion is evident in 50 mol% PC/50 mol% $H_2O$; both large pits and numerous small pits are formed, but the surface still appears to be highly polished. These results can be explained by classical corrosion theory.

**Cross-Cutting Research** is carried out to address fundamental problems in electrocatalysis and current density distribution, solutions of which will lead to improved electrode structures and performance in batteries and fuel cells.

- Mathematical models are being developed at LBL to (i) predict the response to alternating current signals of a redox reaction with soluble reactants and products in a flow-through porous electrode, and (ii) to calculate the frequency response of a rotating disk electrode. Electrosorption phenomena and double-layer theory are being incorporated into the models.

- LBL has observed that the reduction rate for the aqueous sulfide-polysulfide redox couple is enhanced by the addition of 13 mol% dimethylformamide (DMF) to the solution. A porous electrode in the aqueous polysulfide solution containing DMF provides electrode performance that is more than satisfactory for high-performance photoelectrochemical cells or redox cells.

- A micro-mosaic electrode with an electrochemical redox system was used by LBL to study the onset of convection in a fluid with a time-dependent density profile contained in a deep cell. This study showed that a sharp increase in mass-transfer rate occurs immediately after the first deviation from convection-

free behavior on electrodes which are much smaller than the wavelength of the disturbance (e.g., such as those caused by gas evolution).

## AIR SYSTEMS RESEARCH

The objectives of this project element are to identify, characterize and improve materials for air electrodes; and to identify, evaluate and initiate development of metal/air battery systems and fuel-cell technology for transportation applications.

**Metal/Air Cell Research** projects address bifunctional air electrodes, which are needed for electrically rechargeable metal/air (zinc/air, iron/air) cells; and novel alkaline Zn electrode structures, which could be used in either electrically recharged or mechanically recharged cell configurations.

- LBL has demonstrated that flow-through porous electrodes for Zn deposition provide encouraging performance in electrically rechargeable Zn/air cells. Zinc loadings of 160 $mAh/cm^2$ were obtained at 10 $mA/cm^2$, with minimal change in the original structure of the porous substrate as the cell was cycled. Based on data from 1.5-Ah prototype Zn/air cells employing such electrodes, it is projected that a 32-kWh battery should be capable of achieving 110 Wh/kg, with a peak power of 140 W/kg, efficiency of 60%, and a materials cost of <$20/kW.

- CWRU has observed that heat treatment of the polymers polypyrrole and polyacrylonitrile mixed with Co salt produces very active $O_2$ reduction catalysts. Their activity is comparable to that of highly dispersed Pt and heat-treated Co porphyrins, but they are much lower in cost.

- Experiments at LBL demonstrated that Zn can be readily deposited on Zn-coated Cu particles in alkaline zincate solutions. A superficial current density (current per unit area of cell cross section) of 300 $mA/cm^2$ with an electrical energy consumption of 2.7 kWh/kg Zn was achieved.

- Pinnacle Research Institute (PRI) has observed that the addition of 15 g/l sorbitol + 25 g/l $SiO_2$ to 12 M KOH at 55°C enhanced the utilization (78 vs 35%) and capacity (191 vs 87 Ah/l) of Zn in powder slurry electrodes, compared to electrolytes with no additives.

**Aluminum/Air Battery R&D** is directed at improving cell components and solving system integration problems, including the following: (i) air cathode development, (ii) hydrargillite crystallization and separation, (iii) integrated experiments involving a coupled cell/crystallizer, (iv) cell design, and (v) development of improved aluminum anodes. Major achievements of the program include:

- The development of Al/air batteries for electric vehicles has reached the stage that a review committee has recommended transfer of management responsibility of the program from LLNL to SNL. As a result of this recommendation, SNL will assume management responsibility for the engineering development of the Al/air battery and ancillary components, and LBL will retain management responsibility for research on electrodes.

- Experiments were performed at LLNL which showed that a crystallizer/separator with a lamella settler can be started and shut down many times without plugging the lines with solid products. Systems analysis by LLNL indicate that a battery consisting of 100 cells (600-$cm^2$ electrode area) with 2-mm electrode spacing and integrated to a 40-l crystallizer should be capable of delivering 15 to 20 kW.

- Eltech Systems Corporation has built and tested a 5-cell stack, which achieved maximum power density in 4 M NaOH at 400 $mA/cm^2$ with an Al alloy containing In and Ga. The continuous feed of the Al wedge-shaped anode, rapid mechanical rechargeability, high durability of the cathode structure, and continuous, moderate-term operation (10 h) were demonstrated.

- Experimental and theoretical studies are underway at SRI International to elucidate the corrosion mechanism of Al alloys. An experimental cell was designed that allowed the separate examination of $H_2$ evolution and Al electrodissolution reactions in alkaline solution. At 25°C, pure Al showed an active-to-

passive transition, a passive region, and transpassive dissolution region in which the current varies linearly with voltage.

**Fuel Cell Research**, managed by Los Alamos National Laboratory (LANL) includes research in several areas of electrochemistry, theoretical studies, fuel-cell testing, fuel processing, and membrane characterization. Major achievements of the fuel-cell program include:

- LANL has achieved a significant improvement in the performance of low-Pt-loading electrodes in contact with Nafion. Oxygen reduction performance with 0.35 $mg/cm^2$ Pt was comparable to that obtained earlier with electrodes containing 4 $mg/cm^2$ Pt.

- Preliminary evaluation of the Dow perfluorinated polymer by LANL indicates that higher performance should be possible with this material in fuel cells than that achieved with Nafion.

- Methanol reforming on ZnO-CuO catalysts produces equilibrium concentrations of 1 to 3% CO, which are too high for PEM fuel cells. LANL has found that partial oxidation of CO by the addition of a small amount of air to the reformate gas can reduce the CO level to below 0.01%.

- EXAFS studies of pyrolyzed transition metal (Fe and Co) macrocycles (phthalocyanine and tetramethoxyphenylporphyrin) at BNL indicate the presence of reduced metal and some other unidentified material. The pyrolyzed sample remaining after leaching the reduced metal still exhibits catalytic activity for $O_2$ reduction. The remaining material, which is presumed to be the catalyst, has a radial distribution function that is similar to that of the original transition metal macrocycle.

- Oxygen reduction measurements for high-area Pt supported on carbon black porous gas-diffusion electrodes in $K_2CO_3$ and KOH have been carried out by LBL. The reduction current in KOH is kinetically limited, whereas in $K_2CO_3$ local pH changes occur in the pores of the electrode during reduction which result in lower performance than in KOH.

## MANAGEMENT ACTIVITIES

During 1986, LBL managed 30 subcontracts and conducted a vigorous research program in Electrochemical Energy Storage. LBL staff members attended project review meetings, made site visits to subcontractors, and participated in technical management of various TBR projects. LBL staff members also participated in the following reviews, meetings, and workshops:

- Air Systems Review Meeting, Cleveland, OH, April 14-15, 1986.
- First International Workshop on High-Temperature Molten Salt Batteries, ANL, Argonne, Il, April 15-18, 1986.
- Alkali Metal Thermoelectric Converter Workshop, JPL, Pasadena, CA, April 23-24, 1986.
- Spring Meeting of the Electrochemical Society, Boston, MA, May 4-9, 1986.
- Phosphoric Acid Fuel Cell Review Meeting, EPRI, Palo Alto, CA, May 28, 1986.
- International Congress on Corrosion and Electrochemical Behavior of Metals in Non-Aqueous Solutions, Capri, Italy, June 3-6, 1986.
- 32nd International Power Sources Symposium, Cherry Hill, PA, June 9-12, 1986.
- Alcoa Laboratories Centennial Technical Symposium, Farmington, PA, June 9-13, 1986.
- DOE/SNL/LBL Lead Center Coordination Meeting, Washington, DC, June 25-26, 1986.
- EPRI Battery Evaluation Meeting, EPRI, Palo Alto, CA, July 7, 1986.
- SNL/EPRI Na/S and Zn/$Br_2$ Review Meeting, EPRI, Palo Alto, CA, July 8-9, 1986.
- NATO/IDA Workshop on Heat Engines and Batteries for Power Generation, Alexandria, VA, July 16, 1986.
- Gordon Research Conference on Physical Electrochemistry, New London, NH, August 11-15, 1986.
- 37th Meeting of the International Society of Electrochemistry, Vilnius, USSR, August 24-29, 1986.
- 21th Intersociety Energy Conversion Engineering Conference, San Diego, CA, August 25-29, 1986.
- Office of Energy Storage and Distribution Review Meeting, Seattle, WA, August 27-28, 1986.
- LBL/SNL Lead Center Meeting, Washington, DC, September 24-25, 1986.
- Fall Meeting of the Electrochemical Society, San Diego, CA, October 19-24, 1986.
- National Fuel Cell Seminar, Tucson, AZ, October 26-29, 1986.
- Fuel Cell Management Meeting, Washington, DC, November 13-14, 1986.
- SNL/EPRI Na/S and Zn/$Br_2$ Review Meeting, Washington, DC, December 1-4, 1986.
- Technology Base Research Project Review Meeting, Washington, DC, December 16-17, 1986.

## MILESTONES FOR THE TECHNOLOGY BASE RESEARCH PROJECT

Milestones accomplished in Fiscal Year 1986 by the TBR Project include:

- An extensive study of $Pt_xCr_{1-x}$ alloys at the University of Virginia indicate these alloys show improved electrocatalysis for $O_2$ reduction. These results are sufficiently encouraging that further experiments with binary alloys will be continued, and the research will be expanded to include ternary alloys.

- The corrosion behavior of 33 metals and alloys have been examined in sulfur and sodium polysulfides at 350°C by ANL. From these studies it has been concluded that continued development of new alloys will probably not result in a material with sufficiently low cost, low density, and low corrosion rate to be useful as a positive current collector/containment material for Na/S cells.

- ANL has completed a series of tests of the Li-Al/25 mol% LiCl-37 mol% LiBr-38 mol% KBr/$FeS_2$ (upper plateau) bicells with 100-$cm^2$ BN-felt separators. These tests established the following prospects for the new Li-Al/$FeS_2$ cells:

| | |
|---|---|
| Specific energy | 175-200 Wh/kg @ 4-h rate |
| Specific power | $\geqslant$200 W/kg @ 80% DOD |
| Cycle life | $\geqslant$1000 cycles to 100% DOD |

- A glass electrolyte with the composition (in mol%) 42 $Na_2O$, 8 $Al_2O_3$, 5 $ZrO_2$ and 45 $SiO_2$ has been tested in Na/S cells by ANL. Small-scale cells (1-3 mAh capacity) were successfully cycled at 3 to 6 mA/$cm^2$ (C/4-C/8 rate) for 36 to 40 cycles (10-20% DOD) before failure at the containment seals occurred.

- LLNL completed tests with an Al/air cell assembly (two Eltech EL-2 cells) that was coupled to a crystallizer/separator (lamella settler) subsystem. These tests revealed operational problems with the cell/separator assembly: (i) anode dissolution in the cell was irregular, and (ii) partial plugging of various cell components by solid products was encountered. The lamella settler/crystallizer was able to maintain a low solid particle concentration in the cell, and it was able to agglomerate the reaction products. The results of these tests suggested several modifications to the system to improve its overall performance.

## ACKNOWLEDGEMENT

This work was supported by the Assistant Secretary for Conservation and Renewable Energy, Office of Energy Storage and Distribution of the U.S. Department of Energy. The fuel cell effort at LANL was partially supported by the U.S. Department of Energy, Office of Vehicle and Engine Research and Development. The support from the Department of Energy and the contributions to this project by the participants in the Technology Base Research Project are acknowledged.

## ANNUAL REPORTS

1. "Technology Base Research Project for Electrochemical Energy Storage - Annual Report for 1985," LBL-21342 (July 1986).

2. "Technology Base Research Project for Electrochemical Energy Storage - Annual Report for 1984," LBL-19545 (May 1985).

3. "Annual Report for 1983 - Technology Base Research Project for Electrochemical Energy Storage," LBL-17742 (May 1984).

4. "Technology Base Research Project for Electrochemical Energy Storage, - Report for 1982" LBL-15992 (May 1983).

5. "Technology Base Research Project for Electrochemical Energy Storage - Report for 1981," LBL-14305 (June 1982).

6. "Applied Battery and Electrochemical Research Program Report for 1981," LBL-14304 (June 1982).

7. "Applied Battery and Electrochemical Research Program Report for Fiscal Year 1980," LBL-12514 (April 1981).

# SUBCONTRACTOR FINANCIAL DATA - CY 1986

| Subcontractor | Principal Investigator | Project | Contract Value (K$) | Term (months) | Expiration Date | Status in CY 1986 |
|---|---|---|---|---|---|---|
| *EXPLORATORY RESEARCH* | | | | | | |
| **Molten-Salt Cells** | | | | | | |
| Argonne National Laboratory | P. Nelson | Molten-Salt Cells | 300 | 12 | 9-86 | C |
| Gould, Incorporated | G. Barlow | Molten-Salt Electrolytes | 113 | 12 | 7-87 | R |
| Stanford University | R. Huggins | New Battery Materials | 246 | 12 | 11-86 | C |
| **Ambient-Temperature Lithium Cells** | | | | | | |
| Duracell, Inc. | A. Dey | $Li/SO_2$ | 1500 | 48 | 12-85 | T |
| University of Pennsylvania | G. Farrington | Polymeric Electrolytes | 82 | 12 | 2-87 | C |
| University of Minnesota | W. Smyrl | Solid State Cells | 169 | 12 | 6-87 | R |
| EIC Laboratories, Inc. | K. Abraham | Secondary Li Batteries | 150 | 12 | 6-87 | R |
| *APPLIED SCIENCE RESEARCH* | | | | | | |
| Lawrence Berkeley Laboratory | E. Cairns, L. DeJonghe, J. Evans, R. Muller, J. Newman, P. Ross, and C. Tobias | Electrochemical Energy Storage | 1500 | 12 | 9-86 | C |
| **Zinc/Halogen Cells** | | | | | | |
| Illinois Institute of Technology | R. Selman | Zn Deposition | 71 | 12 | 9-86 | C |
| Brookhaven National Laboratory | J. McBreen | Zn Morphology | 100 | 12 | 9-86 | C |
| Lawrence Livermore National Laboratory | D. Miller | Transport Properties | 65 | 12 | 9-86 | C |
| **Components for Alkali/Sulfur Cells** | | | | | | |
| Argonne National Laboratory | P. Nelson | Glass Electrolytes | 250 | 12 | 9-86 | C |
| Massachusetts Institute of Technology | H. Tuller | Li Conducting Glasses | 100 | 12 | 5-87 | C |

C = continuing, T = terminating, R = subject included in a request for proposals (RFP) issued by LBL in FY 1986.

# SUBCONTRACTOR FINANCIAL DATA - CY 1986

| Subcontractor | Principal Investigator | Project | Contract Value (K$) | Term (months) | Expiration Date | Status in CY 1986 |
|---|---|---|---|---|---|---|
| *APPLIED SCIENCE RESEARCH* - cont. | | | | | | |
| **Corrosion Processes in High-Temperature, High-Sulfur-Activity Molten Salt** | | | | | | |
| Argonne National Laboratory | P. Nelson | Polysulfide Containment | 200 | 12 | 9-86 | T |
| Illinois Institute of Technology | R. Selman | Corrosion Resistant Coatings | 163 | 12 | 10-86 | C |
| **Components for Ambient-Temperature Lithium Cells** | | | | | | |
| Case Western Reserve University | D. Scherson | Spectroscopic Studies | 62 | 12 | 11-86 | C |
| Jackson State University | H. Tachikawa | Raman Spectroscopy | 53 | 12 | 3-86 | C |
| Johns Hopkins University | J. Kruger | Corrosion/Passivity Studies | 88 | 12 | 7-87 | C |
| *AIR SYSTEMS RESEARCH* | | | | | | |
| **Metal/Air Cell Research** | | | | | | |
| Case Western Reserve University | E. Yeager | Air Electrodes | 213 | 12 | 4-87 | C |
| Pinnacle Research Institute | L. Morris | Zn/Air Battery | 225 | 12 | 12-86 | C |
| **Aluminum/Air Battery R&D** | | | | | | |
| Lawrence Livermore National Laboratory | A. Maimoni | Al/Air Power Cell R&D | 495 | 12 | 9-86 | C |
| **Fuel Cell R&D** | | | | | | |
| Los Alamos National Laboratory | J. Huff | Fuel Cell R&D | 440 | 12 | 9-86 | C |
| Brookhaven National Laboratory | J. McBreen | Fuel Cell Research | 230 | 12 | 9-86 | C |

C = continuing, T = terminating, R = subject included in a request for proposals (RFP) issued by LBL in FY 1986.

# I. INTRODUCTION

This report summarizes the progress made by the Technology Base Research (TBR) Project for Electrochemical Energy Storage during calendar year 1986. The primary objective of the TBR Project, which is sponsored by the Department of Energy (DOE) and managed by Lawrence Berkeley Laboratory (LBL), is to identify electrochemical technologies that can satisfy stringent performance and economic requirements for electric vehicles and stationary energy storage applications. The ultimate goal is to transfer the most promising electrochemical technologies to the private sector or to another DOE project (e.g., Sandia National Laboratories' Exploratory Technology Development and Testing Project) for further development and scale-up.

Besides LBL, which has overall responsibility for the TBR Project, technical management of several projects is shared with Lawrence Livermore National Laboratory (LLNL) and Los Alamos National Laboratory (LANL). Brookhaven National Laboratory (BNL) and Argonne National Laboratory (ANL) participate in the TBR Project by providing key research support in several of the project elements.

The TBR Project consists of three major project elements:

- Exploratory Research
- Applied Science Research
- Air Systems Research

The objectives and the specific battery and electrochemical systems addressed by each project element are discussed in the following sections, which also include technical summaries that relate to the individual projects. Financial information that relates to the various projects and a description of the management activities for the TBR Project are described in the Executive Summary.

# II. EXPLORATORY RESEARCH

The major thrust of this project element is to evaluate promising electrochemical couples for advanced batteries for electric vehicles. The advanced battery systems that were investigated are various versions of rechargeable lithium cells.

## A. MOLTEN SALT CELLS

**Molten-Salt Cells** based on Li alloy negative electrodes and metal disulfide positive electrodes can exhibit very high performance, ease of manufacture, and freeze-thaw capability. Two organizations are pursuing techniques to stabilize the performance of $FeS_2$ electrodes in these cells.

### Molten-Electrolyte Cell Research

*L.A. Redey and T.D. Kaun (Argonne National Laboratory)*

Research is being conducted to achieve major improvements in the performance and reliability of the Li-alloy/$FeS_2$ system with molten-salt electrolyte. The objective of this task is to bring about innovations in the current technology that will yield a specific energy of 200 Wh/kg at a 4-h discharge rate, a specific power of 200 W/kg and a cycle life of 1000 cycles. Significant progress has been made toward achieving these goals based on improvements in the electrochemical properties of electrode materials (energy and power capabilities, polarization, and area specific resistivities) and innovations in cell design. The two major changes from earlier cells with $FeS_2$ electrodes are (i) a novel electrolyte composition (LiCl-LiBr-KBr rather than LiCl-KCl) with a lower melting point (310°C), and (ii) a higher loading density (2.4 vs 1.5 Ah/cm$^3$) for the $FeS_2$ electrode, which is operated only on its upper plateau (U.P.).

During this period, it was demonstrated that the use of the dense U.P.-$FeS_2$ electrode and the lower-melting LiCl-LiBr-KBr electrolyte eliminated the capacity-loss problem of previous Li-Al/$FeS_2$ systems (with LiCl-KCl electrolyte, a 50% decline in cell upper-plateau capacity occurred in the first 200 cycles). The capacity utilization as a function of cycle number for the U.P.-$FeS_2$ cell is shown in Fig. 1 (cell coulombic efficiency was >99%). The cell capacity was nearly constant (i.e., ~89% at 50 mA/cm$^2$) through more than 400 cycles and 5400 h, and the cell voltage versus capacity curve changed very little during this time.

Compared with previous two-plateau (T.P.) $FeS_2$ cells, the U.P.-$FeS_2$ cell (24-Ah bicell design) had a higher energy density at 50 mA/cm$^2$ as a result of an ~50% higher utilization of the capacity and a 10% higher average discharge voltage. The voltage versus capacity curves of these two Li-Al/$FeS_2$ cells (both with 24-Ah capacity) are compared in Fig. 2. The energy density at higher discharge rates, 100 and 150 mA/cm$^2$, showed even greater improvement, with the utilization of capacity ranging from 82 to 75% at 397°C. The U.P.-$FeS_2$ cell is capable of an 82% utilization at 150 mA/cm$^2$ when operated at 427°C. The cell capacity at a discharge current density of 100 mA/cm$^2$ was only slightly decreased as the temperature decreased from 427 to 388°C. Also, good operability was obtained at temperatures as low as 380°C. Tests with a U.P.-$FeS_2$ cell having a thick positive electrode (48 Ah) showed a four-fold increase in energy storage per unit of separator area compared to previous T.P.-$FeS_2$ cells. The power density at 80% depth of discharge (DOD) was enhanced by at least 100% because (i) the cell voltage at 80% DOD was about 0.3 V higher than that of a T.P.-$FeS_2$ cell, and (ii) the cell resistivity was lower, ranging from 0.65 to 0.85 ohm-cm$^2$ for 5 to 80% DOD, compared with 1.2 to 1.6 ohm-cm$^2$ for the T.P.-$FeS_2$ cell. The higher voltage and lower resistivity of the U.P.-$FeS_2$ cell boosts the power density from 0.3 to 0.8 W/cm$^2$ of separator area at 80% DOD.

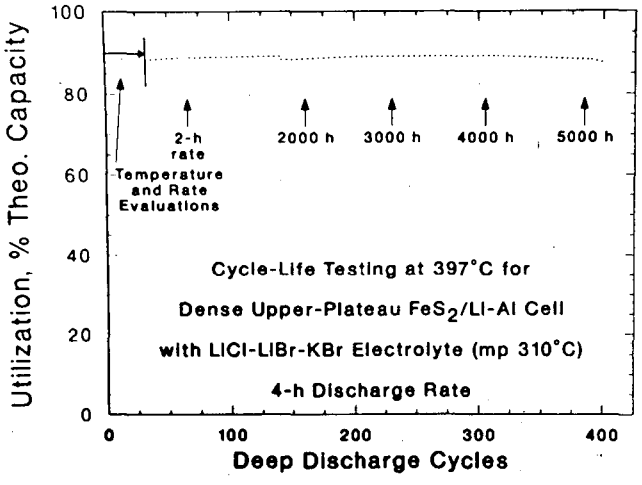


**Figure 1.** Cell discharge capacity (utilization of the U.P.-$FeS_2$ capacity) as a function of cycle life.

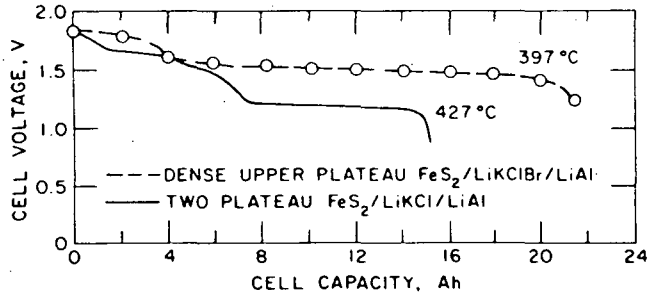


**Figure 2.** Voltage/capacity curves at a discharge rate of 50 mA/cm$^2$.

Electrochemical characterization of $FeS_2$-$NiS_2$ or $FeS_2$-$CoS_2$ active materials has revealed significantly better electrode kinetics when compared to $FeS_2$ active material. In particular, area-specific resistance (ASR) measurements on $FeS_2$-$NiS_2$ (1:1 ratio) electrodes indicated $ASR_{15s}$ values in the range of 0.55 to 0.70 ohm-cm$^2$ for the discharge half-cycle. Under identical discharge conditions, the $FeS_2$ electrode exhibited values in the range of 0.9 to 1.6 ohm-cm$^2$. In addition to the lower ASR values, the narrower range of ASR values results in better overall performance for the mixed-sulfide electrode.

A further decrease and even more uniformity of the ASR values on discharge (0.25-0.35 ohm-cm$^2$) have been observed for $FeS_2$-$NiS_2$ electrodes that were operated in $Li_2S$-saturated electrolytes. The improved power, as indicated by the lower ASR values, is also associated with higher rates of charge and discharge and better utilization of the active material. The power and charge acceptance of Li-alloy/$FeS_2$-$NiS_2$ test cells (1-2 Ah) were significantly improved when $Li_2S$ was used in excess of the stoichiometric amount required by the metal sulfide formation. A sufficient quantity of $Li_2S$ at the end of charge provides a very effective overcharge-protection mechanism.

Studies were initiated to identify materials and mechanisms that afford overcharge protection at the negative electrode. Active materials that will also improve the energy and power density of the negative electrode are also being examined. The initial results of both efforts have been successful and may be patentable. Invention reports are being prepared.

As a result of electrode impedance studies, an ultra-high power capability was revealed during laboratory tests of Li-alloy/$FeS_2$ cells. A specific peak-power of ~18 kW/kg was demonstrated when a power density of 8.8 W/cm$^2$ was achieved with repetitive 1-ms pulses at a current density of 8 A/cm$^2$. The pulse response of the Li-alloy/$FeS_2$ system is illustrated in Fig. 3, which shows plots of cell current and voltage as a function of time. The cell at full charge provides an intense current pulse of 8.04 A/cm$^2$ and 1-ms duration. The current pulse causes a drop in cell voltage of about 0.84 V (from 1.93 V before the pulse to 1.09 V at the end of the pulse) because of an internal cell resistance of ~0.1045 ohm-cm$^2$ ($R_t = \Delta V/\Delta I = 0.84/8.04$). With this $R_t$ (t = 1 ms), a peak power density of 8.91 W/cm$^2$ (32.8 W/cm$^3$ volumetric power density) is available. A system specific peak power of 17.6 kW/kg is projected based on the size (7.91-cm$^2$ area; 2.72-mm thickness) and weight (4 g) of this cell. Full cell capacity was obtained with high-intensity pulses having durations of more than 250 ms and rates of more than 20 pulses a second. This power performance characteristic is orders of magnitude greater than that of the lead-acid battery system. Because of the endothermic nature of the electrochemical discharge reaction, the usual heat generated by internal power ($I^2R$) losses is canceled in the Li/$FeS_2$ system for output pulse power levels as high as 165 kW/kg. This self-cooling feature allows very compact packaging. As a result, a rechargeable bipolar cell array incorporating newly developed active materials and molten-salt electrolytes is projected to have a specific power of 150 to 300 kW/kg.

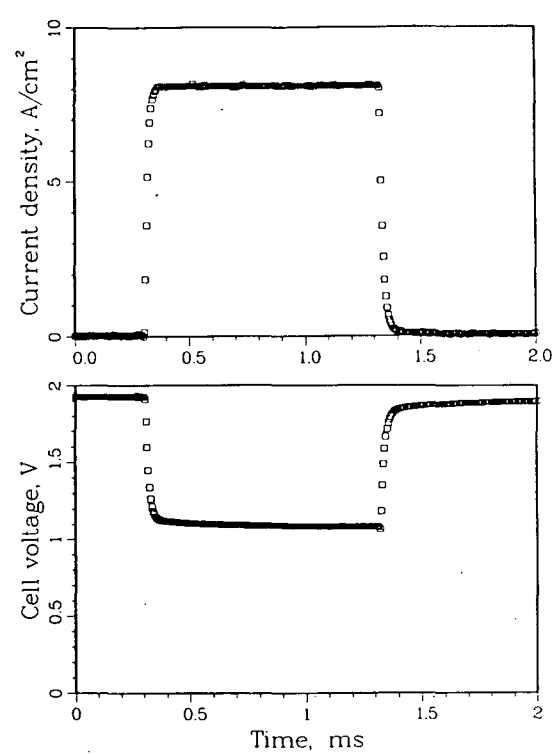


**Figure 3.** Current pulse and the corresponding voltage excursion of a Li-Si-$FeS_2$ cell.

Simplified current-collector shapes are needed to facilitate the fabrication, and to reduce the cost of cells that use Mo current collectors. Modeling and cell fabrication studies were initiated to investigate alternative electrode designs. A model was developed for a cylindrical cell with the positive electrode in the shape of a rod and an outer annulus of separator material (MgO powder). This electrode shape affords simpler and less costly fabrication than that of flat-plate designs. The model was used to evaluate various design options and to identify key components for further study. Calculations for a cylindrical cell design (5-cm O.D. and 19.5-cm length) containing seven positive electrodes (~150 Ah capacity) indicated a specific energy of about 190 Wh/kg and a specific power of ~250 W/kg at 50% DOD (~170 W/kg at 80% DOD) are achievable. The analysis also indicated that an improvement in the electronic conductivity of the positive electrode would result in a significant increase in cell power capability.

PUBLICATIONS


1. L. Redey (1986), "Reference Electrode Systems and Their Application in Li/$MS_x$ Battery Research," *Proceedings of the First International Workshop on High-Temperature Molten Salt Batteries,* Argonne, IL, ANL-86-40, p. B-92.
2. L. Redey (1986), "Power Performance of LiAlSi/(Fe,Ni)$S_2$ Cells," *Proceedings of the First International Workshop on High-Temperature Molten Salt Batteries,* Argonne, IL, ANL-86-40, p. B-131.
3. T.D. Kaun (1986), "Development of the Lithium-Limited FeS Cell," *Proceedings of the First International Workshop on High-Temperature Molten Salt Batteries,* Argonne, IL, ANL-86-40, p. B-101.
4. T.D. Kaun (1986), "A Stable Iron Disulfide Secondary Cell with LiCl-LiBr-KBr Electrolyte," *Proceedings of the First International Workshop on High-Temperature Molten Salt Batteries,* Argonne, IL, ANL-86-40, p. B-138.
5. A.A. Chilenskas, T.D. Kaun, and I.D. Bloom (1986), "Three Super-Batteries Move Closer to Practical Applications," *Logos* **4(2),** 6.
6. T.D. Kaun (1986), "An Advanced Lithium-Aluminum/Iron Disulfide Secondary Cell," *presented at the 32nd International Power Sources Symposium,* Cherry Hill, NJ.
7. T.D. Kaun (1986), "A Stable, High-Performance Lithium/Iron Disulfide Cell with LiCl-LiBr-KBr Electrolyte," *Proceedings of the 21st Intersociety Energy Conversion Engineering Conference,* p. 1O48.
8. L. Redey (1986), "Reference Electrodes for Pyrochemical Applications," *presented at the Sixth Annual Pyrochemical Workshop,* Los Alamos, NM.


## Investigations of $FeS_2$ Electrodes in High-Temperature Li/$FeS_2$ Cells


*G. Barlow (Gould Inc.)*


The lithium-alloy/iron disulfide couple is currently being reconsidered for use in high-temperature molten-salt batteries because of its high theoretical specific energy and power. The successful implementation of the lithium-alloy/iron disulfide couple has not occurred to date, due primarily to an unacceptable decay in the capacity of the upper-plateau discharge reaction. The goal of the present research is to gain a better understanding of the mechanisms which lead to upper-plateau capacity decline and attempt to define a solution to the problem.

Earlier thermogravimetric analyses work performed under this contract showed that iron pyrite thermally decomposes at a relatively high rate at typical cell operating temperatures of ⩾450°C, but at a temperature of ~300°C the rate of decomposition is negligible. This implies that lowering the cell operating temperature in the range of 300 to 400°C by utilizing a lower-melting-point electrolyte would significantly reduce the rate of sulfur loss and hence the loss of upper-plateau capacity.

Three different electrolytes were selected for the in-cell experiments with melting points ranging from 184 to 341°C, thus permitting cells to be operated at temperatures below 400°C. The in-cell experiments were conducted in 20-$cm^2$ pellet cells which were operated over both the upper- and lower-voltage plateaus between an upper charge cut-off of 2.0 V and a lower discharge cut-off of 1.0 V.

Identical cells containing a LiCl-LiF-LiI electrolyte cycled at temperatures of 350 and 450°C, respectively, showed that the average rate of loss in upper-plateau capacity of the cell operated at 350°C was approximately half (0.141% per cycle) that of the cell operated at 450°C (0.295% per cycle). The life of the cell operated at 350°C was also significantly longer than the cell operated at 450°C, 250 cycles compared to 115 cycles. However, the lower-plateau capacity was substantially lower in the cell operated at 350°C than that of the cell operated at 450°C. A cell con-

taining a LiCl-LiBr-LiI-KI-CsI electrolyte operated at 200°C over a period of 650 days exhibited an upper-plateau capacity decline rate of 0.016% per day over the first 500 days. This result reinforces the hypothesis that the rate of capacity decline can be greatly reduced by lowering the cell operating temperature. However, such a low operating temperature greatly reduces the cell reaction kinetics so that charge/discharge current densities are limited to about 5 $mA/cm^2$.

A cell containing a LiCl-LiBr-KBr electrolyte (same composition as used by Kaun[1] at ANL), which has a melting point of 310°C, was also built and tested. This cell differed from the ones in the ANL study in that no $CoS_2$ was incorporated in the $FeS_2$ electrode, and the cell was a starved-electrolyte design with a MgO separator which was operated over both upper- and lower-voltage plateaus. The main findings from this cell were as follows: (i) the upper-plateau capacity declined with cycling at a rate similar to that of the cell containing the all-lithium-halide electrolyte operated at the same temperature; and, (ii) the capacity of the lower plateau was only 20% of theoretical at a discharge current density of 40 $mA/cm^2$. The rate of loss in upper-plateau capacity in this cell differs from that measured by Kaun; however, the loss may be attributed to a degree of irreversibility of the phases formed in the positive electrode when operated over both voltage plateaus, which is not observed when cycling is restricted to the upper plateau only. One concludes from this that the upper-plateau capacity decline is not strictly due to a loss of sulfur from the $FeS_2$. Also, electrolytes containing $K^+$ severely limit the capacity available from the lower plateau at typical electrode operating current densities of $\geqslant 40$ $mA/cm^2$. These results indicate that an upper-plateau cell design should have superior performance and life, compared to a two-plateau cell design.

REFERENCE

1. T.D. Kaun (1985), "Li-Al/$FeS_2$ Cell with LiCl-LiBr-KBr Electrolyte," *J. Electrochem. Soc.* **132,** 3063.

# B. AMBIENT-TEMPERATURE LITHIUM CELLS

These cells have the potential for high specific energy and specific power, but they typically exhibit short lifetimes when tested under deep-discharge regimens. An inorganic-electrolyte system, which offers improved Li-electrode rechargeability and the capacity to withstand limited overcharge, is under investigation, along with an organic-electrolyte system.

## Inorganic Ambient-Temperature Rechargeable Lithium Battery

*A.N. Dey (Duracell, Inc.)*

Duracell, Inc. developed an ambient-temperature Li rechargeable cell in 1980 with an inorganic $SO_2$ electrolyte, positive electrode of porous carbon, $SO_2$ as depolarizer, and $Li_2B_{10}Cl_{10}$ or $LiGaCl_4$ as the electrolyte salt. Cells of D-size had a cycle life of 50 to 140 cycles at 10 to 20% depth of discharge and only 10 to 30 cycles on deep discharge. Degradation of the carbon electrode was believed to cause poor cycle life.

In addition to poor cycle life, the salts $Li_2B_{10}Cl_{10}$ and $LiGaCl_4$ were also very expensive. Development efforts were continued with the exploration of new low-cost electrolyte salts and other positive electrode materials. Various Li and other alkali and alkaline-earth metal salts were found readily soluble in $SO_2$ and formed highly conductive electrolytes. A conductivity of about $1 \times 10^{-1}$ $ohm^{-1}cm^{-1}$ was obtained with the solvated $LiAlCl_4$-$xSO_2$ electrolytes. The solvated electrolytes also provided excellent Li stability and cycling efficiency; Li cycling efficiencies of over 96% were obtained. Studies of various solid positive materials have also identified $CuCl_2$ as one of the promising materials for use in inorganic $SO_2$ electrolyte. Cells using porous carbon and solid active materials such as $CuCl_2$ for the positive electrodes were evaluated with various $SO_2$ electrolytes.

The Li/carbon system with $LiAlCl_4$-$xSO_2$ electrolytes shows an OCV of 3.2 V, and the cell reaction is different from the regular Li/carbon cells with $Li_2B_{10}Cl_{10}/SO_2$ or $LiGaCl_4/SO_2$ electrolytes. These cells have theoretical specific energy of 524 W/kg. In experimental prismatic cells, over 200 cycles at 100% DOD were obtained. The 2/3A-size prototype wound cells delivered about 40 to 60 cycles at 100% DOD and near 200 cycles at 50% DOD. A practical specific energy of about 100 W/kg has been obtained with the prototype 2/3A cells, and a higher specific energy is anticipated for larger sizes of cells.

Li/$CuCl_2$ cells with inorganic $SO_2$ electrolytes have an OCV of 3.4 V with a theoretical specific energy of 606 Wh/Kg to a cut-off of 2.6 V (first electron discharge). Over 400 cycles at a 2 $mA/cm^2$ discharge rate and a 1 $mA/cm^2$ charge rate have been demonstrated in experimental cells. Cells discharged

to 2.2 V with the reduction of $CuCl_2$ to Cu have a lower cycle life. The 2/3A-size prototype wound cells delivered only 15 to 20 cycles, which was probably due to poor fabrication of the positive electrode.

The capability to accept overcharge is one of the important advantages of the inorganic-electrolyte system. All active chemicals present in the systems are inherently reversible. Experiments to demonstrate the overcharge capability and to investigate the balancing reactions were carried out. Oxidation of the electrolyte salt and the recombination of the overcharge products provide the balancing function. The amount of overcharge which the cell can sustain is limited by the chemical stability of the separator to the overcharge products.

Capacity fade, development of internal shorts, and instability of the separator in the presence of overcharge products are the major problems of the prototype wound cells. Further studies of the inorganic rechargeable system to improve the cycle life, specific energy, and the stability of the separator are recommended.

## Ambient-Temperature Secondary Lithium Batteries Using LiAl or Lithium Insertion Anodes

*K.M. Abraham (EIC Laboratories, Inc.)*

The objective of this project is to develop a suitable replacement for Li anodes in ambient-temperature secondary batteries with the intent to eliminate the safety and cycle-life problems associated with the extreme reactivity of elemental Li. The alternative anodes which are being developed are Li-Al, $Li_xWO_2$ and $Li_xFe_2O_3$. The higher equivalent weight and lower Li activity of these materials will be largely compensated for by coupling them to high-voltage cathode materials such as $LiCoO_2$, $Cr_3O_8$ or amorphous $V_2O_5$. The work reported here describes the synthesis, and physical and electrochemical characterizations of the alternative anodes, and studies on the cathodes.

A novel low-temperature chemical synthesis of the anode materials has been developed which involves the reaction of *in situ* generated Li-naphthalide (Li-naph) with powdered Al or metal oxides. Debye-Scherrer X-ray studies confirm that the reaction of Li-naph with Al produces $\beta$-Li-Al. It appears that this is the first time that a room-temperature chemical reaction has produced this alloy. Future work includes improvement of the reaction efficiency and cycle testing of the alloy in a Li-Al/$TiS_2$ cell.

X-ray diffraction data established that the reaction of Li and $WO_2$ involves an insertion process, and the chemical reversibility tests with $I_2/CH_3CN$ solutions confirmed this. The electronic conductivities of $WO_2$ (55 $ohm^{-1}$-$cm^{-1}$) and $LiWO_2$ (1.9 $ohm^{-1}$-$cm^{-1}$) are adequate to allow the materials to function as electrodes without the use of an additive to enhance conductivity.

Although $\alpha$-$Fe_2O_3$ is an insulator, $\alpha$-$Li_6Fe_2O_3$ has a conductivity of 0.40 $ohm^{-1}$-$cm^{-1}$. Thus it is possible to fabricate useful $Li_6Fe_2O_3$ anodes without incorporating additives to enhance conductivity. X-ray analysis revealed that lithiation of $\alpha$-$Fe_2O_3$ results in a loss of crystallinity of the oxide. Thus, $Li_xFe_2O_3$ compounds with $x \geqslant 3$ are amorphous, while those with $x \leqslant 3$ are poorly crystalline. The conductivity of $\gamma$-$Fe_2O_3$ is $3.0 \times 10^{-5}$ $ohm^{-1}$-$cm^{-1}$, and increases to $3.0 \times 10^{-2}$ $ohm^{-1}$-$cm^{-1}$ for $\gamma$-$Li_6Fe_2O_3$. A loss of crystallinity was observed upon Li insertion for this form of $Fe_2O_3$ as well.

Amorphous $V_2O_5$, crystalline $LiCoO_2$ and $Cr_3O_8$ have been prepared and tested. X-ray analysis shows them to be free of impurity phases. The electronic conductivity is $1.98 \times 10^{-5}$ $ohm^{-1}$-$cm^{-1}$ for $\alpha$-$V_2O_5$, $1.78 \times 10^{-4}$ $ohm^{-1}$-$cm^{-1}$ for $LiCoO_2$, and $Cr_3O_8$ is an insulator.

The electrochemical reversibility of the lithiated oxides was studied in Li/PC-$LiClO_4$/metal oxide cells. The maximum reduction capacities corresponded to utilizations of 1.1 Li/$WO_2$, 7.3 Li/$\alpha$-$Fe_2O_3$, and 6.3 Li/$\gamma$-$Fe_2O_3$. The cycling results indicate that $Li_xWO_2$ is useful as a reversible anode with nearly 1 Li/$WO_2$ capacity, and $Li_xFe_2O_3$ is useful as a reversible anode with ~3 Li/$Fe_2O_3$ utilization.

Reaction of a vanadium-containing glass with excess Li-naph resulted in the uptake of 3 Li/$V_2O_5$. Cycling of a Li/PC-$LiClO_4$/$V_2O_5$ cell between 3.6 and 1.5 V resulted in the insertion of 2.4 Li/$V_2O_5$ with 68% recharge efficiency in the first charge. Subsequent cycling efficiency was 97%, and more extensive cycling studies are being performed.

Cycling a Li/PC-$LiClO_4$/$CoO_2$ cell from 3.4 to 4.5 V allowed removal of 0.5 equivalents of Li with 80% recharge efficiency in the first charge.

Discharge of Li/PC-$LiClO_4$/$Cr_3O_8$ allowed insertion of 4.5 Li/$Cr_3O_8$ and 73% of the capacity was regained during charge.

Cells with the configuration $LiWO_2$ or $Li_6Fe_2O_3$/PC-$LiClO_4$/$TiS_2$ were cycled at $\pm$ 0.5 $mA/cm^2$ between the limits of 0.5 and 2.2 V. More than 100 cycles were obtained with each type of cell,

and the coulombic efficiency was 100% for each cycle. The utilization decreased from 0.5 $Li/WO_2$ and 1 $Li/\alpha\text{-}Fe_2O_3$ in the first cycle to ~0.4 equivalents of Li for both materials after 113 cycles. An anode made with chemically prepared $Li_6Fe_2O_3$ was cycled to 0.9 equivalents of Li with 100% efficiency.

# III. APPLIED SCIENCE RESEARCH

The objectives of this project element are to provide and establish scientific and engineering principles applicable to batteries and electrochemical systems; and to identify, characterize and improve materials and components for use in batteries and electrochemical systems. Projects in this element provide research that supports a wide range of battery systems – alkaline, flow, molten salt, nonaqueous, and solid-electrolyte. Other projects are directed at research on improving the understanding of electrochemical engineering principles, corrosion of battery components, surface analysis of electrodes, and electrocatalysis.

## A. ALKALINE CELLS

Zinc is often used as the negative electrode in alkaline cells, and it is this electrode that typically limits the lifetime of these cells. Efforts are underway to identify cell components that will improve the cycle-life performance of the Zn electrode.

### Zinc Electrode Studies

*E.J. Cairns and F.R. McLarnon (Lawrence Berkeley Laboratory)*

The purpose of this research is to study the behavior of electrodes used in secondary batteries and fuel cells, and to investigate practical means for improving their performance and lifetime. Systems of current interest include ambient-temperature rechargeable cells with Zn electrodes: Zn/air, Zn/NiOOH, Zn/AgO, $Zn/Cl_2$, $Zn/Br_2$, and $Zn/Fe(CN)_6^{-3}$.

Micro-electrodes are being used to investigate chemical and transport processes that occur in secondary porous Zn electrodes. The potentials of Zn and Cd micro-electrodes are monitored as the porous electrode is charged and discharged. Examples of Zn micro-electrode data obtained in 30 wt% KOH electrolyte are shown in Fig. 4. Local KOH and $K_2Zn(OH)_4$ molalities were calculated from the $\mu$-electrode potentials, and significant potential gradients were measured at the edge of the electrode during both charge and discharge. There were large changes in the $Zn(OH)_4^{2-}$ concentration during charge and discharge, but the $OH^-$ concentration remained nearly constant.

Three factors under investigation for improving Zn/NiOOH cell cycle-life performance are: 1) electrolyte composition, 2) electrode composition, and 3) charging method. A 15 wt% KOH-15 wt% KF electrolyte was used with electrodes containing 25 to 40 mol% $Ca(OH)_2$, where the $Ca(OH)_2$ is substituted for an equivalent amount of ZnO. Three types of charging methods were successfully employed with these cells: constant-current, constant-current/voltage-limited, and pulsed-current/voltage-limited. The last two methods are preferred because they avoid high overpotentials during charge. A cell employing KF-KOH electrolyte, a Zn-Ca electrode, and a specific pulse-charging regimen (30-ms on/90-ms off, 8 $mA/cm^2$ peak current density) with a 1.95 V cell cut-off voltage has achieved 465 deep-discharge cycles and still maintained 80% of its original capacity! *In situ* X-ray examinations revealed a negative electrode with a slowly-changing mottled appearance against a uniform background attributed to a calcium zincate compound. The NiOOH electrodes for this cell dropped to 80% of their original capacity by cycle 435 and were replaced. Other tests demon-

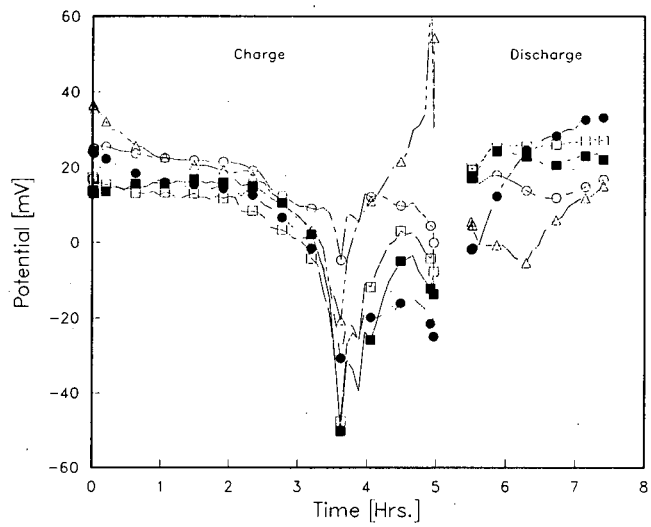


**Figure 4.** Zn micro-electrode potentials during the charge and discharge of a Zn porous electrode in 30 wt% KOH at cycle no. 52. Charge current is 0.1248 A, and discharge current is 0.312 A. Symbols indicate the distance of the micro-electrode from the edge of the porous electrode as follows (a negative value indicates that the probe electrode is in the electrolyte space between the cell wall and the edge of the porous electrode): ■, -.75 mm; □, +.5 mm; •, +2.5 mm; ○, +6.5 mm; Δ, +35.0 mm. (XBL 871-89)

strated that up to 20% of the Zn transfers from the negative electrode to the NiOOH electrode early in cell life. This phenomenon may contribute to the decline of the NiOOH electrode capacity in long-lived cells. A factorial experimental design has been developed to further investigate interactive effects among the three factors under study.

Studies of the electrochemical kinetics of Zn dissolution and deposition have continued. Problems arose using 1-mm Zn disc electrodes due to the low currents involved, so larger electrodes were used. Experiments using 5- to 25-ms pulses were carried out, and the potential step results indicate exchange current densities of 0.75 to 1.0 $mA/cm^2$.

Open-circuit potentials of the NiOOH electrode were measured as a function of state of charge. Four discharge potential-capacity plots were obtained, all showing a similar shape. A multiple-point least-squares method will be used to fit the data for use in a mathematical model of the Zn/KOH/NiOOH cell.

PUBLICATION

1. M.J. Isaacson, E.J. Cairns and F.R. McLarnon (1986), "Activity Coefficients in Concentrated Potassium Hydroxide-Potassium Zincate Electrolytes," *36th Meeting of the International Society of Electrochemistry,* Salamanca, Spain, Paper No. 12080.

## Stable Ionic Polymers for Electrochemical Applications

*C. Arnold and R. Assink (Sandia National Laboratories)*

There is a continuing need for chemically stable, ion-conductive polymers for electrochemical applications. Examples of such applications include battery membranes, solid polymeric electrolytes, and electrode coatings. The purpose of this project is twofold: 1) synthesize and evaluate oxidatively stable ionic polymers, and 2) establish structure/stability relationships and degradation mechanisms by studying the aging of selected model compounds.

*Membrane Synthesis.* Synthesis efforts were focused on polyphenylene (PP), an example of a catenated aromatic polymer, and poly($\alpha$-methylstyrene) (PMS), an example of an aromatic vinyl polymer with no tertiary hydrogens. These polymers were selected for their inherent chemical stability and because the low molecular weights of their repeat units permit the high ion-exchange capacities needed to achieve high conductivities. Polyphenylene was prepared by oxidative coupling of benzene with stoichiometric amounts of either $FeCl_3$ and $H_2O$ or $AlCl_3$ and $CuCl_2$. Sulfonation of PP and commercial PMS was carried out with either fuming $H_2SO_4$ or a complex of 2 moles $SO_3$ and 1 mole $(C_2H_5)_3PO_4$.

Sulfonated polyphenylene (SPP) was only partially soluble in $H_2O$ and other solvents; consequently its fabrication into films was not feasible. Although sulfonated poly($\alpha$-methylstyrene) (SPMS) was soluble in $H_2O$ and could be cast into films, the films were mechanically weak and of little use as membranes. Mechanically strong membranes were made from blends of SSP and/or SPMS with sulfonated polysulfones. These blended membranes exhibited very low area resistivities in a strong base and were non-permeable to electrolytes such as ferricyanide. These findings demonstrate the feasibility of achieving high conductivities and selectivities by blending materials having high ion-exchange capacity and poor mechanical properties with materials having low ion-exchange capacities and good mechanical properties.

*Structure/Stability Relationships.* Earlier studies have shown that the graft of a radiatively grafted membrane often degrades rapidly in an oxidizing environment. The degradation of the active site has tentatively been attributed to the presence of tertiary hydrogens which are known to be particularly susceptible to oxidative attack. In this study the effect of replacing the tertiary hydrogen by a methyl group in a model compound was evaluated. The results suggest that membrane stability can be substantially increased by elimination of tertiary hydrogens.

A membrane of 4-potassium-t-butylbenzene sulfonate was prepared by sulfonation of t-butylbenzene with fuming $H_2SO_4$ followed by neutralization with $K_2CO_3$. Isopropylbenzene-4-sulfonic acid was prepared via sulfonation of isopropylbenzene using a 2/1 complex of $SO_3$ and $(C_2H_5)_3PO_4$ dissolved in 1,2-dichloroethane. Stability was determined by exposure to a saturated solution of $K_3Fe(CN)_6$ in 5 N NaOH at 50°C for various periods of time. This solution was chosen because it is a strong oxidizing agent. Degradation products were identified by proton-decoupled $^{13}C$ NMR at 50.16 Mz.

The $^{13}C$ NMR spectra of sulfonate isopropylbenzene and t-butylbenzene established that sulfonation occurs primarily in the para position. Several degradation products were evident in the spectra of these monomers after they had been aged. The solutions of both model compounds had resonances corresponding to carboxylic acid and carbons next to an alcohol group. In addition, the sulfonated isopro-

pylbenzene spectrum had several peaks corresponding to various aliphatic carbons. It was obvious from the relative intensities of the degradation product peaks that the isopropylbenzene derivative had experienced much more degradation than did the t-butylbenzene derivative. Since the only difference in their structure is the replacement of a tertiary hydrogen by a methyl group, it is concluded that a similar substitution in the grafting monomer of radiatively grafted membranes may result in increased chemical stability.

# B. ZINC/HALOGEN CELLS

Flowing electrolytes are used in Zn/halogen cells to promote the transport of $Zn^{++}$ across the cell and to remove halogen as the cell is charged. The cell performance is limited by the tendency of the electrodeposited Zn to assume unwanted shapes, and efforts are aimed at understanding the complex phenomenon that control the Zn electrode morphology.

## Surface Morphology of Metals in Electrodeposition

*C.W. Tobias (Lawrence Berkeley Laboratory)*

The objective of this project is to gain understanding of the partial processes and their interactions involved in the electrodeposition and electrodissolution of metals. Of particular interest is the influence of hydrodynamic flow on electrocrystallization, and the distribution of charge-transfer rates on advancing and receding metal profiles, as determined by the electric and concentration fields in the solution, and by the kinetics of the charge-transfer reaction. Control of the morphology of metallic deposits has been traditionally effected by addition agents that interfere with the crystallization process. In energy-storage applications, however, other means may have to be employed for the control of morphology.

In a study of the micromorphology and current efficiency of Zn electrodeposited from flowing, acidic chloride solutions, the effects of six variable were examined: flow rate, current density, $Zn^{++}$ and $H^+$ concentrations, concentrations of Ni, Fe and Cd impurity ions, and the nature of the substrate. The development of micromorphology was studied *in situ* by means of videomicrography and *ex situ* by means of scanning electron microscopy (SEM). This investigation focused on the formation of grooved deposits, which are found under a wide range of deposition conditions. The major conclusions from this study are: (i) the most important variable determining whether grooved deposits form is the interfacial concentration; (ii) large protrusions orient themselves parallel to the flow direction with the orientation starting upstream and progressing downstream; (iii) large protrusions become ridges due to growth of the highest current density regions of the electrode under mass transport control. The current efficiency was measured using EDTA titration and weight measurements. The fraction of the current taken by Zn deposition increased with Zn concentration, ranging up to 100%, and decreased with pH. The efficiency of Zn deposition was affected by the flow rate and the substrate employed. Impurities lowered the current efficiency.

Procedures have been developed for the preparation of a micropatterned electrode to be used in the study of electrocrystallization. Using microphotolithography, in conjunction with evaporation and pulse electrodeposition of thin films, a set of artificially roughened electrodes with hemispherical surface features 5 $\mu$ in diameter was developed. Electrodes with different orientations and separations of protrusions will be used to study the interaction of growth centers and the genesis of striations. Voltammetric studies were conducted to determine the material best suited as substrate for the micropatterned electrode. Gold, platinum and various carbon surfaces were evaluated for Zn nucleation density and $H_2$ overpotential. Surface homogeneity was examined by both light and SEM. Gold was determined to possess the best combination of material properties: chemical inertness, low melting point, and a high work function allowing underpotential deposition of Zn which reduces the rate of $H_2$ evolution.

Stripping coulometry was employed to determine Zn limiting currents and evaluate effective diffusion coefficients in concentrated $ZnCl_2$ solutions. Although the method worked well for dilute $ZnCl_2$ and $CuSO_4$ solutions, it failed at higher current densities; the emergence of surface roughness obscured actual limiting current plateaus.

PUBLICATIONS


1. D.P. Sutija, R.H. Muller, and C.W. Tobias (1986), "Development of a Micropatterned Electrode for Studies of Zinc Electrodeposition," (M.S. Thesis), LBL-22576.
2. L. McVay, R.H. Muller and C.W. Tobias (1986), "Studies of Micromorphology and Current Efficiency of Zinc Electrodeposited

from Flowing Electrolytes," (M.S. Thesis), LBL-21492.

## Dendritic Zinc Deposition from Flowing Zinc Halide Solutions

*J.R. Selman (Illinois Institute of Technology)*

The objectives of this project are to investigate the formation and growth rates of dendritic or nodular deposits at Zn electrodes in flowing acidic halide solutions by experimental and analytical methods. The effect of convection on the growth rate and the influence of solution chemistry (speciation) on the kinetics and mass-transfer characteristics of the deposition process are focal points of this research.

The kinetics of Zn dissolution in brominated $ZnBr_2$ have been studied by a rotating hemispherical electrode (RHE). The corrosion potential-current relationships for different $ZnBr_2$ concentrations (0.05-0.35 M) were measured and analyzed. A corrosion mechanism with parallel chemical/ electrochemical reactions:

$$Zn \rightarrow Zn^{+2} + 2e^-$$

$$Br_2 + 2e^- \rightarrow 2Br^-$$

$$Zn + Br_2 \xrightarrow{k} Zn^{++} + 2Br^-$$

was shown to fit the experimental results presented in Fig. 5. The dashed lines plotted in this figure are obtained by a least-square non-linear parameter estimation procedure (simplex method). This analysis leads to the following conclusions:

1. The exchange current density for Zn dissolution (assuming first-order kinetics) is ~20 mA/cm$^2$.
2. The chemical reaction path is dominant at high bromide concentration where $Br^-$ is mostly complexed to form $Br_3^-$. This suggests that the $Br_3^-$ is the reacting species in the parallel chemical reaction.
3. The dominance of the chemical reaction (in solutions containing excess of $Br^-$) suggests that Zn corrosion is appreciable even under cathodic protection. Shown in Fig. 6 are SEM photographs of Zn deposited from solutions containing $Br_2$ and without $Br_2$. In the presence of $Br_2$, the nodules formed tend to be smaller and flatter. This observation also qualitatively confirms the mechanism proposed above.

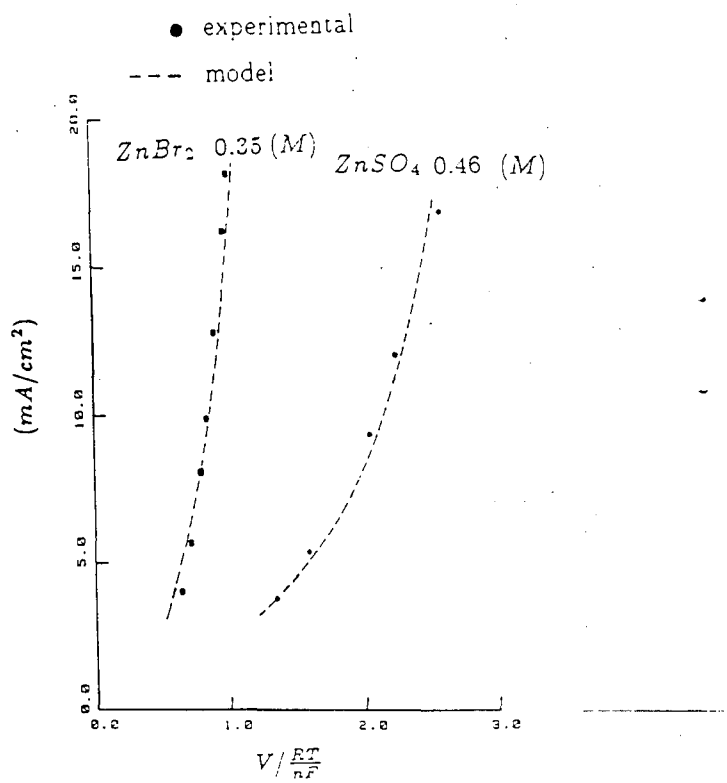


**Figure 5.** Typical corrosion current-potential response in different zinc bromide concentrations and in zinc sulfate solution.

Morphological studies of Zn deposited from 0.2 or 0.8 M $ZnBr_2$ solutions under well-defined convection conditions (RHE) were initiated. The effect of charging methods (DC vs periodic current reversal (PCR)), and of KCl and $Br_2$ as additives are of special interest. The results can be summarized as follows:

1. Charging methods and KCl additions have no apparent effect on the size distribution and crystal structure of the nodules. However, flow lines are visible to the naked eye, except in the case of PCR charging.
2. The presence of $Br_2$ resulted in smaller and flatter nodules, presumably due to chemical attack.
3. The addition of 100 ppm of Tween 60 surfactant caused significant change in structure and made the Zn morphology become wool-like. Under prolonged deposition (3 h at 80 mA/cm$^2$), flow lines of two-dimensional protrusions become visible.

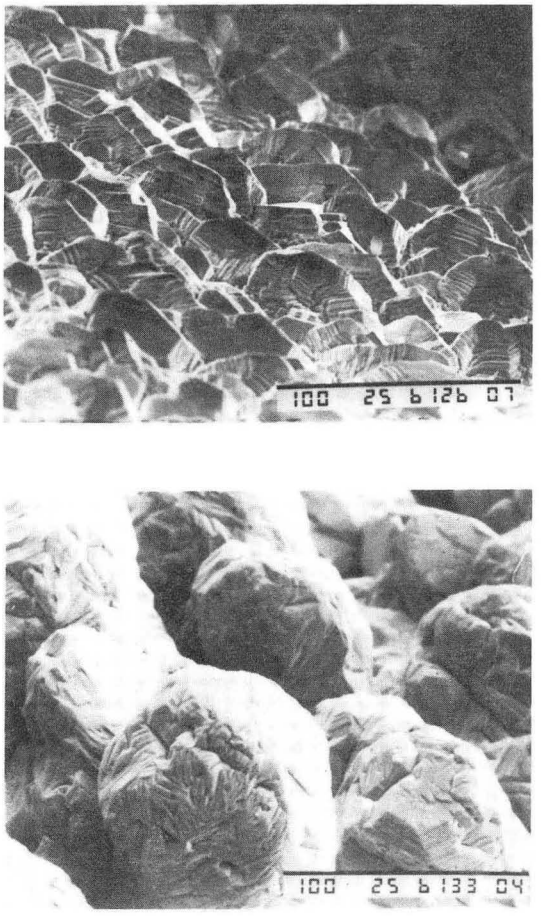

**Figure 6.** SEM photographs of Zn deposits at magnification of 500X. The total loading for both photographs is 75 mA-hr/cm$^2$. The operation conditions for the upper photograph are $ZnBr_2$ = 0.2 M, $\omega$ = 1000 rpm, $C_{Br_2}$ = 10.5 mM, pH = 2.9; and $ZnBr_2$ = 0.8 M, $\omega$ = 1000 rpm, $C_{Br_2}$ = 0 mM, pH = 5.1 for the lower photograph.

KCl were determined from polarographic measurements. The results indicate that Zn-halogen complexes are influencing the migration flux of the reacting species. The effective diffusivities exhibit a minimum at a Cl/Zn ratio of ~3.5 (Fig. 7). A speciation analysis shows that four species ($Zn^{++}$, $ZnCl^+$, $ZnCl_3^-$, $ZnCl_4^=$) are present in varying amounts in the concentration ranges studied. Proton NMR experiments performed on several solutions confirm this behavior.

A computer analysis was undertaken to model the transport of species to the electrode and to subtract the migration effect of the Zn-halogen complexes. A parameter estimation program was used to obtain ionic diffusivities of the Zn species. Corrected diffusivities were then calculated from the migration-corrected experimental currents. The

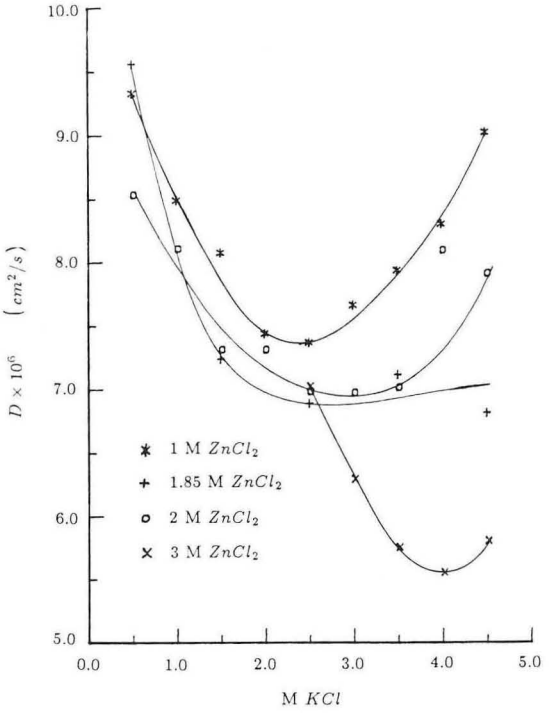


**Figure 7.** Effective diffusivity vs M KCl.

results are in general agreement with a physical interpretation of how diffusivity changes with $ZnCl_2$ and KCl concentrations.

## PUBLICATIONS


1. S.L. Chiu and J.R. Selman (1986), "Corrosion of Zinc by Bromine Under Flow Conditions," *presented at the AIChE Annual Meeting,* Miami Beach, FL.
2. S.L. Chiu and J.R. Selman (1986), "Calculation of Corrosion Rate Distribution of a Rotating Metal Hemisphere," *presented at the AIChE Annual Meeting,* Miami Beach, FL.


# Zinc Electrode Morphology in Acid Electrolytes


*J. McBreen (Brookhaven National Laboratory)*


The purpose of this work is to elucidate the factors, other than mass transport, affecting the kinetics and morphology of Zn electrocrystallization in $ZnBr_2$ and $ZnCl_2$ electrolytes. A further objective is to devise methods to slow the kinetics in $ZnBr_2$ electrolytes, and thereby inhibit dendrite growth and achieve higher capacity densities in $Zn/Br_2$ batteries.

The following research areas were investigated in 1986: (i) investigation of Zn deposition kinetics in modified $ZnBr_2$ electrolytes, (ii) Extended X-ray absorption fine structure (EXAFS) studies of Zn halide electrolytes and, (iii) exploratory work on the use of EXAFS as an *in situ* technique for investigating processes in battery electrodes.

*Modified Zinc Bromide Electrolytes.* Research with modified $ZnBr_2$ electrolytes was extended to include additions of various alkaline and alkaline earth bromides in stoichiometric amounts, as well as $NH_4Br$, were investigated. The Zn deposition and stripping processes on glassy carbon were investigated in these electrolytes using cyclic voltammetry and the potential-step method. The addition of these bromide salts slowed the kinetics in $ZnBr_2$ electrolytes; this effect is mainly related to the $Br^-/Zn^{++}$ ratio. There are secondary effects with $Ca^{++}$ and $Cs^+$ that may be due to the water affinity of $Ca^{++}$ or specific absorption of $Cs^+$. In all of these highly purified electrolytes, including pure $ZnBr_2$, the deposition kinetics were always faster on the second sweep of the cyclic voltammogram, or the second potential step into the Zn deposition region. This effect is believed to be due to an unidentified surface species that remains after the stripping process, which could be eliminated by mechanical polishing. In electrolytes with $NH_4Br$, the effect did not appear. The addition of $NH_4Br$ did not appreciably slow the kinetics, but was beneficial in the stripping process.

*EXAFS Studies of Zinc Electrolytes.* EXAFS studies were carried out on several Zn-containing electrolytes, including zincate ions in 8.4 M KOH, 1 M $ZnBr_2$ with various additions of HBr, and 3 M $ZnBr_2$ with additions of $AlBr_3$. Pure electrolytes (e.g., 1 M $ZnBr_2$ or 3 M $ZnBr_2$) contain several species that have not been identified. Electrolytes with high $Br^-/Zn^{++}$ ratios (e.g., 1 M $ZnBr_2$ + 6 M HBr or 3 M $ZnBr_2$ + 3 M $AlBr_3$) contain tetrabromide ions exclusively. The Zn-Br distance is 2.4 Å in the tetrabromide complex. At intermediate ratios (e.g., 1 M $ZnBr_2$ + 3 M HBr), the Zn ions are coordinated with two water molecules and two bromide ions. Thus, the tetrahedral coordination is maintained. For these complexes the Zn-Br distance is 2.37 Å and the Zn-O distance is 1.83 Å. No evidence was found for tribromide complexes, which suggests that either these complexes do not exist, or they occur only in a narrow composition range. The fast kinetics observed with electrolytes containing low $Br^-/Zn^{++}$ ratios may be due to the waters of hydration permitting close approach of $Zn^{++}$ to the surface. The tetrabromide "cage" inhibits this close approach at higher $Br^-/Zn^{++}$ ratios. Analysis of the zincate data confirm the presence of tetrahedral $Zn(OH)_4^=$ species with a Zn-O distance distance of 1.77 Å. So far no evidence of dimerization or chain formation has been found.

*In Situ EXAFS Studies. In situ* EXAFS of Zn cells presented some problems because of the high solubility of Zn in the electrolyte, which complicates data analysis. Experimental cells were constructed, and the $Ni(OH)_2/NiOOH$ reaction using plastic-bonded nickel oxide electrodes was studied. In this case there is no soluble Ni species in the electrolyte, so data analysis was simple. The results show that *in situ* EXAFS is feasible in cells resembling actual battery cells, and that structural information can be obtained on electrodes during charge and discharge.

PUBLICATIONS


1. J. McBreen and E. Gannon (1986), "Kinetics of Zinc Deposition on Zinc Single Crystals," *J. Electrochem. Soc.* **133,** 2047.
2. J. McBreen, W.E. O'Grady, D. Sayers and C.Y. Yang (1986), "Electrode Kinetics and Electrolyte Structure in $ZnBr_2$: An EXAFS Study," *Extended Abstracts of the 169th Meeting of the Electrochemical Society,* p. 834.
3. J. McBreen, W.E. O'Grady and D. Sayers (1986), "EXAFS Studies of Topochemical Reactions," *Extended Abstracts of the 170th Meeting of the Electrochemical Society,* p. 151.
4. J. McBreen, W.E. O'Grady, K.I. Pandaya, R.W. Hoffman and D.E. Sayers (1986), "An EXAFS Study of the Nickel Oxide Electrode," BNL-38704.


## Transport in Aqueous Battery Systems


*D.G. Miller and J.A. Rard (Lawrence Livermore National Laboratory)*


The aim of this research is to determine mutual diffusion coefficients and osmotic/activity coefficients required for interpreting and modeling the zinc/chlorine batteries (of which other properties have been studied by EDA and its subcontractors). Consequently, LLNL has measured mutual diffusion and density data for aqueous $ZnCl_2$ and $ZnCl_2$-KCl mixtures, and osmotic/activity coefficients for aqueous $ZnCl_2$ at 25°C.

Isopiestic measurements for aqueous $ZnCl_2$ were completed in 1986. Twenty-eight points were measured this year, and the completed data now extend from 0.31358 to 13.134 mol/kg. A detailed com-

parison is being made of the isopiestic data to published isopiestic and emf data. Several conclusions have been reached: (i) previous isopiestic data is in fairly good agreement with LLNL results, to within 0.1 to 0.5%, up to at least 11 mol/kg; (ii) there are a number of emf studies that extend to 12 mol/kg. Emf data only to about 1.0 mol/kg are mutually consistent, and these emf results are also in excellent agreement with isopiestic data. However, a detailed comparison of emfs at higher concentration indicates large differences.

PUBLICATION

1. D.G. Miller, A.W. Ting and J.A. Rard (1986), "Mutual Diffusion Coefficients of Various $ZnCl_2$ (0.5 M)-KCl-$H_2O$ Mixtures at 298.15 K by Rayleigh Interferometry," UCRL-95823.

# C. COMPONENTS FOR ALKALI/SULFUR CELLS

Superior alternatives to the $\beta''$-$Al_2O_3$ ceramic electrolyte and high-temperature sulfur-polysulfide electrode used in Na/S cells, and stable components for Li/S cells are under investigation.

## Low-Temperature Beta″-Alumina Cell

*L.C. DeJonghe (Lawrence Berkeley Laboratory)*

The present focus of this program is to investigate the properties of a novel class of organosulfur positive electrodes and to characterize their behavior in intermediate-temperature high-specific-energy cells. Through determination of the mass transport and electrode kinetic properties of the organosulfur melts, insight can be gained as to the behavior of the sodium/organosulfur cells.

Selected members of a class of novel organosulfur compounds have been studied. These compounds are based on the reversible oxidation of alkali metal thio salts to the corresponding disulfide. Of the many thio/disulfide compounds to choose from, efforts have largely centered on the dithiocarbamate/(thiuram disulfide) system. The overall cell reaction for this couple is:

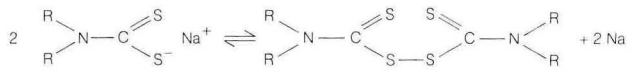

where R is an organic functional group ($C_2H_5$, $CH_3O$, $C_6H_5$, etc.).

The sodium dithiocarbamates are characterized by their low melting points (due to strong resonance stabilization of the thio anion) and reversible oxidation to the thiuram disulfide. Depending on the electronic and/or steric influence of the R groups attached to the nitrogen atom, the Na salts can melt at surprisingly low temperatures (50-150°C). The oxidized species, the thiuram disulfides, $(R_2NCSS)_2$, melt at even lower temperatures (25-100°C), and are easily recrystallized to high purity. Fortunately, the dithiocarbamate salts are also very soluble in the corresponding disulfides, allowing an operating temperature somewhat below the melting point of the salt. There are many thiuram disulfides and related compounds which may have merit as positive electrodes; of these LBL has focused on tetraethylthiuram disulfide (TETD).

The theoretical specific energy of a Na/TETD cell is 360 Wh/kg, and practical cells have been constructed with a maximum specific energy exceeding 110 Wh/kg. The TETD compound melts at ~74°C, while the anhydrous sodium diethyldithiocarbamate (NaDEDC) salt has a melting point of ~145°C. Studies of the ionic conductivity of NaDEDC in molten TETD have been performed as a function of both temperature and salt concentration, indicating reasonable equivalent conductivity in the melt (evidence of ion pairing) which can be further increased by the small addition of a high-dielectric solvent.

More than 30 galvanic cells of the type Na/TETD have been assembled and tested to date. The cell seals were simple since commercially available epoxies were found suitable for this purpose. These epoxies were quite resistant to Na attack at the operating temperature of the cell (120-130°C) but they began to show signs of softening on prolonged exposure to the positive electrode. This was corrected by the use of a second silicone rubber seal which is resistant to the organosulfur melt. Preliminary corrosion studies were also conducted which indicated that Al is not attacked by the positive electrode, even under slightly anodic conditions. This has been supported by the lack of visual signs of corrosion of the Al cell container after prolonged cell testing. Graphite felt seemed to perform better as a current collector than reticulated vitreous carbon. The internal resistance of these cells typically ranges from 0.5 to 2.0 ohms (0.025-0.10 ohms/cm$^2$ electrolyte area) which varies somewhat with state of charge. Results from ionic conductivity studies indicate that the cell internal resistance may be further reduced by the addition of a small amount of sol-

vent. Peak discharge rates of over 100 mA/cm$^2$ (1 min at 1 V) have been demonstrated, as well as 25 mA/cm$^2$ at 1.5 V nominal for 8% of available capacity. However, for charge/discharge cycling to close to available capacity, the Na/TETD cells seem to perform best at a current density of 5 mA/cm$^2$.

PUBLICATIONS


1. L.C. DeJonghe (1986), "Degradation in Sodium-Beta″ Alumina Solid Electrolytes," *J. Electrochem. Soc.* **133,** 355.
2. D.C. Hitchcock and L.C. DeJonghe (1986), "Oxygen Depletion and Slow Crack Growth in Sodium-Beta″ Alumina Solid Electrolytes," *J. Electrochem. Soc.* **133,** 6.
3. D. Olson and L.C. DeJonghe (1986), "Zirconia Toughened Sodium Beta″ Alumina Solid Electrolyte," *J. Mat. Sci.* **21,** 4221.
4. D.C. Hitchcock, C. Mailhe and L.C. DeJonghe (1986), "Electrochemical Cells Utilizing Molten Alkali Metal Electrode Reactant," *U.S. Patent 4,609,596.*


## Mathematical Modeling of the Sodium/Sulfur Cell


*E.J. Cairns and F.R. McLarnon (Lawrence Berkeley Laboratory)*


A mathematical model of the sulfur electrode in Na/S cells has been developed. It consists of a set of partial differential equations which describes the processes of diffusion, migration, and convection occurring during the charge/discharge of such a cell. The solution to the relevant equations will be effected on a digital computer via implementation of the Newman-IAD method for the solution of two-dimensional partial differential equations. The results of this modeling will be compared with data from an operating cell which has been designed to allow measurement of ionic potentials throughout the sulfur electrode. An attempt will be made to predict the effect of various charge-discharge regimens upon cell operation.

PUBLICATIONS


1. S.A. Naftel, F.R. McLarnon and E.J. Cairns (1986), "Studies of the Sulfur Electrode in Sodium/Sulfur Cells," *Extended Abstracts of the 170th Meeting of the Electrochemical Society,* p. 116.
2. M.L. Smith, J. Winnick, F.R. McLarnon and E.J. Cairns (1986), "Stability of a Vitreous Electrolyte for Possible Use in High-Temperature Lithium/Sulfur Cells," *International Workshop on High-Temperature Molten Salt Batteries,* Argonne National Laboratory Report No. ANL-86-40, p. B-153.
3. J.C. Dobson, E.J. Cairns and F.R. McLarnon (1986), "Voltammetry of Lithium Polysulfides at Metal Electrodes," *J. Electrochem. Soc.* **133,** 1549.
4. J.C. Dobson, E.J. Cairns and F.R. McLarnon (1986), "Voltammetry of Sodium Polysulfides at Metal Electrodes," *J. Electrochem. Soc.* **133,** 2069.
5. J.C. Dobson, E.J. Cairns and F.R. McLarnon (1986), "Corrosion of Some Metals in Sulfur-Polysulfide Melts," LBL-20250, submitted to *Corrosion Science.*


## Electrical Conduction and Corrosion Processes in Fast-Ion Conducting Glasses


*H.L. Tuller (Massachusetts Institute of Technology)*


A major objective of this research program has been to develop glasses that exhibit fast-ion conduction (FIC) in the temperature regime of interest (<350°C) for Li/S batteries, and also possess the physical attributes which eliminate the shortcomings of ceramic components, such as current-blocking grain boundaries, anisotropic ion transport (e.g., in $\beta''$-$Al_2O_3$), high-temperature fabrication and relatively large wall thickness. In particular, attention was focused on the transport, electrochemical, and corrosion-resistant properties of alkali-ion conducting glasses.

The influence of modifiers such as CaO, added to improve stability against alkali attack, on $Li^+$ transport in Li borates was examined. Electrical conductivity, density and transition temperature measurements have been performed on two families of FIC glasses, a Li diborate and a Li metaborate in which 1 to 10 mol% of the Li has been substituted with Ca. It is worth noting that conductivities remain within an order of magnitude of Ca-free glasses in sharp contrast to the known depressing effect of Ca additions on alkali-ion transport in alkali silicate glasses. The fact that the Ca-containing Li borate glasses remain highly conductive is of technological impor-

tance since CaO additions are believed to improve durability in contact with Li metal or its alloys.

The decrease in conductivity with CaO additions was found to be due to an increase in activation energy. While the molar volume is only slightly influenced, $T_g$ is observed to be substantially enhanced over that of a corresponding binary glass of like O/B ratio. A preliminary interpretation is that Ca additions serve to strengthen the glass structure which results in lower conductivities and higher activation energies.

The role of the mobile ion radius on conduction and glass structure was examined. Earlier, it was found that K dilates the structure to give reasonably high $K^+$ conductivity above 200°C. The addition of KCl to the K borate glasses generally enhanced transport but not necessarily in the manner observed previously for the Li and Na borate systems. At a fixed O/B ratio of 1.7, the $K^+$ conductivity increased monotonically with increasing chloride content, but in contrast to Li and Na borate glasses, the enhancement in conductivity appears to be tied to an enhancement in the pre-exponential term rather than the activation energy which appears to be about 0.9 eV. Chlorine has a dilating effect on the structure even for the larger K cation. On the other hand, while $T_g$ initially drops with increasing KCl content, it levels off after the 15% value in contrast to observations on Li and Na glasses where $T_g$ drops systematically with Cl additions. It appears that, at least in the case of the K borate glasses, both free volume and stiffness of the structure (related to $T_g$) play important and competing roles in controlling transport processes in high Cl-containing glasses. These features are of interest for further study.

## PUBLICATIONS


1. M.W. Barsoum and H.L. Tuller (1986), "*In-Situ* Determination of the Kinetics of Reaction between Lithium and Fast Ion Conducting Lithium Borate Glasses," *Solid State Ionics,* **18 & 19,** 388.
2. F.A. Fusco, H.L. Tuller and D.R. Uhlmann (1986), "Structure-Transport Relationships in Fast Ion Conducting Alkali Borate Glasses," *Defect Properties and Processing of High-Technology Nonmetallic Materials,* Y. Chen, W.D. Kingery and R.J. Stokes, eds., Materials Research Society, Pittsburgh, PA, p. 251.


# Glass Electrolytes and Advanced Cell Concepts


*I.D. Bloom (Argonne National Laboratory)*


The objective of this research is to develop a glass that has low resistivity (100 ohm-cm at 300°C), is chemically stable in the hostile Na/S cell environment, and is easily fabricable at low cost. A novel glass electrolyte was selected (composition in mol%, 42 $Na_2O$, 8 $Al_2O_3$, 5 $ZrO_2$, and 45 $SiO_2$) for further testing in Na/S cells because of its high ionic conductivity (7.1 X $10^{-3}$ $ohm^{-1}cm^{-1}$ at 300°C) and its chemical stability (comparable to those of the Dow borate glass and $\beta''$-alumina).

Glass electrolytes of sufficient size and quantity for cell tests were prepared by hand directly from the melt at ~1000°C. However, under cycling conditions, cells of 0.1 to 0.8 Ah would fail routinely, after a few cycles. To determine the cause for the rapid cell failures, the glass electrolytes were examined for sources of stress. The glass electrolyte tubes, before and after annealing, showed no signs of internal stress under a polariscope. Furthermore, microscopic examination of a cast disk of ANL glass under back-scatter-electron imaging (30,000X) showed no sign of phase separation. The analysis indicates that failure of these cells is most likely due to water-vapor damage on the glass tube surface, which most likely occurs during the drawing process or subsequent handling at room temperature.

The process under development for the fabrication of precision glass tubes will take into account the physical and chemical properties of the glass. It has been found that the minimum temperature for molten glass stability is ~1350°C. At lower temperatures, such as 1200°C, $Na_2ZrSiO_5$ precipitates as prismatic crystals.

To demonstrate, in part, the electrochemical life of the ANL glass, single-element cells have been tested. A membrane of ANL glass (1-2 mm thick) is attached to the end of an $Al_2O_3$ tube (50-mm long, 3.2-mm od, 1.52-mm id), in which a mixture of sulfur and graphite (10 wt%) is added. A molybdenum wire (0.25 mm) was inserted to serve as the current collector. A glass or Swagelok-based seal was used to contain the sulfur electrode. In tests of small-scale cells (1-3 mAh capacity), no evidence has been found

to indicate a chemical problem native to the glass electrolyte. Cells have been successfully cycled at 3 to 6 $mA/cm^2$ for 36 to 40 cycles (10-20% DOD) before a capacity loss was observed.

The results of these experiments suggest that most of the mechanical problems encountered in the small-scale cell assembly can readily be solved. Thus far, no signs have been found of a chemical or physical problem intrinsic to the glass. Better facilities for glass-structure fabrication are needed to obtain more meaningful test of the electrochemical life of the glass. Once electrochemical life has been demonstrated, further studies are needed for scale-up of tubing manufacture, development of seal and housing, and design of electrode/current collector. Also, studies of freeze-thaw cycling and electrolyte failure containment are needed and efforts to study some of these problems have been initiated.

An ANL glass-membrane sensor/reference electrode has been developed to measure S and Na activity in research and engineering cells for the first time. The membrane electrode provides chemical isolation of the reference electrolyte, thereby allowing measurement of chemical and electrochemical parameters in difficult systems and at temperatures up to 700°C. Concentration and potential distributions can be measured with the resolution of 1 mm in molten-salt cells and in certain molten-metal systems that were previously inaccessible to these investigations.

PUBLICATION

1. G.H. Kucera, I. Bloom and M.F. Roche (1986), "Ionic Conductivities and Glass Transition Temperatures of $Na_2O$-$ZrO_2$-$Al_2O_3$-$SiO_2$ Glasses," *J. Electrochem. Soc.* **133,** 1996.

## New Battery Materials

*R.A. Huggins (Stanford University)*

The objective of this program is to develop materials for high-performance secondary batteries. The emphasis of the research is to understand the important structural, thermodynamic and kinetic properties of these materials which influence their behavior as cell components. The relationships between fundamental thermodynamic and kinetic parameters, e.g., phase equilibria, Gibbs free energy values and chemical diffusion within solid phases, and the microscopic and macroscopic electrochemical phenomena of the new battery materials are investigated in this project.

*Negative Electrode Materials.* Work under this program on negative electrodes has focused on the investigation of Li alloys which undergo displacement reactions, and have Li activities less than unity. It has been found that solid-state diffusion and heterogeneous reactions are rapid in a number of Li-alloy systems at room temperature, a very positive indication for their potential use in practical systems.

Work has continued on the characterization of several Li binary alloys, in particular Li-Cd, Li-Zn and Li-Sn, enabling suitable pairs of alloys to be considered for use in a mixed-conducting matrix electrode. Such an electrode has been constructed containing a finely dispersed reactant, in this case $Li_xCd$ ($1 < x < 3$), in a solid mixed-conducting matrix, i.e., $Li_{22}Sn_5$. The matrix material is a good electronic conductor and has a high diffusion coefficient for Li, $\sim 10^{-7}$ $cm^2/s$. Furthermore, it is stable towards the reactant material (i.e., the three phases $Li_{22}Sn_5$, LiCd and $Li_3Cd$ lie at the corners of a tie triangle on the Li-Cd-Sn ternary phase diagram) and is stable at the potential at which the reactant is operated, 55 mV for the two-phase LiCd-$Li_3Cd$ plateau. A typical composite electrode containing equimolar amounts of Cd and Sn has been cycled repeatedly at ~55 mV vs pure Li, using a current density of 0.1 $mA/cm^2$.

*Positive Electrode Materials.* Progress has been made in the study of the room-temperature electrochemical behavior of ternary-phase oxide bronzes in the Li-Mo-O system. Only $Li_4Mo_5O_{12}$ has a significant capacity for Li, inserting up to three moles of Li per mole. The Li diffusion coefficient is of the order of $10^{-8}$ $cm^2/s$ at room temperature. Powder X-ray diffraction results suggest that, for the bronzes mentioned above, Li insertion proceeds without major structural rearrangement of the host material. It has been further determined that the electrochemical behavior of $Li_4Mo_5O_{12}$ may be enhanced significantly if it is prepared with an excess of $MoO_2$. This enhancement makes $MoO_2$-rich $Li_4Mo_5O_{12}$ potentially interesting as a positive electrode material in reversible nonaqueous Li batteries. By determining the electrochemical behavior of several compositions in the Li-Mo-O system, a room-temperature ternary phase diagram has been constructed for comparison with the high-temperature (equilibrium) phase diagram. Such a phase diagram, showing the presence of metastable phases, enables the prediction of the room-temperature electrochemical behavior of any composition within the $Li_2O$-$MoO_2$-Mo-Li region.

*The Li-Si-S System.* This system contains structures with parallel chains of edge-sharing tetrahedra found in $SiS_2$. Compositions in the Li-Si-S system, both

crystalline and amorphous, are being considered for use as both positive electrode materials (with suitable dopants to enhance the electronic conductivity) and electrolytes.

The Li-Si-S phase diagram has been determined using a variety of electrochemical methods and powder X-ray diffraction. The Gibbs free energies of formation of $Li_2SiS_3$ and $Li_4SiS_4$ have been calculated from electrochemical data to be -197 and -335 kcal/mol, respectively. Further, the $Li_2S$-$SiS_2$ binary phase diagram has been determined as a function of temperature using differential thermal analysis. Powder X-ray data for $Li_2SiS_3$ and $Li_4SiS_4$ have been indexed for the first time. For $Li_2SiS_3$ the unit cell is orthorhombic with lattice parameters: a = 6.61 Å, b = 11.44 Å and c = 6.50 Å. $Li_4SiS_4$ is also orthorhombic, with lattice parameters: a = 6.88 Å, b = 7.80 Å and c = 6.13 Å. Various glasses in the composition range $Li_4Si_3S_8$-$Li_6Si_2S_7$ have been prepared in graphite-lined quartz tubes and their $Li^+$ conductivities and activation energies were measured using AC impedance spectroscopy.

*Preparation of Thin-Film Electrode and Electrolyte Materials.* The atmospheric-pressure chemical-vapor-deposition (CVD) technique is being used to prepare battery materials. In this technique, a continuous belt carrying the desired substrate is moved under a carefully designed gas-injector system that permits CVD at atmospheric pressure. Impressive uniform and defect-free films of a number of highly reactive materials have been made continuously at temperatures well below their melting points. A special small-scale mock-up of the critical parts of this type of apparatus has been engineered and constructed by Watkins-Johnson Co.

Work on the deposition of $ZrO_2$ has been undertaken as a precursor to various Li-conducting $ZrO_2$ phases. $ZrO_2$ was deposited by the pyrolysis of zirconium n-butoxide at substrate temperatures between 385 and 535°C. The temperature of the chemical source through which the $N_2$ carrier gas was passed was varied from 170 to 215°C. Substrates were primarily single-crystal Si, although deposits have also been made on Ni, Al and Mo.

Work has been initiated on the deposition of $FeS_2$ films using $Fe(CO)_5$ and $H_2S$ as source materials. The feasibility of this method has been demonstrated using a small-scale apparatus at low temperature (~100°C).

# D. CORROSION PROCESSES IN HIGH-TEMPERATURE, HIGH-SULFUR-ACTIVITY MOLTEN SALTS

The aim of these projects is to develop low-cost containers and current-collector materials for use in alkali-sulfur and other molten-salt cells.

## Polysulfide Containment Materials

*J.E. Battles (Argonne National Laboratory)*

During the past 2 to 3 years, the corrosion behavior of 33 metals and alloys in S and $NaS_x$ at 350°C was examined. The objectives of these studies were to obtain a basic understanding of the corrosion reactions and to develop an alloy for use as a positive current collector/container in the Na/S cell. Work on this project has now been completed, and it was concluded that the continued development of new alloys would probably not result in an alloy material of sufficiently low cost, low density, and low corrosion rate to be useful for Na/S cells.

In general, a remarkable difference was found in the corrosion behavior of the metals and alloys in pure S, as opposed to a polysulfide composition of $Na_2S_3$. For most of the metals and alloys studied, corrosion rates were higher in $NaS_x$ than in S. Cr and Ni were the only exceptions, and only with Cr was the corrosion rate markedly lower in $Na_2S_3$ than in S. The corrosion penetration of the metals and alloys after 2500 h of exposure varied by as much as two orders of magnitude between S and $Na_2S_3$.

The principal cause for the higher corrosion rates in $Na_2S_3$ is due to the corrosion-scale composition and morphology. The high basicity of $Na_2S_3$ results in the formation of ternary sodium-metal-sulfides, which are partially soluble in the corrosion medium, e.g., Fe forms $Na_3FeS_3$, Cr forms $NaCrS_2$, and Al forms several different phases depending on the polysulfide composition. Even when a ternary sulfide phase is not formed, the binary metal sulfides often exhibit sufficient solubility in the $Na_2S_3$ to modify the scale morphology, e.g., Ni-based alloys of high Cr content form $NiS_2$, and Al-Mg alloys form MgS.

Based solely on considerations of corrosion resistance, Mo is the only metal or alloy that can be recommended as a positive current collector/ container material for the Na/S cell. Electrochemically dynamic or in-cell testing of selected Ni-based super alloys of high-Cr content might result in an expensive but more easily fabricable container material that is corrosion resistant. If the metal or alloy is used as a substrate for a corrosion-resistant coating, then the best metal or alloy to provide adequate protection against coating defects would be a stainless steel with a composition near to Fe-26Cr-3Mo, such as Ferralium 255.

PUBLICATION

1. A.P. Brown and J.E. Battles (1986), "Corrosion of Nickel-200 and AISI-1008 Steel in Sodium Polysulfides and Sulfur at 350°C," *J. Electrochem. Soc.* **133,** 1321.

## Corrosion Resistant Coatings for High-Temperature High-Sulfur-Activity Applications

*J.R. Selman (Illinois Institute of Technology)*

The refractory compounds of Mo and Ti with N and C possess unique combinations of chemical and physical properties which are well-suited for applications demanding high-temperature corrosion resistance. Besides Mo and Cr, TiN and $Mo_2C$ are possible candidate materials in the form of coherent coatings on a mild steel substrates for current collectors in sulfur-containing secondary batteries. The purpose of this project is to investigate the optimal conditions for producing Mo and $Mo_2C$ coatings by molten-salt electrodeposition and Mo and TiN coatings by chemical vapor deposition (CVD). The corrosion resistance of these coatings in polysulfide melt and in (Li-K)Cl eutectic containing sulfide ions is also determined.

Molybdenum was plated as a dense coating from an all-fluoride bath with additions of alkali molybdate at temperatures between 750 and 800°C. Current densities between 50 and 100 mA/cm$^2$ were found optimal. Film thicknesses of up to 10 $\mu$m were obtained, whose surface morphology showed crystallites of variable sizes.

Molybdenum carbide was plated from a similar bath at 850°C or higher, with alkali carbonate additions as source of carbon. Current densities between 100 and 150 mA/cm$^2$ yielded dense coatings 30- to 40-$\mu$m thick, with superficial crystallites of 1 to 10 $\mu$m in size. A SEM micrograph of a cross-section of such a coating is presented in Fig. 8. The X-ray diffraction confirmed the formation of $\alpha$-$Mo_2C$ with some preferential orientation. The electrolysis conditions for both Mo and $Mo_2C$ are given in Table 1.

The chemical vapor deposition of TiN from a mixture of $TiCl_4(g) + N_2 + H_2$ at a substrate temperature of 915°C resulted in coatings with reduced adhesion due to substrate deformation, which results from the rapid variation in temperature caused by induction heating. Using $NH_3$ as a N source permitted the deposition temperature to be lowered to 600 to 700°C, and permitted coating deposition on Al substrates. However, the relationships between the properties of the coating and the deposition parameters are not well understood. Significant quantities of white solid $NH_4Cl$ and a black, poorly adherent coating on the Al substrate indicated that this system is extremely sensitive to impurities and prone to form by-products. A different approach such as plasma-enhanced CVD appears to be necessary.

The behavior of Mo and $Mo_2C$ coatings in $Na_2S_3$ melt was studied using cyclic voltammetry. Only unimportant differences were observed in the potential range -1.0 to +0.8 V with respect to a $Mo/MoS_2$ reference electrode. In contrast to Mo metal, which in polysulfide melt is covered with a thin black sul-

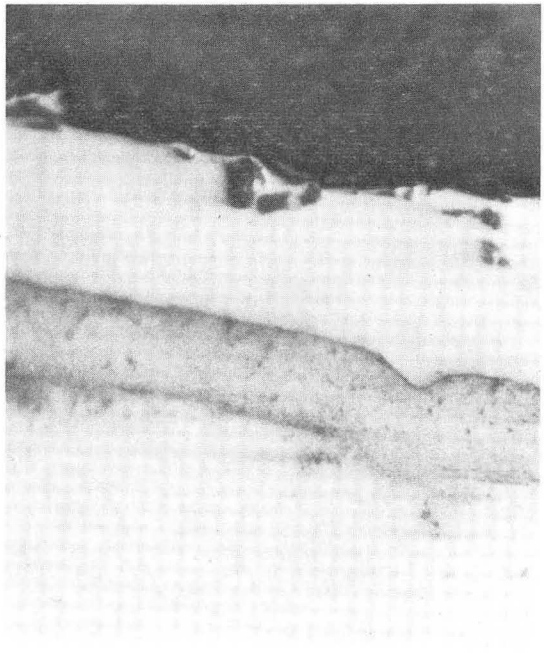

**Figure 8.** Micrograph of a cross-section of $Mo_2C$ after exposure to $Na_2S_4$ melt for ~25 h at 310°C. Sample polarized between -1.0 and +0.6 V.

| Table 1. Electrolysis conditions for Mo and $Mo_2C$ coating deposition. | | |
|---|---|---|
| | Molybdenum | Molybdenum Carbide |
| Bath composition | FLINAK<br>$K_2MoO_4$ (5-7 w/o) | FLINAK<br>$K_2CO_3$ (4-6 w/o)<br>$Na_2MoO_4$ (5-7 w/o) |
| Atmosphere | inert, dry | inert, dry |
| Temperature, °C | 780 | 850 |
| Current density, $mA/cm^2$ | 60 | 150 |
| Current efficiency, % | 22 ($3e^-$) | 45 ($10e^-$)<br>76 ($16e^-$) |
| Deposit | coherent coating | coherent, dense coating |
| Thickness, $\mu m$ | 10 | 30-40 |

fide layer, $Mo_2C$ was not discolored and no variation in weight was observed after more than 24 hours of exposure at 300°C.

In $Na_2S_4$ melt at 310°C, the $Mo_2C$ coating shows a peculiar behavior in the cathodic part of the voltammogram: the principal peak, assigned to the formation of a blocking $Na_2S_2$ film, is associated with a second peak, suggesting a continued reduction to $Na_2S$. After exposure to this melt for more than 24 hours a black color was observed on the surface of the sample. A SEM micrograph showed some dissolution of the sharp edges of $Mo_2C$ grains resulting in a more or less flat area. This action seems not to be extended deeply into the coating. Examination of a cross-section confirmed that a solid, dense coating covered the substrate evenly over some surface imperfections and resisted sulfur attack.

PUBLICATIONS


1. D.C. Topor and J.R. Selman (1986), "Corrosion Resistant Coatings for High-Temperature Sulfur and Sulfide Batteries," *Proceedings of the First International Workshop on High-Temperature Molten Salt Batteries,* Argonne, IL, ANL-86-40, p. C-20.
2. D.C. Topor and J.R. Selman (1986), "Molybdenum and Molybdenum Carbide Coatings for Sodium/Sulfur Batteries," *Extended Abstracts of the 170th Meeting of the Electrochemical Society,* p. 127.


# E. COMPONENTS FOR AMBIENT-TEMPERATURE NONAQUEOUS CELLS

Metal/electrolyte combinations that improve the rechargeability of ambient-temperature nonaqueous cells are under investigation.

## Surface Layers on Battery Materials

*R.H. Muller (Lawrence Berkeley Laboratory)*

The purpose of this work is to provide direct experimental information about formation and properties of surface layers on battery-electrode materials and to find new means for controlling properties that enhance cell performance. Present studies are concerned with anodic oxide formation and the behavior of Li in different ambient-temperature nonaqueous battery electrolytes.

Lithium nitride has been studied as a possible solid-electrolyte interphase between the Li electrode and an organic electrolyte. The $Li/Li_3N$ electrode has been obtained by exposing Li to a pure $N_2$ atmosphere at ambient temperature. This procedure is found to lead to the formation of a porous $Li_3N$ film, resulting from a decrease in the molar volume during the reaction. Mercury porosimetry has shown

that most of the pore radii are less than 25 Å (Fig. 9). The impedance behavior of the $Li/Li_3N$ electrode can be interpreted by a porous-film physical model deduced from a transmission-line electrical model. The slow filling of the micropores of the film and reaction of Li with the electrolyte at the base of the pores are responsible for changes in the impedance and open-circuit potential with time and under cycling.

## PUBLICATIONS


1. J.G. Thevenin and R.H. Muller (1986), "Impedance of Lithium Electrodes in a Propylene Carbonate Electrolyte," LBL-21192.
2. J.G. Thevenin and R.H. Muller (1986), "Study of the $Li/Li_3N$ Electrode in an Organic Electrolyte," LBL-21191.
3. J.G. Thevenin and R.H. Muller (1986), "Study of the Impedance Behavior of the Surface Layer Formed on the Lithium Electrode in Propylene Carbonate-Based Electrolytes," LBL-20660.
4. J.G. Thevenin and R.H. Muller (1986), "The $Li/Li_3N$ Electrode: Study of Its Electrochemical Behavior in an Organic Electrolyte by means of Electrode-Impedance Spectroscopy," LBL-20659.


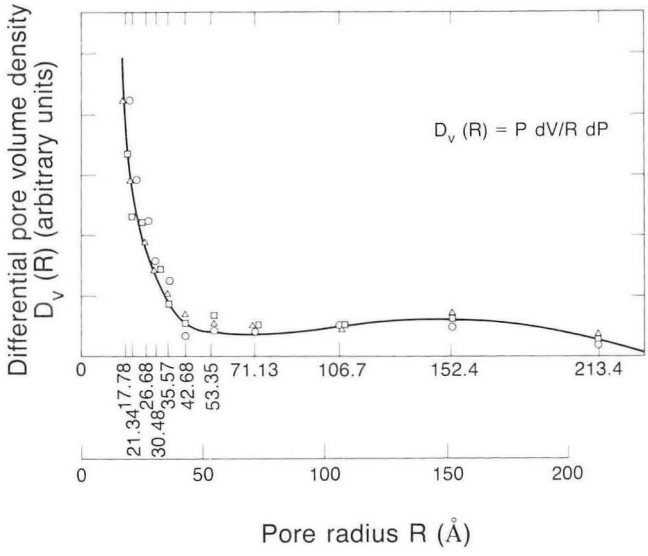


**Figure 9.** Mercury porosimetry of $Li_3N$ samples 0.7-cm thick and 0.3-cm diameter. Differential pore-volume density as a function of pore radius, derived from cumulative pore-volume as a function of applied mercury pressure.

# Spectroscopic Studies of the Passive Film on Alkali and Alkaline Earth Metals in Nonaqueous Solvents


*D.A. Scherson (Case Western Reserve University)*


The objective of this research is to investigate the interaction, reactivity and energetics of nonaqueous solvent/alkali and alkaline earth metal systems. The specific approach being utilized involves the vapor deposition of the reactive metal onto a host single-crystal metal surface followed by their exposure to the nonaqueous solvent in the gas phase. These operations are performed under ultra-high vacuum conditions in order to avoid contamination, and the reactions are monitored by *in-situ* work-function measurements. An array of electron-based analytical techniques including low energy electron diffraction (LEED), Auger electron spectroscopy (AES), and ultra-violet photoelectron spectroscopy (UPS) are used to determine the surface structure and elemental composition. Information regarding bonding and energetics is obtained from high-resolution electron energy loss (HREELS) and thermal desorption spectroscopies (TDS). The results obtained from this investigation are expected to provide considerable insight into the physicochemical nature of the passive film on Li and other alkali and alkaline earth metals.

During the second year of this project the operation of each of the spectroscopies currently available in the ultra-high vacuum chamber, as well as the overall methodology associated with the actual experiments, have been carefully examined. The adsorptions of CO and $O_2$ on Ni(111) were selected as model systems for analysis, and the results are in accordance with those reported earlier by other workers.

No other features, except those associated with K and Ni, were found in the Auger electron spectra recorded before and after vapor deposition of the alkali metal, indicating that within the limits of detectability of this technique the K deposits are free of impurities. LEED patterns for the Ni(111)/K system have provided evidence for the formation of a super-structure for low K coverages. Preliminary TDS experiments have shown that the presence of K on the surface shifts the desorption of CO towards higher temperatures. Such information is particularly relevant to the analysis of the proposed experiments as CO is believed to be a common product in reactions involving a variety of nonaqueous solvents.

Several measurements were conducted in which the work function ($\Delta\phi$) was monitored *in-situ* during exposure of Ni(111) to CO, both in the absence and presence of K on the surface. A representative curve for Ni(111)/CO is shown in Fig. 10, for which the final value of $\Delta\phi$ (1.24 V) was found to be in good agreement with that reported earlier.

Based on these studies it can be concluded that the system components and the procedures involved in the experiments appear to yield satisfactory results, and thus may be expected to afford reliable data in the case of the alkali and alkaline earth metals/nonaqueous solvent systems.

Mass spectroscopy measurements indicate that the long-term stability of propylene carbonate (PC) is not as good as reported. Specifically, the presence of $CO_2$ in amounts much larger than those expected have been consistently observed upon opening a glass-stainless steel container with PC to the ultra-high vacuum chamber connected to a mass spectrometer. Although it is well-known that PC undergoes decomposition at about 150°C, and thus much lower than its boiling point, the present observations may be the first indication that degradation might indeed occur at even lower temperatures.

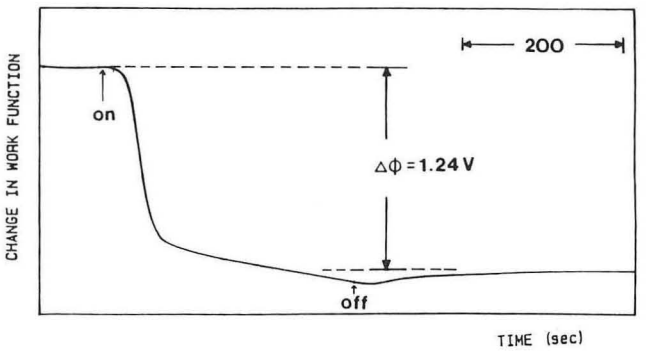


**Figure 10.** Change in work function vs exposure time for CO adsorption on Ni(111) at 85°C. The arrows indicate opening (on) and closing (off) of the leak valve to the CO bottle. The total exposure was 30 Langmiurs.

# *In Situ* Raman Spectroscopy of Lithium Electrode Surface in Ambient-Temperature Lithium Secondary Battery

*H. Tachikawa (Jackson State University)*

The objectives of this project are (i) to develop *in situ* Raman spectroscopic technique for the identification of substances in surface layers on Li electrodes in nonaqueous-electrolyte systems, and (ii) to apply *in situ* Raman spectroscopy to study other electrodes (e.g., Zn) in aqueous solutions which are used in secondary batteries. Structural information on films and other compounds, which form on Li electrode surfaces during charging, will be obtained by *in situ* Raman spectroscopy. The electrode surfaces will also be studied during discharge in order to find the effect of the applied potential on the surface layers. Lithium electrodes in such solute and solvent systems as $LiAsF_6$/PC, $LiAsF_6$/THF, $LiAsF_6$/2-Me-THF, $LiClO_4$/2-Me-THF, $LiClO_4$/THF, $LiClO_4$/PC, and $LiBF_4$/THF are being studied. Surface layers on the following Li electrode are being investigated: (i) Li foil electrode and (ii) Li electrode which are electrodeposited onto thin metal films, such as Al, Ni, Au and Pt.

An electrochemical cell with Pyrex windows, three electrode holders (fabricated from Ni), a medium-size frit which separates working and auxiliary electrodes, and a reservoir for deaerating solution has been built for *in situ* Raman spectroscopy studies. Lithium foil is used as the reference electrode, and either a Pt helix or Li foil is used as the auxiliary electrode. The cell is operated either under vacuum or Ar atmosphere. *In situ* Raman spectra of a Li electrode surface which was electrodeposited on an anodized Ag electrode were recorded in 0.75 M $LiAsF_6$/PC. The Raman spectrum recorded at -0.68 V vs $Li/Li^+$ showed 23 separate bands, most of which are due to the vibrational modes of PC.

Three bands in the low-frequency region are in close agreement with the vibrational modes of $Li_2CO_3$ (reported for polycrystalline $Li_2CO_3$). Another band in the low-frequency region may be due to $Li_2O$. The above results clearly indicate the formation of $Li_2CO_3$ and $Li_2O$ on the Li electrode surface. These preliminary results demonstrated the feasibility of Raman spectroscopy for the *in situ* analyses of surface layers on Li electrodes.

## Polymeric Electrolytes for Ambient-Temperature Lithium Batteries

*G.C. Farrington (University of Pennsylvania)*

The objective of this program is to investigate the chemical and electrochemical characteristics of polymeric electrodes for use in high-specific-energy batteries. A principal goal of this work has been to understand the factors of structure and composition which determine the transport properties of these materials, in particular, those aspects which influence the relative transport numbers for anions and cations. Over the past year, a number of novel solid polymer electrolytes containing poly(ethylene oxide) [PEO] were prepared. Among them were solid solutions of cations such as Cd(II), Zn(II), Ni(II), and Co(II) with various anions. Mixed solid solutions containing divalent cations and Li ions were also prepared.

*PEO Electrolytes Containing $ZnX_2$ Salts.* Electrolytes containing $ZnX_2$ salts (X = Cl, Br, I and $ClO_4$) were prepared and studied over a wide range of compositions, typically from $ZnX_2(PEO)_4$ to $ZnX_2(PEO)_{30}$. The composition which has the highest specific conductivity varies from salt to salt. Of those studied, $ZnI_2(PEO)_{16}$ has the highest conductivity, $3.6 \times 10^{-4}$ $ohm^{-1}$-$cm^{-1}$ at 140°C. The initial transport number measurements show that the $ZnX_2$ electrolytes are essentially pure anion conductors.

*PEO Electrolytes Containing Transition Metal Cations.* Electrolyte compositions containing $NiBr_2$ and $CoBr_2$ were prepared. With both of these ions, it has been possible to use optical spectroscopy to study the coordination of the cations, both in dry electrolytes and during various states of hydration.

The $NiBr_2$ compositions are the most unusual. It appears possible to activate the transport of Ni(II) in these materials by careful hydration and dehydration. For example, a freshly-prepared $NiBr_2$ electrolyte that has been carefully dried has a Ni(II) transport number of less than 0.1. However, if the sample is allowed to hydrate first and then slowly dried, the Ni(II) transport number increases to about 0.7 (both transport numbers measured at 145°C). The change in transport number is accompanied by a large increase in the total film conductivity, from about $10^{-6}$ $ohm^{-1}$-$cm^{-1}$ to $10^{-3}$ $ohm^{-1}$-$cm^{-1}$ at 150°C. The electrolytes formed with $CoBr_2$ do not appear to be affected by the same treatment. Optical spectroscopy studies are underway to understand the mechanism by which purposeful hydration and dehydration can produce such a dramatic increase in ionic conductivity, as observed in the case of Ni(II).

PUBLICATIONS


1. L.L. Yang, R. Huq and G.C. Farrington (1986), "Preparation and Properties of PEO Complexes of Divalent Cation Salts," *Solid State Ionics* **18/19,** 291.
2. L.L. Yang, A.R. McGhie and G.C. Farrington (1986), "Ionic Conductivity in Complexes of Poly(ethylene oxide) and $MgCl_2$," *J. Electrochem. Soc.* **133,** 1380.


## Exploratory Cell Research and Fundamental Processes Study in Solid State Electrochemical Cells

*W.H. Smyrl (University of Minnesota)*

The objectives of this program are to perform research to support the development of high-performance and low-cost rechargeable batteries that are desired for the development of viable electric vehicles or utility load-leveling systems. The program has two specific thrusts that will be concurrently addressed: (i) to investigate the electrochemical performance of novel types of thin-film polymer electrolyte, with emphasis on their feasibility for scale-up from performance, safety and cost aspects, and (ii) to apply advanced techniques for assessing the basic mechanisms occurring at the electrode/electrolyte interfaces of novel electrochemical cells with emphasis on solid-state systems. The study will emphasize solid polymer electrolyte systems, especially those systems that will allow the use of Na, Ca, Mg and other low-cost metals.

Effort has been focused on a theoretical analysis of transport in polymeric electrolytes and the techniques of measuring transference numbers at steady state. Preliminary conclusions of the analysis are at variance with the literature on the subject, and this study may be the basis for new techniques for transference-number determination in polymer elec-

trolytes. In the steady state, measurement of the cell thickness, initial concentration of electrolyte, initial conductivity, and the current and voltage across a cell will allow the determination of the diffusion coefficients of both ions of a binary electrolyte, and the transference numbers of each. The electrodes must be identical and must have a negligible contribution from surface overvoltage effects to determine transference numbers by this method. Our new technique is based on the use of microstructured electrodes and offers the advantage of being rapid, and broadly applicable to all solid electrolytes.

A mass transport-kinetic model for metal dissolution has been extended to include homogeneous reaction effects. It has been derived for metal dissolution reactions that involve multiple valence states, the lower states of which may be oxidized in a homogeneous reaction in the bulk of the electrolyte. The steady-state analysis has been completed and will be extended to treat the impedance of the coupled system, as a possible analog of behavior at a reacting battery electrode.

As part of the study of possible electrodes for further exploratory cell research, an investigation has begun on the electrochemical impedance of both electrode reactions and transport in the electrolyte. Results have been obtained on the electrochemical behavior of electronically conducting polythiophene, poly(3-methyl)thiophene, and polypyrrole. The behavior has some similarities to that observed earlier on the redox polymer polyvinylferrocene. The materials behave as porous electrodes, with properties that depend on the concentration of injected charge in the films.

The selection of alternative systems for study in this program has begun, based on both fundamental and practical bases. Systems based on polymeric electrolytes (including but not necessarily limited to polyethylene oxide), on materials less expensive than Li (primarily Na), and on multivalent metals (e.g., Ca, Mg and Al) will be emphasized.

## Metals Couples in Nonaqueous Electrolytes

*C.W. Tobias (Lawrence Berkeley Laboratory)*

The objective of this project is to explore practical alternatives to high-temperature molten-salt systems for the efficient electrochemical reduction and oxidation of reactive metals. Recent developments in advanced primary cells and projected high-energy rechargeable battery systems involve the use of alkali-metal negatives. To expand the possibilities for application of reactive metals at near-ambient temperatures, new ionizing media are being sought that have high decomposition potentials and are capable of dissolving ionic compounds. The reduction of alkali metals, with reasonably high efficiency in the PC family of solvents at room temperature, has been demonstrated in this laboratory. However, solvent stability in the presence of reactive metals remains a critical issue, especially so in the case of rechargeable galvanic-cell applications.

Cyclic voltammetry and limiting currents to a rotating-disk electrode (RDE) have been used for the determination of $H_2O$ in the 0.3 to 20 ppm range in PC electrolytes. Carefully dried solutions yielded voltammetric peaks proportional to the amount of $H_2O$ added. In $KPF_6$ electrolytes, the cathodic current corresponding to the reduction of $H_2O$ was observed at 0.48 V, whereas in $KAlCl_4$ solutions reduction started at 2.8 V, both relative to a $K/K^+$ reference electrode. At these potentials, the current to a RDE showed Levich-type dependence on rotation rate and was proportional to the concentration of $H_2O$ in the range of 0.5 to 20 ppm. The calculated diffusion coefficients of $H_2O$ are higher than expected: at 25°C, $D_{H_2O}$ is 8.5 $\sim\pm\ \sim 2\mu$ x $10^{-6}$ $cm^2/s$ in 0.5 M $KPF_6$, and 10 $\sim\pm\ \sim 2\mu$ x $10^{-6}$ cm $^2/s$ in 0.25 M $KAlCl_4$.

### PUBLICATIONS


1. R.T. Atanasoski, H.H. Law and C.W. Tobias (1986), "Electrochemical Reduction of Potassium from Potassium Chloride in Propylene Carbonate Electrolyte with Aluminum Anodes," *Electrochim. Acta* **16,** 339.
2. K.J. Hanson and C.W. Tobias (1986), "Electrochemistry of Iodide in Propylene Carbonate: I. Cyclic Voltammetry Monitored by Optical Spectroscopy," LBL-22008.
3. K.J. Hanson, M.J. Matlosz, J. Newman, and C.W. Tobias (1986), "Electrochemistry of Iodide in Propylene Carbonate: II. Theoretical Treatment," LBL-22009.
4. R.T. Atanasoski, H.H. Law, R.C. McIntosh and C.W. Tobias (1986), "Electrochemical Analysis of Trace Amounts of Water in Propylene Carbonate Electrolytes," LBL-22467.

## Corrosion, Passivity and Breakdown of Alloys Used in High Energy Density Batteries

*(J. Kruger, The Johns Hopkins University)*

The objective of this research is to further the understanding of the passivity of metals and alloys in nonaqueous and mixed solvents. There is a paucity of data in this area, despite its importance in construction materials for high-specific-energy batteries. This work is concerned with analyzing the nature, mode of formation, and mode of breakdown of passive films that exist on alloys in nonaqueous and mixed solvents.

The first phase of this project has concentrated on studying the effect of additions of PC and 0.01 M $Cl^-$ (as LiCl) on the current-potential characteristics of Au and Armco Fe in 0.5 M $LiClO_4$.

Slow potentiodynamic scans (0.1 mV/sec) of Armco Fe in 0.5 M $LiClO_4$ with various additions of PC (resulting in solutions of 0 to 100 mol% PC) have shown that while Armco Fe can passivate in all solutions studied upon anodic polarization, it pits upon further anodic polarization in solutions containing greater than or equal to 50 mol% PC as a co-solvent with $H_2O$, without the addition of $Cl^-$. It has also been found that the pit morphology depends strongly on the $H_2O$ content. In nominally dry PC, the pits are small ($\sim$20 $\mu$m) and widely spaced (Fig. 11). In 50 mol% PC, there is a radical change in the morphology of the attack (Fig. 12). The morphology observed in nominally dry PC is classical pitting attack due to a localized breakdown of a passive film. The scratches after polishing with 800-grit paper can still be clearly seen. There is no apparent crystallographic nature to the attack. The attack on the majority of the surface in 50 mol% PC/50 mol% $H_2O$ shows a crystallographic nature which Pickering and Frankenthal[1] ascribe to active dissolution from a film-free surface, i.e., activation-controlled dissolution. A polished surface with numerous pits can also be observed in Fig. 12, and these pits are widely scattered over the entire specimen surface. Such a smoothly polished surface is characteristic of dissolution in the presence of a rate-limiting film which forms in the active region at high current densities.[2] Again, the tests cited above were conducted without the addition of $Cl^-$. When 0.01 M $Cl^-$ is added, passivity is destroyed in all of the solutions studied.

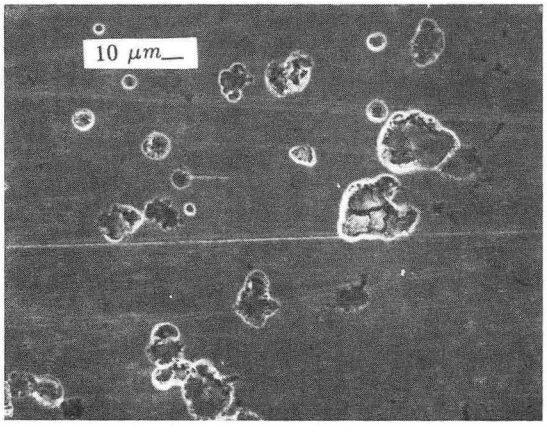


**Figure 11.** Pitting in Armco Fe in nominally dry PC.

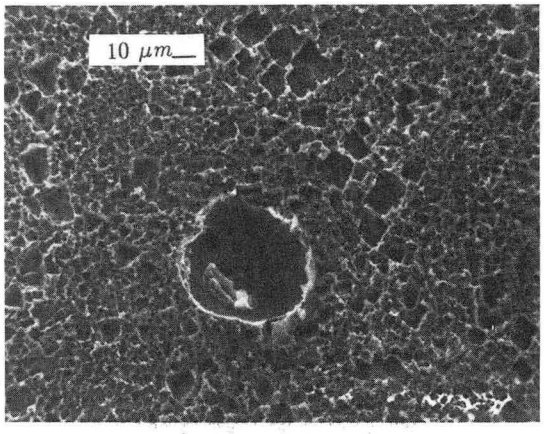


**Figure 12.** Pitting in Armco Fe in 50 mol% PC.

REFERENCES


1. H.W. Pickering and R.P. Frankenthal (1974), *Localized Corrosion,* Staehle, Brown, Kruger, Agarwal, eds., National Association Corrosion Engineers, Houston, TX, p. 261.
2. K.F. Bonhoeffer (1953), *Z. Metallkde.* **44,** 77.


# F. CROSS-CUTTING RESEARCH

Cross-cutting research is carried out to address fundamental problems in electrocatalysis, current density distribution and gas evolution, solution of which will lead to improved electrode structures and performance in batteries and fuel cells.

# Analysis and Simulation of Electrochemical Systems

*J.S. Newman (Lawrence Berkeley Laboratory)*

The objective of this program is to improve the performance of electrochemical cells used in the inter-conversion of electrical energy and chemical energy by fundamental investigations of the transport and interfacial phenomena. Results of this work are used to analyze experimental data, to identify important system parameters, and to aid in the design and scale-up of these systems.

A mathematical model of the electrode/electrolyte interface is being developed to calculate the frequency response of a rotating disk. The working algorithm accounts for the effect of surface coverage owing to specific adsorption and charge-transfer reactions. Double-layer theory is used to calculate the potentials at the interfacial planes and the surface excesses of all the electroactive species present in the solution. Presently, the microscopic model of the interface predicts qualitatively the measured complex impedance for the $ZnCl_2$ solutions. This mechanistic approach allows the proposed reaction process to be changed to account for the experimental observations. Finally, the generalized model can be used to identify system limitations and to guide further experimental research. This microscopic model of the interface will be coupled with the previously developed macroscopic model accounting for convection, migration, and multicomponent diffusion in concentrated solutions, in addition to homogeneous and heterogeneous reactions.

A computer model is being developed to predict the response to alternating current signals of a redox reaction with soluble reactants and products in a flow-through porous electrode. Terms accounting for double-layer capacity have been added to the model. An experimental investigation is underway to accompany the modeling efforts.

The corrosion of iron in sulfuric acid is being studied experimentally using rotating Fe hemispherical electrodes. The anodic polarization curve, the sustained electrochemical oscillations, and the alternating current impedance for this system are being determined. The impedance data are being checked for consistency with the Kramer-Kronig relations. Finally, the experimental impedance results will be compared with the predictions of recently developed theoretical models to elucidate the fundamental processes governing the behavior of the $Fe\text{-}H_2SO_4$ system.

Double-layer adsorption is an important phenomenon in heavy-metal ion removal from waste streams and in discharge transients in high-pulse-power battery systems. An experimental and theoretical investigation of double-layer adsorption of Zn ions on high-surface-area porous carbon is underway.

The solution of Laplace's equation is important to many modeling efforts. Its solution is often expensive and difficult to obtain accurately. The feasibility of a boundary-integral technique for use in current-distribution problems is being investigated. Preliminary observations appear promising. This technique is being applied to primary and secondary current distributions and can be used for more general problems involving Laplace's equation. In addition, a theoretical and experimental study is underway to determine how the conductivity varies in solid mixtures of several phases used in solid electrodes of varying composition.

## PUBLICATIONS


1. C.G. Law, Jr., and J. Newman (1986), "Corrosion of a Rotating Iron Disk in Laminar, Transition, and Fully Developed Turbulent Flow," *J. Electrochem. Soc.* **133,** 37.
2. P. Russell and J. Newman (1986), "Anodic Dissolution of Iron in Acidic Sulfate Electrolytes: I. Formation and Growth of a Porous Salt Film," *J. Electrochem. Soc.* **133,** 59.
3. M.M. Jaksic and J. Newman (1986), "The Kramers-Kronig Relations and Evaluation of Impedance for a Disk Electrode," *J. Electrochem. Soc.* **133,** 1097.
4. M. Matlosz and J. Newman (1986), "Experimental Investigation of a Porous Carbon Electrode for the Removal of Mercury from Contaminated Brine," *J. Electrochem. Soc.* **133,** 1850.
5. P. Russell and J. Newman (1986), "Current Oscillations Observed within the Limiting Current Plateau for Iron in Sulfuric Acid," *J. Electrochem. Soc.* **133,** 2093.
6. D. Bernardi (1986), "Mathematical Modeling of Lithium (alloy), Iron Sulfide Cells and the Electrochemical Precipitation of Nickel Hydroxide," (Ph.D. Thesis), LBL-20858.
7. M. Matlosz and J. Newman (1986), "Solving One-Dimensional Boundary-Value Problems with BandAid: A Functional Programming

Style and a Complementary Software Tool," LBL-21589.
8. D. Bernardi and J. Newman (1986), "Mathematical Modeling of Lithium(alloy), Iron Disulfide Cells," LBL-21764.
9. V. Edwards (1986), "Design of Thin-Gap Channel Flow Cells," (Ph.D. Thesis), LBL-21848.
10. J. Newman (1986), "Modeling of Porous Electrodes in Molten-Salt Systems," LBL-21867.

## Ambient-Temperature Alkaline Sulfur-Polysulfide Electrodes

*E.J. Cairns and F.R. McLarnon (Lawrence Berkeley Laboratory)*

The objectives of the present work are to obtain information on the electrochemical and chemical reactions of the aqueous sulfide/polysulfide redox couple and to use that information to design a stable and efficient redox electrode for use in photoelectrochemical cells (PECs) and redox batteries.

The kinetics of the aqueous polysulfide redox couple were investigated using a transient potential-step technique in a solution 1 M in $S^0$ and 1.3 M in total $S^{2-}$, at pH 12. This pH was selected in order to minimize the disproportionation of polysulfides to thiosulfate and sulfide. The low-overpotential region (-25 to +25 mV) was investigated for Co and Pt electrodes from 25 to 80°C. The active species concentration was found to be several orders of magnitude lower than those of any of the major (poly)sulfide ions, and its temperature dependence corresponded to an $E_a$ of about 10 kcal/mole. These results are consistent with the idea that the electrochemically active species is $S_2^-$. Deviations were found between experimental data for temperatures above 45°C and the simple analytical form of the current response for an electrode reaction with one rate-determining step. The results agree with a new model proposed here that considers two rate-determining steps, one of which is the homogeneous chemical reaction:

$$S_4^{2-} \rightleftarrows 2S_2^- \,. \qquad (1)$$

The rate constants for this reaction determined using this new model agree with those measured for similar reactions. Exchange current densities were on the order of 1 mA/cm$^2$ at 60°C.

The steady-state current density-overpotential relationships for Co and Pt rotating disk electrodes were determined for a range of temperatures. A model was developed to take into account the rate of Reaction 1 as well as a finite heterogeneous reaction rate. The parameters determined by the potential-step method could be used with this model to explain the current density-overpotential behavior in the low-overpotential cathodic region. At higher overpotentials in the cathodic region a second cathodic reaction was evident. This second cathodic reaction was less prominent when the current densities were lower (as on Pt electrodes) or when the $S_2^-$ concentrations were higher (as temperature increased).

The addition of 13 mol% DMF to the aqueous polysulfide solution was found to increase significantly the current density, at a given temperature and overpotential, by increasing the equilibrium concentration of the electrochemically active sulfur radical anion. In the range of overpotentials studied, the first cathodic reaction wave becomes much more prominent. Although independent quantitative data are lacking for the DMF-water mixtures, the use of reasonable values for the exchange current density and the rate constant for Reaction 1 allows the quantitative prediction of the observed cathodic behavior in the temperature range of 25 to 77°C.

The results of the rotating disk work indicate that porous electrodes are required for the counterelectrode in a PEC utilizing the aqueous sulfide/polysulfide redox couple in order to meet a design goal of supporting 10 to 20 mA/cm$^2$ at less than 50 mV overpotential. A flow cell for testing flow-through porous electrodes was constructed and operated. The effects of electrode material, temperature, flow rate, and the addition of DMF on electrode performance were studied. Co (plated on Ni screens) and $MoS_2$ (grown by reaction of sulfur vapor with Mo on expanded-metal mesh) electrodes gave similar performances which were more than adequate to meet the design goals. Flow rate variation between 0.1 and 1.6 liter/min had only a small effect on the current density-overpotential curves. Raising the temperature and/or the addition of DMF had much larger effects. These observations are in accord with the steady-state results obtained on the rotating disk electrodes. The demonstrated electrode performance is more than satisfactory for a high-performance photoelectrochemical cell or redox cell.

### PUBLICATIONS

1. P.M. Lessner (1986), "Kinetics and Transport Processes in Aqueous Polysulfide Electrode Reactions," (Ph.D. Thesis), LBL-22399.
2. P. Lessner, J. Winnick, F.R. McLarnon, and E.J. Cairns (1986), "Kinetics of Aqueous Polysulfide Solutions: Part I. Theory of Cou-

pled Electrochemical and Chemical Reactions, Response to a Potential Step," *J. Electrochem. Soc.* **133,** 2510.

3. P. Lessner, J. Winnick, F.R. McLarnon, and E.J. Cairns (1986), "Kinetics of Aqueous Polysulfide Solutions: Part II. Electrochemical Measurement of the Rates of Coupled Electrochemical and Chemical Reactions by the Potential Step Method," *J. Electrochem. Soc.* **133,** 2517.
4. P. Lessner, J. Winnick, F.R. McLarnon, and E.J. Cairns (1986), "Kinetics of Aqueous Polysulfide Solutions: Part III. Investigation of Homogeneous and Electrode Kinetics by the Rotating Disk Method," LBL-22802.

## Engineering Analysis of Gas Evolution

*C.W. Tobias (Lawrence Berkeley Laboratory)*

The objective of this project is to establish the influence of electrode geometry and surface morphology, and of electrolyte composition, on bubble size and residence time, and to elucidate the role of free and forced convection as it affects overpotential behavior and ohmic resistance in gas evolution processes.

A micromosaic electrode with an electrochemical redox system was used in a study of the Benard-Rayleigh problem of onset of convection in a fluid with a time-dependent density profile contained in a deep cell. The electrochemical technique offers several advantages over thermal techniques, the most important one being the precise control of the surface condition. The well-controlled experiment lends itself to a thorough analysis of the time-dependent base state, the case of diffusion and migration into a semi-infinite column of electrolyte. In addition, the electrode serves as the monitoring device, allowing a precise detection of the onset of convection, the criterion for which is a percentage deviation of the Sherwood number (current) from base-state behavior.

The critical Rayleigh number for the problem of onset of convection at a rigid, conducting boundary, due to a step change in the surface condition, was found to be ~1350, based on the equivalent, linear-segment concentration profile and using a deviation criterion of 5% of the Sherwood number. For the redox system employed here, a maximum in the density profile was calculated. The relevant length for the equivalent, linear-segment density profile, based on an equivalent destabilizing buoyant force below the density maximum, is 16% lower than that for the concentration profile of the reactant. The critical Rayleigh number based on this length is ~800.

At sensing elements much smaller than the wavelength of the disturbance, a sharp increase (or decrease) in mass-transfer rate occurs immediately after the first deviation from convection-free behavior. Over a larger area, some averaging takes place and a significant enhancement of the mass-transfer rate does not occur until tens of seconds after the first deviation in the mass-transfer rate is detected.

A model has been developed for predicting the current distribution and the increment in cell voltage caused by the presence of bubbles attached to the electrode surface. In describing the geometric configuration of the bubble layer, great computational savings are achieved by approximating the hexagonal symmetry cell with a cylindrical one. This approximation is shown to be successful by comparison with analogue measurements of primary resistance.

When supersaturation effects do not influence the problem (either because they have been omitted or because they are precluded by irreversible electrode kinetics), both the current distribution and the resistance increment associated with attached bubbles can be accurately correlated, for a given geometric configuration, by a single parameter, the Wagner number. When supersaturation does influence the problem, the solution depends on five parameters, and the model predicts a lower voltage increment than would be calculated without including concentration effects. In this case, the current distribution is strongly non-uniform, with highest current density to the electrode region nearest the bubble contact area. These effects depend strongly on electrode kinetics as well as on contact angle and on the density of the attached-bubble layer.

### PUBLICATIONS

1. J.O. Dukovic and C.W. Tobias (1986), "The Influence of Attached Bubbles on Potential Drop and Current Distribution at Gas Evolving Electrodes," LBL-18818.
2. G.M. Whitney and C.W. Tobias (1986), "The Limiting Current Technique at a Sectioned Electrode for the Study of Buoyancy Induced Convection," *Proceedings of the Symposium on Significant Questions in Buoyancy Affected Enclosure or Cavity Flows,* 107th Meeting of the ASME, HTD Vol. 60, p. 105; LBL-22036.

3. D.W. Dees and C.W. Tobias (1986), "Experimental Observations of Free Convection Mass Transfer at a Horizontal Surface with a Micromosaic Electrode," LBL-16176.

4. D.W. Dees and C.W. Tobias (1986), "Mass Transfer at Gas Evolving Surfaces; A Microscopy Study," LBL-22311.

# IV. AIR SYSTEMS RESEARCH

The objectives of this project element are to identify, characterize and improve materials for air electrodes; and to identify, evaluate and initiate development of metal/air battery systems and fuel-cell technology for transportation applications.

## A. METAL/AIR CELL RESEARCH

Projects on metal/air cell research address oxygen electrocatalysis; bifunctional air electrodes, which are needed for electrically rechargeable metal/air (Zn/air, Fe/air) cells; and novel alkaline Zn electrode structures which could be used in either electrically recharged or mechanically recharged cell configurations.

### Electrocatalysts for Oxygen Electrodes

*E.B. Yeager (Case Western Reserve University)*

The overall objective of the research is the development of more-effective electrocatalysts for $O_2$ reduction and generation, combining high activity with long-term stability. Research emphasis is on achieving a fundamental understanding of $O_2$ electrocatalysis.

*Transition Metal Macrocycle Catalysts.* The research has continued on catalysts which promote the 4-electron reduction of $O_2$ to $OH^-$ or $H_2O$ without producing solution-phase peroxide. The spectroscopic and electrochemical studies of iron phthalocyanine (FePc) and its $\mu$-oxo species have been completed. These included FTIR and Mossbauer spectroscopy, scanning electron microscopy, voltammetry and rotating ring-disk electrode, as well as measurements on gas-fed electrodes. These catalysts dispersed on carbon (Vulcan XC-72) show very little peroxide formed in the solution phase at low polarization and the activity, particularly with the $\mu$-oxo species, is comparable to commercially available Pt-based catalysts in alkaline solution. Iron tetra-pyridino porphyrazines (FeTPyPz) adsorptively attached to graphite also show voltammetry and $O_2$ reduction kinetics similar to FeTsPc, which catalyzes the direct 4-electron pathway in alkaline electrolytes.

Attempts have been made to prepare sandwich-type dimeric structures as adsorbed layers on pyrolytic graphite, using positive- and negative-charged water-soluble transition metal macrocycles. Thus far these layers have shown no synergistic improvement in the activity for $O_2$ reduction in alkaline solutions. These ligands may not possess sufficient structural compatibility to form the desired sandwich-type species with proper spacing for binding of $O_2$. Mono- and bi-nuclear metal chelates of tetradentate Schiff-base ligands (obtained from Tanta University, Egypt) have also been characterized. The catalytic activity for $O_2$ reduction of the metal chelates is much lower than that of the transition metal porphyrins or phthalocyanines. One reason for low activity may be the lack of p-electron delocalization in the ligand structure symmetrically about the central metal ion, which may result in a tetrahedral geometry.

Work has also continued on surface-enhanced Raman spectroscopy involving adsorbed monolayers of phthalocyanine molecules on Ag electrodes and AgBr substrates. The analysis of electronic energy levels in semiconducting AgBr and the adsorbed phthalocyanine molecules suggests a new mechanism for the high enhancement factor in surface-enhanced Raman scattering.

*Heat-Treated Catalysts Based on Nitrogen-Containing Polymers.* The high catalytic activity for dioxygen reduction, that is achieved by bonding transition metal ions (e.g., Co and Fe) and nitrogen on high-area surfaces, is believed to be due to the strong $O_2$ interaction with d-orbitals of the transition metal. Guided by this concept, the polymers, polypyrrole black and polyacrylonitrile heat-treated with Co salts, have been identified as very active $O_2$ reduction catalysts in alkaline electrolytes. The activity is comparable to highly dispersed Pt. These catalysts function through a peroxide mechanism, similar to that involved with heat-treated Co porphyrins, and have comparable activity but much lower cost. Life testing of these catalyst systems is in progress.

*Perovskite Electrocatalysts and Possible Use in Bifunctional $O_2$ Electrodes.* One focus of the ongoing research on perovskite electrocatalysts for $O_2$ reduction and generation has been the catalysis of peroxide decomposition. The methods (volumetric and RDE) for monitoring $HO_2^-$ concentrations, which

have been used with catalyst suspensions, typically yield first-order dependence of the reaction rate on peroxide concentration. The open-circuit potential decay (OCPD) method using gas-fed electrodes, however, yields both first- and second-order behavior, depending upon the current density and the elapsed time after opening the circuit. This apparent discrepancy with the OCPD method has been explained recently by the discharge of the double layer and Faradaic capacitance of the high-surface-area carbon and the perovskite. A mathematical model has been developed which quantitatively describes this behavior.

*Bifunctional Oxygen Electrodes.* The development of catalysts, which are active for both $O_2$ reduction and generation in alkaline electrolytes, is continuing. The catalysts receiving the most attention are those which consist of tetramethoxyphenyl porphyrin (TMPP), either metal-free or containing Co, heat-treated on carbon and mixed with transition metal-containing perovskites.

The presence of the perovskite does not appreciably affect the $O_2$ reduction performance of heat-treated CoTMPP on carbon. Cobalt-containing perovskites, however, have been found to greatly increase the performance of heat-treated $H_2$TMPP on carbon, probably because small amounts of Co(II) can go into solution and re-adsorb at nitrogen-containing sites on the macrocycle-carbon surface. Since the loss of Co from heat-treated CoTMPP-based catalysts may be an important failure mechanism in long-term operation, perovskites may provide a back-up source of the transition metal.

It should be noted that most of the perovskites examined have been found to undergo irreversible surface reduction, some even in the potential range where $O_2$ reduction takes place. This surface reduction can seriously affect the catalytic activity for $O_2$ generation.

## PUBLICATIONS


1. E. Yeager (1986), "Dioxygen Electrocatalysis: Mechanisms in Relation to Catalyst Structure," *J. Molecular Catalysis* **38,** 5.
2. D. Scherson, A.A. Tanaka, S.L. Gupta, D. Tryk, C. Fierro, R. Holze, E.B. Yeager, and R.P Lattimer (1986), "Transition Metal Macrocycles Supported on High Area Carbon: Pyrolysis-Mass Spectrometry Studies," *Electrochim. Acta* **31,** 1247.
3. R. Holze, A.T. Riga and E. B. Yeager (1986), "Thermal Decomposition of Surfactants in PTFE-Dispersions," *J. Materials Science Letters* **5,** 819.
4. B. Simic-Glavaski (1986), "Spectroscopic and Electrochemical Studies of Transition-Metal Tetrasulfonated Phthalocyanines: 9. A Correlation Between Surface-Enhanced Raman Scattering and Photography," *J. Phys. Chem.* **90,** 3863.
5. S.L. Gupta, D. Tryk, M. Daroux, W. Aldred and E. Yeager (1986), "Heat-Treated Pyrrole Black Based Electrocatalysts for $O_2$ Reduction," *Proceedings of the Symposium on Load Levelling and Energy Conservation in Industrial Processes,* D.T. Chin, ed., The Electrochemical Society, Inc., Pennington, NJ, p. 207.


# Electrode Research for Electrically Rechargeable Zinc/Air Alkaline Battery


*P.N. Ross (Lawrence Berkeley Laboratory)*


A new concept for an alkaline Zn electrode was explored that would overcome the cycle-life limiting phenomena characteristic of most Zn electrode concepts. The new concept is a flow-through porous Zn electrode with recirculating supersaturated zincate solution. An alkaline Zn battery with recirculating zincate is not a new concept itself, but many of the prior systems used an inert (usually flat) current collector with recirculating Zn particles. The concept employed here uses an inert substrate having an open "honeycomb" type porosity onto which Zn is plated (and from which it is stripped) while electrolyte circulates through the open pores. Materials having this type of porous structure are commercially available as either "metal foams" or "carbon foams." The use of Cu foam-metal, which has an open honeycomb or reticulated structure (nominal "cell" diameter is 0.2 cm and characteristic diameter of the filaments is ~0.4 mm) was investigated. This particular foam has a bulk density of 3% (97% porosity) of the bulk density of Cu with a total BET surface area of $\sim 10^4$ $m^2$ per $m^3$. Using a 0.3-cm thickness, the internal surface area is roughly 30 times the superficial area, so the "true" current density for Zn deposition/stripping will be more than an order of magnitude lower than the nominal current density. Low current density is known to promote uniform Zn deposition/stripping and should extend cycle-life. A full parametric study of the influence of current density, electrolyte flowrate, and zincate concentration of Zn distribution was conducted. The maximum amount of Zn that could be deposited uni-

formly was about 160 mAh/cm$^2$ (at 10 mA/cm$^2$). The Zn deposit mirrored the cellular structure of the substrate and the distribution was found to be uniform and invariant with the number of cycles over a wide range of conditions of flowrate, zincate concentration and current density.

Two types of carbon materials were identified for air electrodes: (i) graphite fibers woven into a "cloth" that serves as the current collector, and (ii) a high-surface-area graphite powder formed by heat-treatment of a carbon black. The latter was impregnated with a mixture of transition metal oxides to form the active catalyst. The electrode was fabricated by bonding the catalyst layer to one side of the graphite cloth, and a hydrophobic polytetrafluoroethylene (PTFE) film bonded to the other. The electrode still showed acceptable voltage in the current density region of 10 to 20 mA/cm$^2$ after 300 cycles in 12 N KOH containing 200 g/l zincate.

Proof-of-principle experiments were conducted on 1.5-Ah Zn/air prototype cells employing the new concepts in Zn and air electrodes described above. The cell was cycled at the three-hour rate producing 1.2 V on discharge, required 2.0 V on charge, and operated satisfactorily for over 150 cycles. Based on the 1.5-Ah prototype performance characteristics, engineering design calculations were made for a 32-kWh battery. These calculations project specific energy of 110 Wh/kg, peak power of 140 W/kg, electrical efficiency of 60% and an attractive materials cost of $<$ \$20/kW. The prototype testing revealed a number of problem areas that would have to be addressed in further studies using multi-cell prototypes: (i) shunt currents in the electrolyte manifold, (ii) the effect of air electrode dissolution products in the electrolyte on Zn cycling, and (iii) component reliability.

## Electrical and Electrochemical Behavior of Particulate Electrodes

*J.W. Evans (Lawrence Berkeley Laboratory)*

The objective of this research is to provide the basic knowledge to enable particulate electrodes to be designed, evaluated and scaled up. One possible particulate electrode is a fluidized-bed electrode where Zn particles are maintained in a state of agitated suspension by the upward-flowing electrolyte. Such electrodes have been the main subject of this investigation to date.

The local, instantaneous and time-averaged potentials have been measured in fluidized-bed and moving-bed electrodes at LBL. These measurements support the concept that such beds function electrochemically by the conduction of electricity along "chains" of particles that have a fleeting existence in the bed. This suggests that of the three types of particulate electrodes, slurry electrodes (where the particles remain suspended in the electrolyte and flow through the cell with it) are likely to be inferior to fluidized-bed or moving-bed electrodes where the particles are less widely separated. For discharge (electrodissolution of metal) the moving-bed electrode appears advantageous because of its lower pumping requirements than a fluidized-bed electrode. For charging (electrodeposition of metal) fluidization is essential to avoid attaching the particles to each other and by "bridges" of deposited metal. Hence both types of electrodes are under study at LBL. Moving-bed cells with particulate Zn electrodes and air counter-electrodes have been built and are in the process of testing and improvement. Testing consists of measurement of current-voltage characteristics and voltage-time characteristics on discharge at constant current. Fluidized-bed cells are being operated to study the deposition of Zn from alkaline zincate electrolyte.

Experimental measurements have shown that Zn can readily be deposited from alkaline zincate electrolyte onto fluidized beds of Cu particles with a Zn coating. The laboratory cell could be operated at a superficial current density (current per unit area of cell cross section) of 300 mA/cm$^2$ with an electrical energy consumption of 2.7 kWh/kg Zn. This compares very favorably with the 3-4 kWh/kg Zn typical for the present day industrial electrodeposition of Zn (from acid sulfate electrolytes). The Zn-coated Cu particles that are produced are most suitable for discharge in a moving-bed cell. Complete (planned or accidental) discharge can occur without impacting the ability to recharge in a fluidized bed. The density of the particles changes only slightly on charge or discharge; this facilitates their fluidization (in the fluidized bed) or downward motion (in the moving bed).

Laboratory cells with moving-bed electrodes have been constructed using the Zn-coated Cu particles and commercially available air cathodes. Discharge characteristics of these cells have been measured. The discharge efficiency of these cells (of the order of 30%) is poor, but there is ample opportunity for improvement in efficiency by changes in cell design.

PUBLICATION

1. H. Choi (1986), "An Investigation of Zinc Electrodes Relevant to Zinc-Air Batteries," (M.S. Thesis), LBL-22705.

# Technology Base Research on Zn/Air Battery Systems

*J.L. Morris (Pinnacle Research Institute)*

The slurry Zn/air battery is a good candidate to power electric vehicles because it permits the energy and power specifications to be designed independently of each other, and *in situ* or centralized recharging is possible. The research effort reported here addresses the development of the discharge and the recharge processes in separate cells. The objective of the discharge studies was to find ways to increase the capacity and power by studying the effect of (i) capacity-extension additives, (ii) KOH concentration, (iii) temperature, (iv) coated polymeric bead slurries, (v) Zn powder slurries, and (vi) air and $O_2$ depolarizers. Fundamental studies on the effect of additives on passivation were also started by determining the potentiodynamic critical currents and transition times from galvanostatic transients at the rotating disk electrode. The objective of the recharge studies was to find a practical method to recharge either the bead or Zn particle slurries. A fluidized-bed cell was designed to recharge the beads. Engineering improvements are required to solve buoyancy and other problems in this cell. A scraped rotating cylinder cell was built to produce dendritic Zn slurries from discharged Zn particle slurries. Magnesium and glassy carbon cathodes were evaluated both in the rotating cylinder cell and in a static disk cell. Zinc dendrites, which were more easily removed, were obtained at a lower cell potential on glassy carbon than on Mg substrates, but they were produced with a lower current efficience (i.e., 80%).

*Additives to Extend Capacity.* A summary of the additive study is presented in Fig. 13, where a bar shows the capacity, in Ah/$\ell$ of Zn powder slurry, achieved when the indicated compounds were added to 12 M KOH at 55°C. The hatched bar indicates the corresponding % utilization of Zn powder, starting from 300 g/l Zn to full discharge. Sorbitol is an additive that is believed to increase the discharge capacity by stabilizing the polymer chains involving $\{OZnO\}_n...\{[Zn(OH)_4^{2-}]\}...\{OZnO\}_n$, by means of hydrogen bonding. Sorbitol by itself extends the

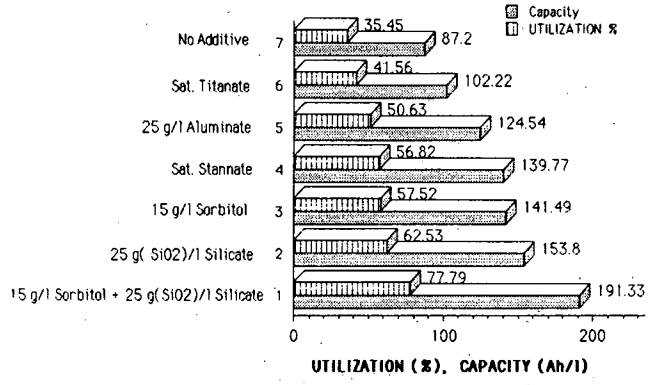


**Figure 13.** Zinc utilization and capacity of selected additives. Discharge of 300 g/l simulated dendritic Zn powder at 200 mA/cm$^2$ in 12 M KOH in a 200-cm$^2$ bicell at 55°C using 4.5 x rate of stoichiometric air.

capacity just below that obtained by silicate. Titanate, aluminate, stannate and silicate additives are believed to act by stabilizing micelles of ZnO or zincate. However, when sorbitol was combined with silicate, a 20% increase in capacity was obtained compared to that with silicate alone, indicating complementary mechanisms.

*Comparison of Bead and Zn Particle Slurries.* Slurries made with a mixture of Zn powders outperformed the coated beads (from Sorapec) in discharge with silicate additive in 12 M KOH, as shown in Fig. 14. The beads presented buoyancy problems that were more difficult to manage in the fluidized bed used for recharge than in the moving-slurry bed used for discharge. The effect of pure $O_2$ versus air as depolarizers was assessed. Better cell potential and power at higher current densities were possible with $O_2$, as shown in Fig. 14.

*Scraped Rotating Cylinder Recharge Cell.* The fundamental concept of mechanical removal of dendrites to form a slurry was verified. Complete scraping was possible both from Mg and glassy carbon (GC) cylindrical electrodes. However, with both substrates, agglomerations at the fixed scrapers favor preferential growth at the blades that short-circuits the cell. Preliminary measurements with the rotating cylinder using 12 M KOH (saturated with ZnO, ~90 g/l) yielded current efficiencies of 83 and nearly 100% for glassy carbon and Mg substrates, respectively. These preliminary data were obtained from comparisons of the mass of Zn scrapped from the electrodes. More reliable current efficiencies were obtained from the quantity of $H_2$ evolved at the static disk electrode, and these data are shown in Fig. 15.

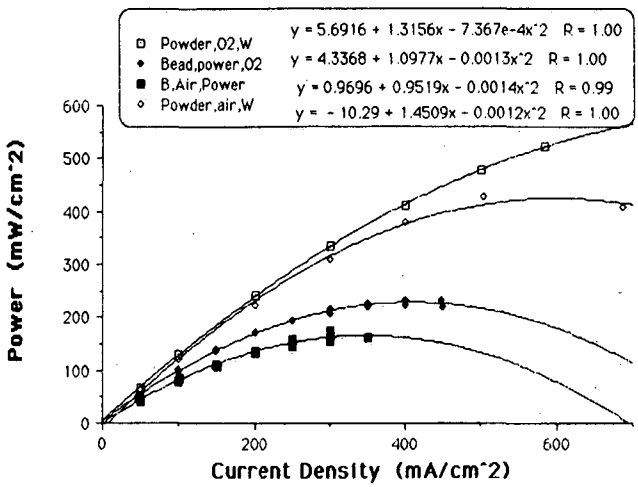


**Figure 14.** Performance of bead and Zn powder slurries.

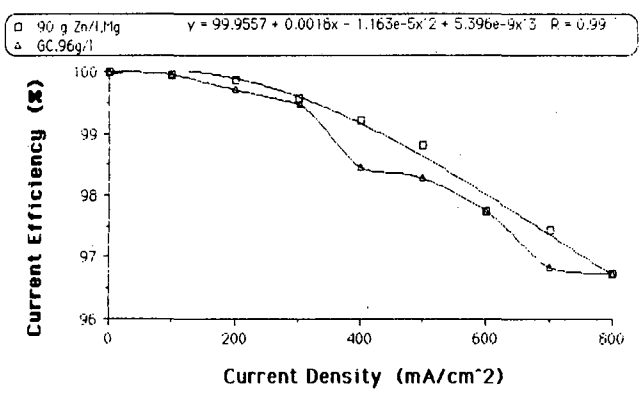


**Figure 15.** Current efficiencies for Zn deposition on glassy carbon (Δ) and Mg (□) substrates vs current den-

# B. ALUMINUM/AIR BATTERIES

Projects on Al/air battery R&D are directed at improving cell components and solving system integration problems.

## Aluminum/Air Power Cell Research and Development

*A. Maimoni (Lawrence Livermore National Laboratory)*

The objectives of this program are to develop an electric power source as an alternative to the internal combustion engine, and to evaluate its ability to provide general-purpose vehicles with the range, acceleration, performance, and rapid refueling capability of current internal combustion engines. During 1986 LLNL conducted research and provided program direction on the development of the Al/air battery. Most of the work was carried out under a cost-shared contract with Eltech Systems Corporation, which has formed a consortium with Alcan International Ltd., CWRU, SRI International, the University of Akron and Oklahoma State University.

### CELL DESIGN AND PERFORMANCE

The design efforts at Eltech focused on the development of cell hardware that combines the qualities of reliability and ease of assembly with low-cost construction techniques. The following discussion briefly identifies those design improvements.

*Modular Air Cathode.* A reliable seal between the air cathode, current collector, and air-cathode module was developed which maintained good electrical contact to the main electrical bus.

*Anode Current Collector.* The solution-side current collector for the anode was eliminated because of manufacturing difficulties and low reliability of electrical insulation on the conducting tines. An external connection to the anode was developed and continuous anode recharge was demonstrated.

*Anode/Cathode Separator.* A low-cost plastic separator was developed with internal grooves to optimize electrolyte flow through the battery. A constant anode feed was demonstrated with this separator, and the "scalloped" leading edge on the anode was eliminated.

*Cage Support for the Aluminum Anode.* A vertical cage support for the anode was developed which could replace the separator tynes. The plastic cage served the secondary purpose of increasing the rigidity of the cell by acting as a compression member, i.e., as a three-sided filter press.

*Performance.* An EL-2 five-cell stack was built and integrated into a laboratory system. Hydraulic control of the cathode compartments was accomplished with one valve for all ten cathodes, and it allowed reproducible air-cathode pressure drops. The cell voltages obtained were as follows:

| Cell Number | Cell Voltages (V) |
|---|---|
| 1 | 1.20 |
| 2 | 1.20 |
| 3 | 1.20 |
| 4 | 1.20 |
| 5 | 1.16 |

The maximum power density in 4 M NaOH electrolyte occurred at 400 mA/cm$^2$ using an Al alloy containing In and Ga manufactured by Reynolds. There were substantial resistive drops (~210 mV) in the external busbar. The performance criteria characterized by the EL-2 cell design were repeated with the five-cell stack; namely the continuous feed of the Al wedge-shaped anode, rapid mechanical rechargeability, high durability of the cathode structure, and continuous, moderate-term operation (10 h).

## COMPONENT DEVELOPMENT

*Air Cathode.* The best catalyst identified by CWRU for high-current $O_2$ reduction was ~5 wt% CoTMPP on a highly conductive carbon black, such as Vulcan XC-72 or Gulf Shawinigan acetylene black (steam-activated), which was heat-treated at 450 to 800°C. The catalysts were fabricated into a relatively thin active layer (0.1-0.2-mm thick) structure on a conductive hydrophobic backing layer. These electrodes were capable of reducing pure $O_2$ at 1 A/cm$^2$ at about -1 V (vs Hg/HgO) in 4 M NaOH at 60°C. A model was developed to explain the processes occurring during heat treatment as well as the $O_2$ reduction performance. Heat treatment, especially at 800°C, destroys the structure of the macrocycle considerably, but a sizable fraction of the $N_2$ content remains, probably in a form which can complex the transition metal ion. This complex containing the transition metal is thought to be the active site for $O_2$ reduction and/or peroxide decomposition. The portion of the transition metal that is not complexed can easily be converted to an oxide. The hydrated Co oxide is active for peroxide decomposition, but the Fe oxide has little activity.

Two types of N-containing polymers, polypyrrole and polyacrylonitrile (PAN), were used to prepare highly active catalyst for $O_2$ reduction. They were heat-treated with either Fe or Co acetates at 300 to 900°C, with optimum $O_2$-reduction performance obtained at 700 to 850°C, depending on the particular combination of polymers and transition metal.

The primary emphasis of the Electromedia program was to develop long-lived electrode structures using CoTMPP catalyst. Initially, the electrode was targeted for operation at 60°C in 4 M KOH, however, this specification was changed to 80°C in 5 M KOH during the latter stages of the research. Electrodes were fabricated using active carbon and carbon black substrates. The structures tested included (i) Double Layer Single Grid (DLSG) electrodes, (ii) Single Layer Double Grid (SLDG) electrodes, and (iii) Double Layer Double Grid (DLDG) electrodes.

Superior, long-lived, active carbon electrodes were developed which operated for a full year in KOH and NaOH at 60 and 80°C. Specifically, for active carbon electrodes, long-term cycle life was enhanced in KOH and at the lower temperature. These electrodes still have a major drawback in Al/air batteries because their potential showed a steady decline from start-up to failure, with no stable plateau. In order to insure uniform battery performance with a well-defined, predictable failure point, further innovation in electrode fabrication is needed. Alternative carbon black substrates with increased hydrophobicity and corrosion resistance compared to the active carbons were selected. A new electrode structure was tailored specifically for the carbon black substrates. The result was an electrode with superior voltage performance (ca. 700 mV, RHE at 600 mA/cm$^2$) at both 60 and 80°C, with a well-defined failure point, but shorter life than the active carbon electrodes (<1500 cycles).

The tests at 80°C showed a drastic shortening of the life of the standard DLSG electrodes, whether they were made from active carbon or from carbon black. The wetting tests revealed that the AB (conducting) layer absorbed more electrolyte and lost more gas permeability at 80°C than at 60°C in a one-week immersion test. Redesigning the electrode structure resulted in SLDG electrodes which lasted longer than the DLSG electrodes at 80°C. Cycle tests, on the other hand, identified the DLSG electrodes as the best-performing air cathodes, particularly for the DLSG electrodes containing RB carbon or Norit carbon. The program now focuses on combining the technology reported above to develop and optimize an air cathode which will satisfy the demands of both constant current and cyclic operation.

*Aluminum Anodes.* The compositions of seven families of alloys were investigated at Eltech based on the following criteria:

- Al-based alloys are commercially available,
- literature is available on the effect of certain metals on the electrochemical characteristics of Al, and
- alloys can be prepared specially for the Al/air battery by either Alcan or Reynolds.

The best-performing alloys are fabricated with high-purity Al, either 99.99 or 99.999% pure, with no or very little Fe contamination. Indium is a common alloying agent which improved the electrode performance. Thallium was found to be beneficial but later abandoned because it is highly toxic. Gallium was shown to improve electrode potential, but also increased parasitic corrosion of the electrode. The best-performing alloy had proprietary composi-

tion (designated BDW) which yielded 4.2 kWh/kg Al at 200 mA/cm$^2$.

Operating the anodes at 80°C increased the parasitic corrosion of most alloys, but BDW showed only a slight increase in corrosion. At high current densities, the increase in anode potential outweighs the increase in parasitic corrosion, thus leading to improved energy yields. The performance in 5 M KOH was comparable to that obtained in 4 M NaOH.

An acceptable anode composition was identified which exceeded the 0.6 W/cm$^2$ target and attained over 90% of the specific energy target of 4.5 kWh/kg Al.

Experimental and theoretical studies were undertaken at SRI International in order to optimize the development of Al alloy anodes for the Al/air battery. Experimental techniques were developed for delineating the anodic and cathodic reactions by oxidizing evolved $H_2$ in a porous platinized-nickel electrode located downstream of the Al specimen. This technique allowed the separate examination of the $H_2$ evolution and Al electrodissolution reactions over a wide range of potential (-1.9 to -1.3 V) and temperature (25-80°C). At 25°C, and possibly higher temperatures, pure Al showed an active-to-passive transition, a passive region, and transpassive dissolution in which the current varies linearly with voltage. At the higher temperatures, the potential could not be displaced to sufficiently negative values to observe the active-to-passive transition, but the passive region was still observed, at least at 50 and 60°C. In the case of the alloys containing Ga, In, and Tl as alloying elements, the anodic curve displayed a wide passive range from -1.9 to -1.5 V (Hg/HgO), at which point the current/voltage curve made the transition to that for pure Al. Activation of the Al alloy anode at -1.5 V was attributed to the oxidation of a layer of the metallic alloying elements on the surface, which exposed the underlying base Al metal. The potential at which activation occurred at 25°C (-1.5 V) coincided well with the calculated equilibrium potential for the Ga/$GaO_2$-couple in concentrated hydroxide solution, so that activation tentatively could be attributed to the oxidation of metallic Ga.

The electrodissolution mechanism of Al for pure Al and Al alloys has been investigated using wide-band-width AC Impedance Spectroscopy (ACIS). The impedance spectra display both pseudo-capacitive and pseudo-inductive relaxations; their number and characteristics depend strongly on the DC-bias potential. These relaxations were attributed to the formation of adsorbed hydroxyl species from a series of one-electron discharge steps coupled with $H_2$ evolution, with all reactions competing for surface sites. Additionally, a surface film is envisaged to form that blocks reaction sites, or it imparts resistive control over the current flow. In the case of the alloys, the impedance spectra are complicated by the metallic alloying species on the surface. However, at potentials more positive than -1.5 V (activation voltage), the impedance spectra are similar to those for pure Al, as expected, because of the oxidation and loss of the alloying elements from the interface.

Oklahoma State University conducted an exploratory study into the metallurgical characterization of Al alloy anodes. The program was divided into three separate objectives: (i) computerized literature search, (ii) a review of the literature, and (iii) metallurgical analysis. The results show that it is possible to use Raman and Fourier transform infrared spectroscopy techniques to analyze the Al anode corrosion products.

## CRYSTALLIZATION AND PRODUCT SEPARATION

Research at LLNL focused on developing an Electrolyte Management System (EMS) for the Al/air battery. The experiments to validate the EMS design were carried out at 80°C, using NaOH and KOH electrolytes, and the following Al samples: 99.999% pure Al, Alcan's BDW alloy and Eltech's 353 and 1QY alloys. The solids concentration at the bottom of the crystallizer was maintained at below 20 vol%.

*Lamella Crystallizer/Separator System.* Two Al/air cells provided the aluminate feed to the crystallizer system. During standby or shut down, the electrolyte resides in the electrolyte storage tank (EST) and in the lamella crystallizer. The cells are started by activating the electrolyte flow from the bottom of the EST to the cells. The overflow from the cells returns by gravity to the EST. The conductivity of the electrolyte entering the cells is monitored by a Foxboro conductivity meter. A peristaltic pump circulates electrolyte from the bottom of the EST to an annular passage at the bottom of the crystallizer.

The bottom of the crystallizer is a cone, 12.1-cm ID at the top with 65° angle. The bottom of the crystallizer acts as an elutriator to concentrate the coarsest particles at the bottom, from which they are sent to the product separation and wash section. The annular flow at the bottom of the crystallizer re-suspends the particles that have settled into the sides of the cone. The return flow from the separation and wash section enters near the top of the crystallizer. The lamella settler that makes up the top

portion of the crystallizer consists of 5 parallel plates, 5-cm wide with 1-cm plate spacing, 60-cm long with 30° angle of inclination to the vertical. A Foxboro conductivity meter at the top of the crystallizer monitors the conductivity of the electrolyte returning to the EST.

The experimental results indicate that plate spacing in the settler can be reduced to 0.5 cm or less, leading to crystallizer volume for a 100-cell vehicle system of about 40 $\ell$.

The product separation and wash section consists of a 1-cm ID, 30-cm long, 1-cm ID tube settler. At the bottom of the tube settler there is a splitter which directs the underflow to a 1-cm ID zig-zag wash section where the hydrargillite product flows counter-current to the incoming make-up water to the cells. The splitter has an adjustable baffle to control the solids flow into the zig-zag section. When the baffle is open, solids are removed at a rate corresponding approximately to a 300 mA/cm$^2$ current density (180 Amp). When the system is operated at lower current densities, the baffle is opened intermittently. As the product falls into the moving water stream at the end of each zig-zag, it is washed of entrained caustic and only the finer particles are retained in the liquids. The product is collected in any one of four product receivers.

The system operated very well, it was started and shut down many times without plugging of the lines by solids. However, it was found that trouble-free operation at high solid concentrations required adherence to fixed operating sequences for startup and shut down of the system.

The experimental results indicate that the aluminate concentration approaches closely the equilibrium value when electrolyte is circulated between the crystallizer and the EST for one hour after cell shut down, and that none of the alloys tested had alloying elements that unduly interfered with the crystallization process.

*Lamella and Tube Settlers.* For hydrargillite powders of four widely different particle size distributions and a settler (60-cm long, 1-cm plate spacing, 5-cm wide) inclined at 30° to the vertical, there is good agreement between the calculated and experimental values of the ratio of solids concentration in the overhead divided by the solids concentration in the feed, as well as in the overall material balance.

*System Analysis.* It is of interest to estimate steady-state performance of a system, which in this analysis is assumed to consist of 100 cells with 600-cm$^2$ active area each with 2-mm anode/cathode gap and a 40-$\ell$ crystallizer. The most frequent operating mode for the system is for the aluminate concentration to fluctuate between the equilibrium value and a peak concentration determined by the average power density during vehicle operation. When the system is shut down for an extended period and the system temperature is about 20°C, the initial Al concentration is below 0.6 M.

The power densities (W/cm$^2$) and energy densities (kWh/kg Al) were calculated for several aluminate concentrations (1-2.9 M). The analysis indicates that the Al/air system can easily deliver 15 to 20 kW of steady-state output power, and it performs at its highest energy density (~4 kWh/kg) under those conditions.

PUBLICATION

1. Maimoni, A. (1986), "Aluminum-Air Batteries: Materials Related Research," *Mat. Res. Soc. Bull.* **11**, 19.

# C. FUEL CELL RESEARCH

Fuel cell research includes projects in several areas of electrochemistry: theoretical studies, fuel-cell testing, fuel processing, and fuel-cell component characterization.

## Fuel Cells for Transportation

*J.R. Huff (Los Alamos National Laboratory)*

The objectives of this program are to conduct basic and applied research in electrochemistry necessary to take fuel-cell technology from its present status to a proof-of-concept level where it becomes a practical alternative to internal combustion engines (ICE) for vehicular propulsion. The goals of the effort are to improve the specific power and transient response of the fuel-cell system and to reduce the materials and manufacturing costs. Program emphasis has been on the optimization of Nafion-impregnated electrodes with low Pt loadings (0.35 mg/cm$^2$), long-term testing of single cells based on such electrodes, characterization and modeling of membranes for polymer-electrolyte-membrane (PEM) fuel cells, and investigation of the kinetics and mechanisms of reforming required for fast-response reformers.

*Optimization of PEM Electrodes.* A significant improvement in the performance of low-Pt-loading electrodes has been achieved. This has been accomplished by spraying the electrodes, by heating the

modified electrodes after spraying, and by hot-pressing the electrodes onto the Nafion electrolyte. With 0.35 mg Pt/cm$^2$, the best electrodes have an IR-free-oxygen-reduction-reaction (o.r.r.) current of 600 mA/cm$^2$ at 570 mV (RHE) at ambient temperature and 1 atm.

Rutherford Backscattering (RBS) measurements have been used to determine that the Nafion content of the modified electrodes is not uniform with depth. The results showed that most of the Nafion was concentrated in the first 1 $\mu$m, using a single spray of 5% Nafion solution. This implies that, despite the marked improvement in performance with such treatment, the match between the depth that the proton conductor can penetrate and the Pt catalyst layer in a Prototech electrode is still very poor. It should be stressed, however, that the performance of Nafion-impregnated electrodes with 0.35 mg Pt/cm$^2$ is already comparable to that of electrodes with 4 mg Pt/cm$^2$.

Impedance results of Nafion-impregnated electrodes in contact with Nafion membranes have been analyzed with the aid of a powerful computer program developed at LANL for this purpose. For the o.r.r., a feature in the impedance plot due to diffusion can be clearly resolved at high current densities. The value of the apparent charge-transfer resistance changes at a rate of one decade per 240 mV for potentials below about 0.75 V vs RHE. This doubling of the Tafel slope is due to the distributed nature of the Faradaic process. At higher potentials, a lower slope is seen. At about 0.5 V, the resistance approaches an almost constant value. Such behavior implies that an interplay between mass transport and charge transfer effects determines the behavior of the Nafion-impregnated $O_2$ cathode at potentials between 0.8 V and the onset of limiting-current behavior. The relative contributions of protonic and gas transport limitations to the polarization of the impregnated cathode in the intermediate current domain still have to be clarified. The high-frequency electrolyte (membrane) resistance shows a significant dependence on the current density for the $H_2$ oxidation reaction, the most likely explanation being local drying of the membrane. For the o.r.r., the high-frequency resistance tends to decrease with increased current density, which could also be due to interfacial $H_2$ content.

The performance of the modified electrodes at higher temperatures (50°C or above) and at atmospheric pressure did not improve. Neither the electrolyte resistance nor the kinetic components of the overpotential changed very much with an increase in temperature. It appears that the membrane may not be adequately hydrated at higher temperatures. There is also evidence that kinetic parameters are adversely affected by partial dehydration. These results provide additional evidence that stabilization of the interfacial $H_2$ content is essential for high-performance PEM fuel cell systems.

Measurements of the o.r.r. currents at a Pt RDE that was coated with a recast Nafion film yielded the permeability of $O_2$ through such films. Combined with results from linear-potential sweep experiments on similar electrodes, these measurements also allowed the separate evaluation of the concentration of $O_2$ and its diffusion coefficient in such films. This information is required to analyze the effects of the recast Nafion film on the kinetics of the interfacial process and on the transport of the reactant gas to the catalyst site in Nafion-impregnated electrodes. The diffusion coefficient of $O_2$ in the recast film (4 x $10^{-6}$ cm$^2$/sec) and the $O_2$ concentration in it (3 mM) should allow $O_2$ fluxes as high as 10 mA/cm$^2$ of catalyst area (i.e., $\sim$10 A/cm$^2$ of electrode area) through recast films 0.5-$\mu$m thick. Experiments with Pt RDE were also performed to evaluate the potential of Nafion coatings to improve the performance of cathodes, particularly in $H_3PO_4$ fuel cells, based on the increase of $O_2$ solubility next to the catalyst surface. The enhancement of o.r.r. kinetics due to $O_2$ enrichment in the recast Nafion film was found to be marginal at best in either dilute $H_2SO_4$ or 85% $H_3PO_4$ at room temperature. Based on this result, it was further concluded that the addition of a recast Nafion film to the catalyst side of a fuel cell cathode is most probably advantageous because of the great improvement in protonic access to catalyst particles and not because of a significant enhancement of local $O_2$ concentration.

*Electrode Fabrication and Fuel Cell Evaluation.* Electrodes produced in-house by the filtration method (0.35 and 0.5 mg Pt/cm$^2$), which were impregnated with Nafion and hot-pressed onto Nafion membranes at 120°C and 50 atm for 15 seconds were studied. Similar experiments were carried out with Prototech electrodes (0.35 mg Pt/cm$^2$), both as-received and Nafion-impregnated. The results showed that: (i) the performance (in $H_2$, $O_2$ and air) of Nafion-impregnated electrodes in contact with Nafion membranes match the performances of similar electrodes in contact with $CF_3SO_3H$ at concentrations of more than 0.5 M; and (ii) the performance of the electrodes prepared at LANL are comparable to the Prototech electrodes, except the diffusional overpotential is higher with the LANL electrodes at high current densities.

Single-cell tests were conducted to demonstrate good, long-term performance of PEM fuel cells using low-Pt loading electrodes. A General Electric/ Hamilton Standard (GE/HS) membrane and electrode assembly (4 mg Pt/cm$^2$) was used for comparison. For the test cells, as-received and Nafion-impregnated Prototech electrodes were hot-pressed onto Nafion membranes or onto Dow experimental membranes at 120°C and 50- to 60-atm pressure. Cell potential-current density measurements were made periodically by interrupting the constant current density operation of the cells at 25 and 50°C. The high frequency (~1 KHz) resistances of the cells were measured at several current densities.

The cell potential-current density data were analyzed using an equation of the form

$$E = E_o - b \log i - Ri . \qquad (1)$$

In this equation, $E_o$ is a constant and, if it is assumed that the $H_2$ oxidation reaction is considerably faster than the $O_2$ reduction reaction (evident from the half cell tests), the Tafel slope, b, is representative of the $O_2$ reduction reaction. R is the slope, which includes contributions from ohmic as well as activation and transport overpotentials, the last being due to rate limitations within the catalyst layer. The parameters $E_o$, b and R were evaluated by means of a least-squares fit of the experimental points. Figure 16 shows the least-squares plots and the experimental points for the GE/HS control, the as-received and the Nafion-impregnated Prototech electrodes. These results clearly demonstrate that the difficulty in achieving access of protons to Pt sites within the catalyst layer in the Prototech electrode is solved effectively by Nafion impregnation. Using these electrodes hot-pressed onto the Dow experimental membrane yielded a high-frequency resistance, $R_{HF}$, which was about half that for the other cells, indicating even higher performance should be possible with this membrane.

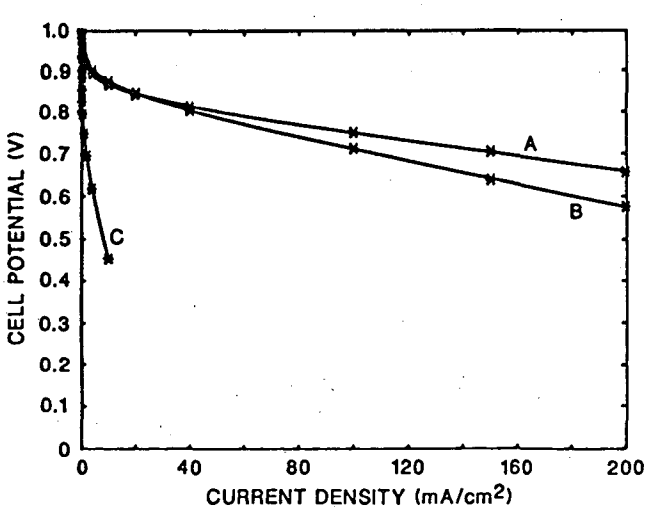


**Figure 16.** Cell potential vs current density for $H_2/O_2$ fuel cells at 50°C and 1 atm. (A) GE/HS control; (B) Nafion-impregnated Prototech; (C) as-received Prototech; solid line - least-squares fit; x - experimental points.

The electrochemically active surface area of the electrodes was approximately the same for the GE/HS and the Nafion-impregnated Prototech electrodes; however, it was at least an order of magnitude less for the as-received Prototech electrodes. The results clearly demonstrate the extension of the active reaction zone by incorporation of a proton conductor into the electrode.

Electrodes prepared at LANL by the filtration method (0.35 and 0.5 mg Pt/cm$^2$) were tested for $H_2$, $O_2$, and air performance at room temperature in $H_2SO_4$ and $CF_3SO_3H$ of varying concentrations. The $H_2$ overpotential is quite small (< 20 mV) up to current densities of 500 mA/cm$^2$, and only a small dependence of $H_2$ overpotential on acid concentration is observed. At high current densities, the $O_2$ overpotential is markedly dependent on acid concentration. With $H_2SO_4$ at concentrations of 0.5 M or less, there are significant effects of combined ohmic and mass transport control. With $CF_3SO_3H$, this occurs at a lower concentration.

*Membrane Characterization and Modeling.* Experiments were conducted to measure the rates of $H_2$ transport in Nafion membranes. The results of thermogravimetric, IR spectroscopy and conductivity measurements led to the following observations:

- During fuel cell operation, polymers maintain rather low $H_2$ content (~5 $H_2O/R\text{-}SO_3H$).
- Water motion is the result of two forces in the polymer under steady-state conditions. First, $H_2O$ moves through the polymer as the result of hydraulic permeability, driven by a $H_2O$ activity gradient. Second, $H_2O$ is pumped by the movement of $H^+$, which is a function of cell current.
- High current densities can result in the transport of $H_2O$ away from the anode-membrane interface at a rate that is faster than it can be restored, thereby causing dehydration. The extent of this dehydration is a direct consequence of the rate of hydraulic permeability, the back-diffusion rate of $H_2O$ from cathode to anode. Local partial dehydration can lead to cell failure.
- Comparison of Nafion 1100 and Nafion 1200 showed clear differences in conductivity and

$H_2O$ permeability rate (1100 gave higher values in both cases). These results indicate that lower-equivalent-weight polymers are closer to optimum and also that $H_2O$ management requires high hydraulic permeability.

Several new polymers have been characterized that have resistances half that of Nafion or lower. With these membranes, current densities near 4,000 $A/cm^2$ at a reasonable voltage have been obtained with single cells by industrial collaborators. Such new membranes are a major advance in PEM fuel cell technology. These membranes are not optimized, and future work is expected to yield performance levels for $H_2$/air PEM fuel cells that are comparable to those obtained with alkaline fuel cells.

*Reformer Kinetics and Mechanisms.* Considerable experience has been gained with a stirred (forced convective) heat-transfer reactor, which uses recirculation to sustain a uniform catalyst temperature. Depending upon the recirculation rate, the temperature variation across the catalyst bed is held to 10°C or less, which is closer to isothermal than the $\geqslant$200°C temperature variations found in conventional reformer hardware.

This reformer produces equilibrium values (1-3%) of CO in the reformate; levels which are too high for PEM fuel cells. Therefore, CO removal from the process stream following the reforming step was pursued. The effectiveness of a partial oxidation process for this step was initially suggested by Ballard Technologies. The partial oxidation process was investigated by examining the addition of small quantities of $O_2$ (or air) to the reformer product mixture and then passing the mixture over an oxidation catalyst. Experiments, first with $O_2$ and then with air, showed the utility of this approach. Gaseous mixtures of $H_2$ containing 1% CO were reacted on 0.5% Pt on $Al_2O_3$. As predicted, no reaction was apparent at low temperatures. At temperatures near 165°C (gas-phase temperatures), the CO concentration was decreased to below 0.01%. This was done by the addition of 2% $O_2$ (2x stoichiometry). No $O_2$ was found in the effluent so the excess $O_2$ was consumed to produce $H_2$. At higher catalyst temperatures, CO could be removed only by addition of ever larger quantities of $O_2$, at the expense of consuming more and more $H_2$. Therefore, this technique is successful, in a narrow regime of temperatures. The ability to operate low-temperature fuel cells with reformed fuels depends on control of CO content.

## PUBLICATIONS


1. M.T. Paffett, J.G. Beery, and C.J. Maggiore (1986), "Ion Beam Analysis of Fuel Cell Electrodes," *Proceedings of the 22nd Annual Symposium of the New Mexico Chapter of the American Vacuum Society,* Albuquerque, NM, p. 37.
2. L. Borodovsky, J.G. Beery, and M.T. Paffett (1986), "Platinum Loss and Migration in Porous Gas Diffusion Fuel Cell Electrodes as Studied by Rutherford Backscattering," *Conference on the Application of Accelerators in Research and Industry,* Denton, TX.
3. S. Gottesfeld, M.T. Paffett, and A. Redondo (1986), "Ellipsometric Measurements of Structure and Dynamics at the Metal-Electrolyte Interface," *International Conference on Structure and Dynamics of Solid/Electrolyte Interfaces,* at the Fritz Haber Institute of the Max Planck Geselschaft, Berlin, West Germany.
4. I.D. Raistrick (1986), "Modified Gas Diffusion Electrode for Proton Exchange Membrane Fuel Cells," *Extended Abstracts of the 169th Meeting of the Electrochemical Society,* p. 660.
5. T.E. Springer (1986), "Electrostatic Modeling of Porous-Electrode/Electrolyte Interfaces," presented at the *Cube Symposium,* Livermore, CA.
6. N.E. Vanderborgh, B.E. Goodby, and T.E. Springer (1986), "Oxygen Exchange Reactions During Methanol Steam Reforming," *32nd International Power Sources Conference,* Cherry Hill, NJ.
7. P.C. Rieke and N.E. Vanderborgh (1986), "Pyrolyzed Macrocycle/Carbon Blends for Advanced Electrocatalysts," *Carbon '86,* Baden-Baden, FRG.
8. P.C. Rieke and N.E. Vanderborgh (1986), "Influence of Temperature and Water Content on the Proton Conductivity and Tertiary Structure of Polyperfluorosulfonic Acid Membranes," *Extended Abstracts of the 170th Meeting of the Electrochemical Society Meeting,* p. 891.
9. B.E. Goodby, J.E. Pemberton, and N.E. Vanderborgh (1986), "Hydrogen from Methanol: Oxygen Exchange," *Extended Abstracts of the 170th Meeting of the Electrochemical Society Meeting,* p. 223.
10. J. Leddy and N.E. Vanderborgh (1986), "Microstructural Enhancement of Mass Transport through Nafion/Nuclepore Composite Membranes," *Extended Abstracts of the 170th Meeting of the Electrochemical Society Meeting,* p. 885.
11. J. Leddy, A.E. Iverson, and N.E. Vanderborgh (1986), "Modeling of the Electrode/Ionomer Interface in a Solid Polymer Electrolyte Fuel

Cell," *Extended Abstracts of the 170th Meeting of the Electrochemistry Society Meeting,* p. 196.
12. J.L. Fales, N.E. Vanderborgh, and P. Stroeve (1986), "Water Flows within Ion-Exchange Membranes during Fuel Cell Operation," *Extended Abstracts of the 169th Meeting of the Electrochemical Society,* p. 661.
13. I.D. Raistrick (1986), "Application of Impedance Spectroscopy to Materials Science," *Ann. Rev. Mater. Sci.* **16,** 343.

## Advanced Chemistry and Materials for Fuel Cells

*J. McBreen (Brookhaven National Laboratory)*

The objectives of this work are to understand electrocatalysis at a molecular level, to minimize or eliminate the need for noble metals in fuel cells, and to enhance the kinetics of $O_2$ reduction and the oxidation of $C_1$ compounds. In 1986, research was focused on: (i) EXAFS studies of pyrolyzed metal macrocyclics on carbon and of carbon-supported Pt electrocatalysts, (ii) *in situ* EXAFS studies in operating phosphoric acid fuel cells, and (iii) the synthesis of new electrocatalysts based on conductive polymers and tetrasulfonated metal phthalocyanines (M-TsPc).

*EXAFS Studies of Pyrolyzed Metal Macrocyclics.* The structure of the active catalyst in pyrolyzed Fe or Co macrocyclics on carbon is not known. There is some evidence that the Co material has a maximum activity after pyrolysis at 600 to 800°C. At these temperatures, the pyrolysis products show no X-ray diffraction pattern, and thus are amorphous.

An EXAFS study was carried out on pyrolyzed Co and Fe macrocyclics supported on carbon (Vulcan XC-72). Both phthalocyanine (Pc) and TMPP materials were studied. The Fe macrocycles were pyrolyzed at 920°C, and the Co macrocycles were pyrolyzed at 800 and 900°C.

At 900°C, the Co macrocycles were reduced to the metal possibly by carbothermic reduction. At 800°C, the Fourier transform of the EXAFS spectra was very complex, however, it indicated the presence of Co metal and some other materials. When the pyrolysis product was leached in hot KOH solution to remove Co, a bluish filtrate was observed. This procedure removes up to 50% of the Co without decreasing the catalytic activity. The remaining material, which is presumably the catalyst, has a radial structure function similar, in most respects, to the original Co-TMPP material. Apparently, some core moiety of the macrocyclic compound remains after pyrolysis. After pyrolysis at 920°C, the Fe-TMPP on carbon consists of both Fe metal and another material. Leaching in either hot HCl or oxalic acid removes the Fe and leaves a material with a structure similar to the macrocyclic. Analysis is continuing to fully elucidate these pyrolysis products.

*EXAFS Studies of Platinum on Carbon.* Extensive EXAFS studies have been done on commercial carbon-supported Pt electrodes. This includes work on as-received electrodes and electrodes in operating fuel cells. The Pt-C interactions on these electrodes were elucidated from EXAFS on reduced electrodes (to remove the oxide) and by subtracting the Pt-Pt contribution in the data analysis. This reveals two Pt-C interactions – one with a Pt-C bond of 2.58 Å, and the other with a Pt-C bond of 3.40 Å.

In operating cells, changes in the EXAFS were observed in going from open circuit to load. Even further changes were observed when operating on hydrogen. These data are being analyzed.

*M-TsPc Compounds in Conductive Polymers.* Several M-TsPc compounds were successfully prepared by direct chelation with $H_2$-TsPc in aqueous solution. The M-TsPc compounds of Ti and Mo were synthesized for the first time. The ions ($Mn^{2+}$, $Fe^{2+}$, $Ni^{2+}$, $Zn^{2+}$, $Pd^{2+}$, $Co^{2+}$ and $Sn^{2+}$) that could be chelated had ionic radii between 0.68 and 1.0 Å.

Several polypyrrole electrodes were prepared with M-TsPc compounds (M = Fe(III), Co, Mn, Ni, Ga, Os, Ru, VO [vanadium in the +2 state with an axial O ligand] and Ir) as the counter anion in the conductive polymer. The redox behavior of these materials is being investigated.

### PUBLICATIONS

1. C.A. Linkous, H. Teoh and M. Velazquez-Rosenthal (1986), "Characteristics of Polypyrrole/Sulfonated Metal Phthalocyanine Electrodes," *Extended Abstracts of the 169th Meeting of the Electrochemical Society,* p. 416.
2. C.A. Linkous, W.E. O'Grady, D. Sayers and C.Y. Yang (1986), "Spectrophotometric and X-ray Absorption Edge Study of Complexation of Carbon Monoxide with Ferric Tetrasulfophthalocyanine in Alkaline Solution," *Inorg. Chem.* **25,** 3761.
3. M. Velazquez-Rosenthal, T.A. Skotheim and C.A. Linkous (1986), "Polypyrrole-Phthalocyanine," *Synthetic Metals* **15,** 219.
4. V. Danginis, S.N. Levine and C.A. Linkous (1986), "Electrochemical Properties of Polypyrrole-Phthalocyanine and its Metal Derivatives," *Extended Abstracts of the 169th*

*Meeting of the Electrochemical Society,* p. 418.
5. W.E. O'Grady and D.E. Sayers (1986), "X-ray Studies of the Solid Electrolyte Interface," *Abstracts of the American Chemical Society Meeting,* NY.
6. C.A. Linkous, C.E. Shea, W.E. O'Grady, D. Sayers and C.Y. Yang (1986), "Electronic Structural Effects of Carbon Monoxide Coordination with Ferric Tetrasulfonated Phthalocyanine in Alkaline Solution," *Abstracts of the American Chemical Society Meeting,* NY.

## Oxygen Reduction on Platinum in Fuel Cell Electrolytes

*E.J. Cairns and F.R. McLarnon (Lawrence Berkeley Laboratory)*

The reduction of $O_2$ on Pt electrodes in aqueous alkali hydroxide and carbonate electrolytes were studied over a concentration range approaching practical fuel cell conditions. Parallel studies of the mechanism on smooth electrodes and fuel cell behavior on gas-diffusion electrodes are also being carried out.

Kinetically limited currents at an electrode potential of 880 mV vs RHE (reversible hydrogen electrode at the same conditions as the working electrode) are shown in Fig. 17 for KOH and $K_2CO_3$ as a function of electrolyte concentration. The right-hand scale shows the same data corrected for the large differences in $O_2$ solubility which occur over this concentration range. The smooth electrode studies also indicated that Pt with low oxide coverages showed negligible peroxide production when in contact with the carbonate electrolytes during $O_2$ reduction. In the higher-pH hydroxides, however, peroxide production accounted for from 2 to 15% of the total $O_2$-reduction current. From a kinetic point of view, therefore, carbonates are superior to hydroxides at the same concentration, showing an average of 60% higher kinetic currents and lower peroxide production rates.

Oxygen reduction currents were also measured for high-area Pt supported on carbon black porous gas-diffusion electrodes (obtained from Prototech, Inc.). The area of Pt actually in contact with the electrolyte in these electrodes can be estimated from the charge associated with hydrogen desorption. The measured $O_2$-reduction currents can then be compared directly with the purely kinetically limited results mentioned above. For the hydroxide electrolytes, this comparison indicated that kinetics, as opposed to mass transfer of reactants and/or products or ohmic effects, is the controlling process over most of the potential range of interest (800-1000 mV vs RHE). This is not true for the carbonate electrolytes. Local pH changes occur in the pores of the electrode due to hydroxide-ion production during operation. This is believed to be the major cause of the lower performance observed in carbonate vs hydroxide shown in Fig. 18 (solid curves). Preliminary experimental work indicates that addition of $CO_2$ to the $O_2$ feed may be a way to improve this situation by converting to carbonate some of the excess hydroxide (dashed curves).

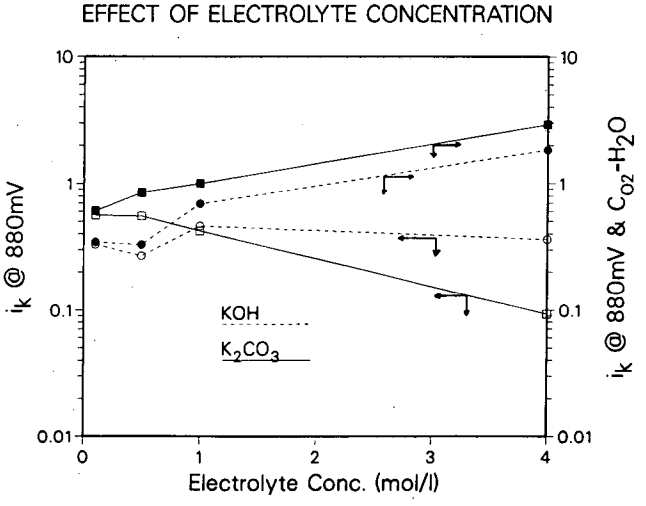


**Figure 17.** Kinetic current density dependence on electrolyte concentration in KOH and $K_2CO_3$ for $O_2$ reduction on Pt. (XBL 8610-3873)

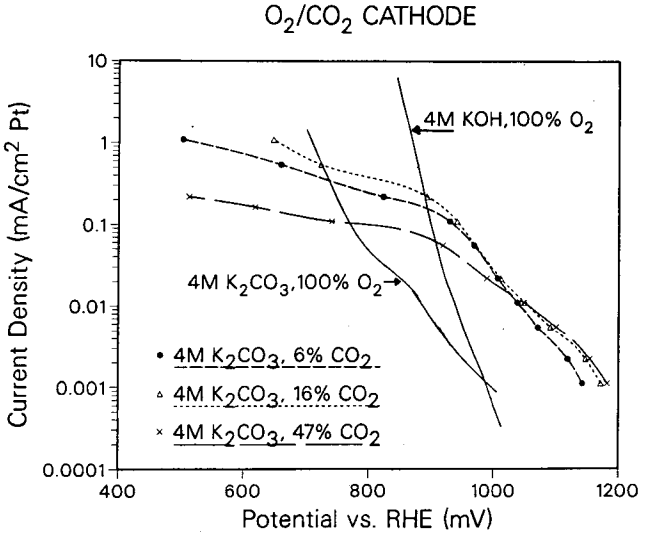


**Figure 18.** Performance curves for a Prototech electrode (0.3 mg Pt/cm$^2$) at 25°C in alkaline electrolytes with various gas compositions. (XBL 871-92)

*LAWRENCE BERKELEY LABORATORY*
*TECHNICAL INFORMATION DEPARTMENT*
*UNIVERSITY OF CALIFORNIA*
*BERKELEY, CALIFORNIA 94720*